Structure of the organo-phosphatic shell of the brachiopod *Discina*

ALWYN WILLIAMS[1], SARAH MACKAY[2] AND MAGGIE CUSACK[3]

[1,3] *Department of Geology and Applied Geology and* [2] *Department of Anatomy, University of Glasgow, Glasgow G12 8QQ, U.K.*

CONTENTS

SUMMARY

The secondary shell of *Discina* is composed of a succession of thin, impersistent, organo-phosphatic layers (laminae) pervaded by a vertical canal system and anastomosing organic strands. Four types of biomineral laminae are distinguishable, all composed of the same basic unit, an apatitic granule, between 4 and 8 nm in size, with a chitino-proteinaceous coat. These units are assembled and aggregated into spherules within the outer epithelium of the mantle. During exocytosis, spherules are further aggregated into mosaics, varying from flattened discs to spheroids, which are added incrementally to the shell succession more or less in their final polymerized and crystallized states. The distinctiveness of a lamina depends on the relative proportions of its organic and biomineral components and the aggregation of its apatitic mosaics. Compact laminae are composed almost exclusively of apatitic mosaics. In contrast, stratified, rubbly and baculate laminae respectively consist of plates, lenticles (or nodules) and rods of apatite in an increasing proportion of chitino-protein, culminating in wholly organic membranes. There is a discernible rhythmic sedimentation from a predominantly (or exclusively) organic to a mainly apatitic deposition, which reflects a recurrent cycle of secretion by the same group of cells. Spheroidal mosaics of apatite characterize the shell structure of extinct acrotretides and paterinides and probably represent traces of the original fabric.

Exceptionally, swarms of inclusions, up to 1 μm or more in diameter and consisting of spheroidal mosaics grouped around central cavities, are embedded in laminar successions. The inclusions have thick, mainly proteinaceous coats and are encased in meshes of coarse particles representing nodes in the apatitic framework of the enclosing laminae. The inclusions appear to have crystallized immediately before or during exocytosis. Hemispherical hollows found in other shells are believed to be the casts of related structures. Arrays of pits and tubercles on the external surfaces of many extinct organo-phosphatic brachiopods may have originated in the same way.

The sporadic development of discrete walls of spherular mosaics of apatite enclosing vertical canals also serve as a living model for the growth of the columnar laminae of Palaeozoic acrotretoids.

Phil. Trans. R. Soc. Lond. B (1992) **337,** 83–104
Printed in Great Britain

1. INTRODUCTION

Species of the inarticulate brachiopod, *Discina*, and its close relatives, *Discinisca* and *Pelagodiscus*, are the only living survivors of an ancient order, the Acrotretida, which was widely represented among early Cambrian marine faunas. Apart from the development of skeletal apophyses, inferentially for the support of muscles and the tentacular feeding organ (lophophore) in some extinct acrotretoids, the morphology of the bivalve shell has always been conservative with little more elaboration than that resulting from variability in the emergence of the holdfast organ (pedicle) from the ventral valve. The shell itself, on the other hand, is complex in composition and intricate in structural design; so much so that it is difficult to reconcile some of the more esoteric skeletal successions of extinct stocks with those of living species. The difficulties have been compounded by inadequate information on the ultrastructural development of the living shell which has a very complicated periostracum (Williams & Mackay 1979, p. 728); and to remedy this deficiency a comprehensive study of fossil and extant discinoid species is now under way.

In the course of these researches ultrastructural variations in the *Discina* shell have been found which help to explain some of the more bizarre skeletal successions of extinct organo-phosphatic groups, including the pillared laminae of acrotretides (Poulsen 1971). Moreover, the *Discina* shell may contain microscopic biomineralized bodies which, in some respects, are little more than curiosities as they have been found in only a few valves and are not, therefore, manifestations of the standard secretory regime. Their occurrence and structure, however, afforded an opportunity to reconsider the nature of microscopic pits and tubercles ornamenting the surfaces of a wide range of extinct organo-phosphatic brachiopods. Such pits, which tend to be characteristic of particular stages in ontogeny, were first identified in the larval shells of acrotretoids by Biernat & Williams (1970). They have since been reported on the post-larval shells of some linguloids (Holmer 1989) and some extinct discinoids (Holmer 1989; Williams & Curry 1991). In contrast, tubercles, albeit of a comparable size range to that of the pits, ornament the larval shells of the Cambro–Ordovician paterinides (Popov *et al.* 1982), which are also remarkable for having a skeletal fabric of coarse polygonal crystals of apatite (Popov & Ushatinskaya 1987). The current interest in such features, which is being further stimulated by international collaboration in the impending revision of the brachiopod volumes (Part H) of the Treatise on Invertebrate Paleontology, has prompted us to describe the *Discina* shell succession independently of our main findings which will be completed within the next year or so.

2. MATERIALS AND METHODS

Specimens of *Discina striata* (Schumacher) were collected intertidally at Solifor Point about 3 km west-southwest of the village of Tanji in The Gambia. Some were fixed within a day or so of collecting in glutaraldehyde (3% by volume) made up in phosphate buffer (0.1 M, pH 7.2 containing sodium chloride ($30\ g\ l^{-1}$)), for two hours at 4°C. Other specimens were brought back alive and most survived for six months or so on a diet of 'Liquifry Marine' in an aerated solution of 'Tropic Marin' seasalt at normal salinity and a temperature of 25°C. This living sample provided material for certain soft tissue studies under the transmission electron microscopy (TEM) and, with dead shells collected in The Gambia, for all scanning electron microscopy (SEM) work and the enzymic digestion programmes.

(*a*) *Preparation of materials for the TEM*

After a buffer rinse, specimens that had been fixed in glutaraldehyde in the manner just described, were decalcified in EDTA ($10\ g\ l^{-1}$), washed in 0.2 M sucrose and postfixed in 2% osmium tetroxide (all solutions buffered to pH 7.2 with phosphate buffer). For 'undecalcified' specimens the EDTA treatment was omitted. Embedding in Spurr's resin followed dehydration through an ascending alcohol sequence. Thin sections were cut on a Reichert E ultramicrotome using a Diatome diamond knife. After staining with an aqueous solution of lead citrate and uranyl acetate, sections were examined on a Jeol JEM 100S transmission electron microscope.

(*b*) *Preparation of materials for the SEM*

Dried valves of *Discina* were first sonicated for about 10–15 min in a gentle detergent to remove extraneous particles (including bits of mantle tissue from the internal surfaces). They were then left in the natural state or broken to provide oriented fracture surfaces or embedded in London resin and cut in a preferred plane for polished sections. Some of these surfaces were used as controls and did not undergo chemical treatment; others were bleached or subjected to enzymic digestion as described below. Finally, some specimens were coated with carbon and, later, gold to furnish energy dispersive X-ray (EDX) analysis and back scattered electron (BSE) detection as well as normal electron scans of the same area(s) under a Cambridge Stereoscan 360. Others were coated with gold or gold–palladium dependent on whether they were to be viewed under the Cambridge 360 or a Hitachi 900 for resolutions down to about 100 Å† and 7 Å respectively.

The few fossils used in this study were prepared for viewing under the Cambridge 360 in the same way as untreated fracture surfaces of *Discina*.

(*c*) *Chemical and enzymic treatment of specimens*

Natural and fracture surfaces and especially sections of London resin-embedded specimens were subjected to various treatments in an attempt to identify and map out the distribution of the organic components of the *Discina* shell.

† $1\ Å = 10^{-10}\ m = 10^{-1}\ nm$.

(i) *Sodium hypochlorite treatment*

Non-specific degradation of the organic components of the shell was achieved by incubating samples at 22°C for 24 h with an aqueous solution of sodium hypochlorite (10% by volume).

(ii) *Enzymic digestion*

Five enzymes in various concentrations over different periods were applied to specimens before the following procedures were adopted. They involved incubating the surfaces under treatment with aqueous buffered solutions of enzyme at 22°C for 48 h with the enzyme solution being replenished every 24 h.

A selection of proteinases, encompassing a range of specificities, was employed to locate the protein component of *Discina* shells. The cysteine proteinase papain (E.C.3.4.22.2), from *Carica papaya*, hydrolyses peptide bonds at the carboxyl side of arginine, lysine, glutamine, histidine, glycine and tyrosine residues (Smith & Kimmel 1960). Such a broad range specificity for hydrolysis was favoured because few details of the proteins of the *Discina* shell are available. Papain is activated by a variety of thiol compounds such as cysteine or β-mercaptoethanol. Papain was applied at a concentration of 40 μM with the activating agent β-mercaptoethanol (50 μM), both reagents in sodium dihydrogen phosphate buffer (100 mM, pH 7).

The serine proteinases, trypsin (E.C.3.4.21.4) and subtilisin (E.C.3.4.21.14), require no reducing agent for activation and may therefore be more appropriate than papain for this study since the organic components in a control section treated with only β-mercaptoethanol in buffer underwent some degradation. Trypsin specifically hydrolyses peptide bonds at the carboxylic side of the basic residues, lysine and arginine (Geiger & Fritz 1983). Trypsin was employed at a concentration range of 200 μM to 2.6 mM, the highest concentration being the most efficacious. Therefore, in later experiments trypsin from bovine pancreas was dissolved in sodium dihydrogen phosphate buffer (100 mM, pH 7) and applied at a concentration of 2.6 mM. Subtilisin is less specific than trypsin and cleaves peptide bonds at the carboxylic side of neutral or acidic residues (Markland & Smith 1971). Subtilisin from *Bacillus licheniformis* was applied at a concentration of 2 mM after initial experiments employed subtilisin in the concentration range of 200 μM to 2 mM.

The specificity of collagenase (E.C.3.4.24.3) resides in a sequence common in the collagen molecule, of -P-X-G-P-Y-, where P and G are proline and glycine residues respectively and X and Y are any amino acid residues. Enzyme action occurs between -X-G- residues (Seifter & Harper 1970). Binding of collagenase to collagen requires Ca^{2+} ions. Collagenase from *Clostridium histolyticum* was applied at a concentration of 0.02 mM in an aqueous solution of Tris buffer (80 mM, pH 7.8) with $CaCl_2$ (0.1 M). Control samples, incubated with buffer in the absence of any enzyme, were included in all programmes of digestion. They confirmed that the buffers on their own were ineffectual.

Chitin was digested by chitinase (E.C.3.2.1.14) from *Serratia marcesens* dissolved in MES [2-(N-morpholino)ethanesulphonic acid] buffer (100 mM, pH 6) and employed at a concentration 0.2 mM. Lower grade preparations of chitinase were employed at higher concentrations of 0.5, 1 and 2 mM. The higher grade chitinase at 0.2 mM was most efficacious.

(iii) *Successive digestions*

Successive polished surfaces of the same resin-mounted specimens were prepared. After treatment with an efficacious enzyme, resin-mounted sections were polished to remove all digested material. One such sample was exposed to chitinase, trypsin and finally sodium hypochlorite in that order. A reciprocal treatment system was also established whereby an embedded dorsal valve of *Discina* was cut in half and one section, after polishing, incubated with subtilisin, the other with chitinase in preparations described above. Following incubation of the valves with the enzymes, the embedded samples were cleaned by sonication in Milli Q™ water and the valves examined by SEM and then polished to remove the treated material. The reciprocal enzymes were then applied and the specimens re-examined. After another cycle of polishing, chitinase and subtilisin were applied together.

3. TERMINOLOGY OF SHELL STRUCTURE

The shell of adult *Discina striata* (Schumacher), 1 cm or so in diameter, is variable in thickness. Some ventral valves may be little more than translucent, flexible sheets, about 100 μm thick. Even fully grown dorsal valves are up to three times as thick around the margins and beneath the muscle bases as in the mid-region where the full succession seldom exceeds 400 μm.

This variation in thickness reflects the nature of the shell succession which is most easily categorized in montages of backscattered electron micrographs showing the distribution of apatite in fracture and cut sections. In such micrographs (figures 1 and 2), banding is usually clearly delineated by changes in electron density between the extremes of light and dark representing apatitic and organic concentrations respectively. The bands may be mottled, striped with a high-angled cleaved or jointed appearance, or cavernous with high density patches commonly in bedded arrays; or they may be stratified, either coarsely or in alternating, fine, electron-light and -dense units, disposed more or less parallel to their boundaries. Few layers, as represented by bands in the section examined, were large enough to have completely lined a valve interior (figure 1). In a median sections of a dorsal valve, 8.8 mm long, a finely stratified apatitic band, about 40 μm thick, could be traced continuously for almost 6 mm and may have represented a mineralized sheet covering the entire floor of the valve at an earlier growth stage. Generally, however, bands thin out within short spans, grading laterally into other kinds of successions or being abruptly overlapped unconformably by inner, later deposits (figures 2 and 3). In fact, montages so closely resemble stratigraphic profiles of sedimentary

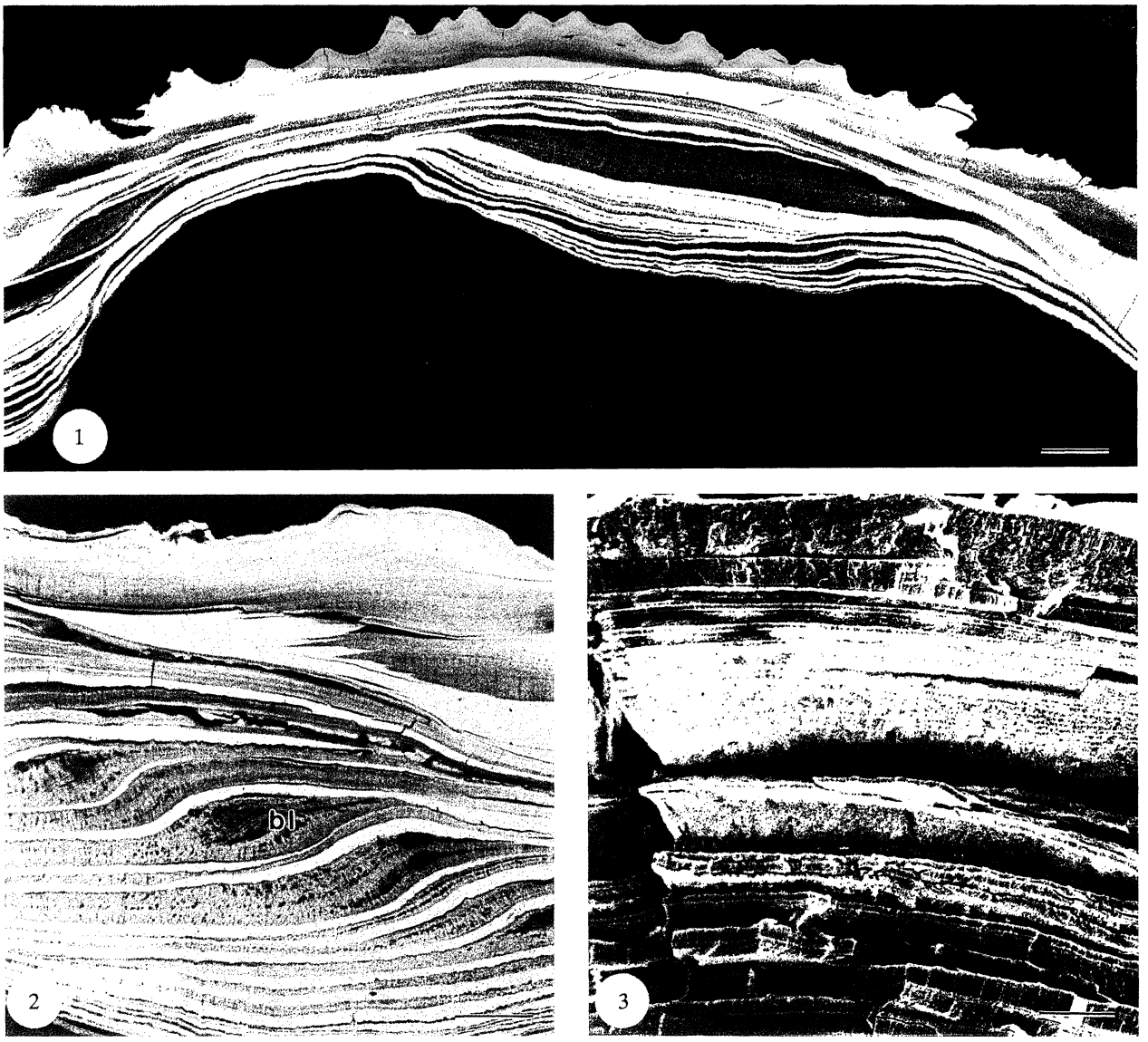

Figures 1–3. Scanning electron micrographs of dried dorsal valves of *Discina striata* with their external surfaces immediately underlain by the primary layer at the top.

Figure 1. Backscattered electron micrograph of a chordal section cut near the umbo and digested in chitinase (0.2 mM in MES buffer) and papain (40 μM in phosphate buffer with mercaptoethanol (50 μM)) and coated with carbon to show the distribution of the apatitic (white) and organic (grey to black) components of the shell succession. Scale bar = 250 μm.

Figure 2. Backscattered electron micrograph of a bleached radial section through the intramarginal zone coated in carbon and showing the distribution of apatitic (white) and organic (grey to black) components of the shell succession with lateral gradations and unconformable oversteps between baculate laminae (bl). Scale bar = 100 μm.

Figure 3. Vertical fracture surface digested in trypsin (1 mM in phosphate buffer) and coated with carbon then gold to show the main types of lamination in a shell succession. Scale bar = 50 μm.

basins that a stratiform terminology is eminently appropriate for labelling the various constituents of the shell. Thus, 'layer' will be used for major divisions of the shell succession, especially in distinguishing between primary and secondary shell. The subperiostracal primary layer is uniformly electron-light in backscattered scans for phosphate; and, as its growth is by marginal increment only, it is isotopic (but not isochronous) with a fairly constant thickness throughout a valve although varying between 2 and 8 μm in the 30 or so shells sectioned for electron microscopy. The underlying succession, which includes all other constituents of the shell, is the secondary layer.

The stratiform components of the secondary shell in the related genus *Discinisca* have also been referred to as 'layers' and in another 'chitino-phosphatic' inarticulate, *Lingula*, as 'layers' made up of 'zones' (Iwata 1982). In this paper they will be referred to as 'laminae' with the implication that they are structurally homogeneous and normally bounded by isochronous interfaces. As already noted, laminae, which had been coated with carbon to facilitate back-scattered electron scans, varied widely in composition as measured

by the proportions of their apatitic and organic constituents. The differences were correlated with structural details revealed by gold or gold–palladium coating of the same specimens. Such correlations suggested that discinid laminations are most aptly distinguished as: compact, rubbly, baculate, stratified and membranous (figure 4). These terms are textual but they also reflect a progressive compositional change from a predominantly apatitic lamina to an exclusively organic one.

The most extensive recent studies of biomineralization of the brachiopod organo-phosphatic shell, are those conducted, mainly on *Lingula*, by Japanese biologists (see Watabe 1990). They continually refer to 'mineralized' and 'organic' layers of the inarticulate shell. For the most part, it seems that a mineralized layer is equivalent to a compact lamina as here defined and the organic layer to the four other laminae.

On a nanometric scale, a distinction has been drawn (compare Carter *et al.* 1990) between spheroidal aggregates of acicular crystallites radially disposed about a common centre (spherulite) and rounded bodies, in which polygonal constituents may be concentrically, radially or even randomly packed (spherule). In using the term 'spherule' to describe a biomineral aggregate of *Discina*, prime consideration has been given to the structure and disposition of its constituents rather than its shape which can change as the spherule becomes incorporated within the growing shell. An attempt has also been made (figure 5) to categorize the nature of aggregate components by distinguishing between a 'mosaic' biomineral and its constituent 'composite crystallites' (Williams 1984, p. 412).

The shell of *Discina*, as of other living organo-phosphatic brachiopods, is perforated by an orthogonal system of fine canals (figures 21, 24 and 25), between 300 to 500 nm in diameter, which occur at intervals of about 1 μm, usually in groups delineated by the intercellular boundaries of outer epithelium. These canals are frequently described as 'punctae' (Iwata 1981; Pan & Watabe 1988), a term used for perforations of the brachiopod carbonate shell. True punctae, however, accommodate papillose extensions of outer epithelium and may exceed 20 μm in diameter (Owen & Williams 1969). In contrast, perforations of the organo-phosphatic shell are, at most, membrane-lined and seldom have an organic core. They will be referred to as 'canals' or the 'vertical canal system' when it becomes necessary to distinguish them from anastomosing tunnels sometimes with comparable diameters, which are also found in the shell.

4. RESULTS

(*a*) *Basic components of Discina shell*

The structure of the *Discina* shell, like that of the closely related *Discinisca* (Jope 1965, p. H158; Iwata 1982, p. 960) is determined by four principal components: apatite, chitin, an acidic protein and the amino acid, hydroxyproline. Their structural relationships have been established by comparative electron microscopy studies; and their compositions by EDX and BSE

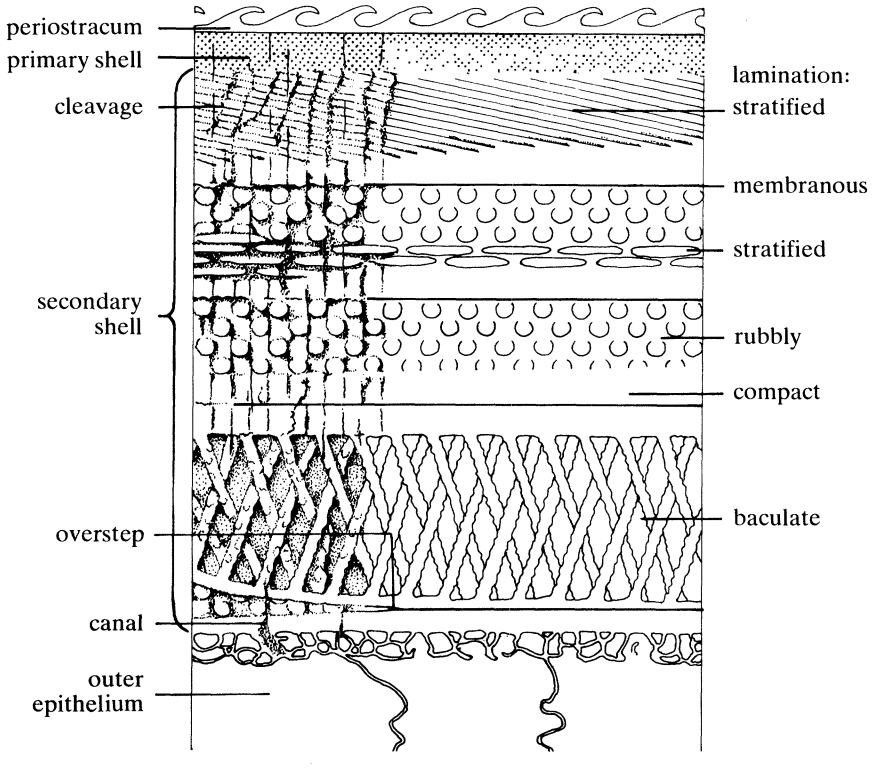

Figure 4. Diagrammatic representation of the main constituents of the integument secreted by the outer epithelium of *Discina*; the left side of the diagram is a stylized version of the various components as they appear on a cleaved surface of a dried dorsal valve.

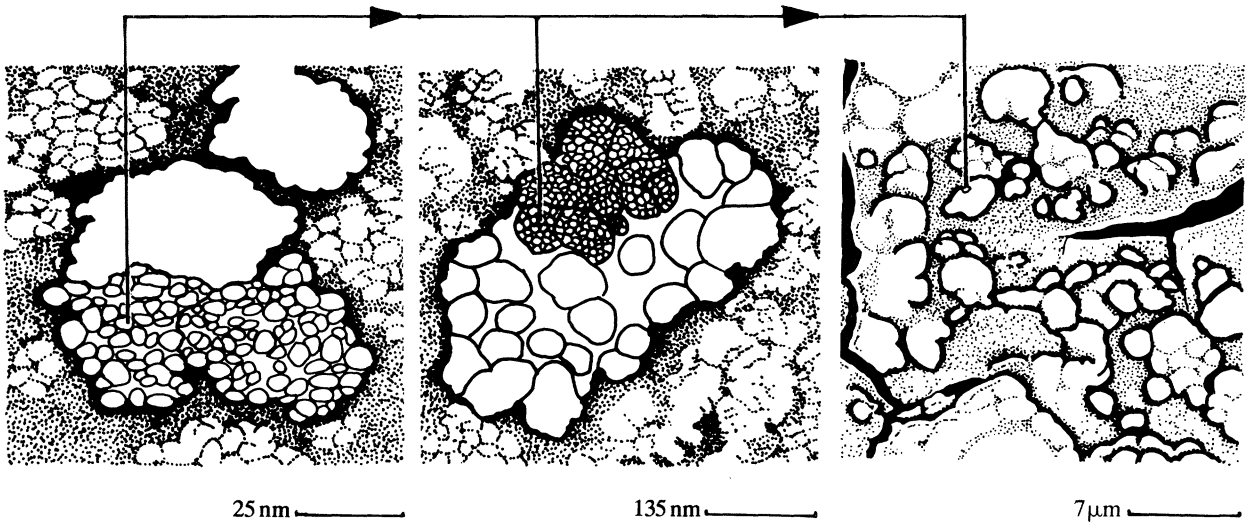

Figure 5. Diagrammatic representation of various apatitic structures to illustrate the aggregation of granules (left) into spherules of composite granules (centre) and of mosaics of spherules (centre) into spheroidal and hemispherical masses (right).

scans, differential enzymic digestion and various staining techniques. All four constituents are present throughout the secondary shell in varying proportions which determine the nature of lamination. Their inferred distribution will, therefore, be described before dealing with variations in the shell succession as a whole.

(i) *Apatitic aggregates*

The basic apatitic unit and its naturally occurring aggregates are most clearly seen on surfaces and in sections subjected to bleaching, proteolysis and chitinase digestion. At resolutions down to 1 nm, the unit is a subrounded crystallite or granule (figures 6 and 7), ranging in diameter from under 4 to about 8 nm (compare the granular crystallite in *Discinisca* as described by Iwata (1982, p. 966)). Variations in shape reflect the nature of granular packing. Stripped of organic covers, the granules are normally discrete, closely stacked units in overlapping arrays. Small groups can, however, be contiguous with one another along flat surfaces with a prevalence of triple or quadruple junctions (figure 6).

At resolutions between 10 and 20 nm, granules can form relatively smooth surfaces over several square micrometres, sporadically studded with low domes up to 100 nm in diameter. Usually, however, they aggregate into either flattened jigsaw pieces (figure 8), normally about 500 nm across or spherular composite masses between 100 and 200 nm in diameter which, when compacted, may also interlock like jigsaws. These spherules, which must also be organically coated, may themselves cluster into ovoidal or spheroidal mosaics up to 1 μm in size (figure 9). The spherular constituents of the mosaics are normally discrete but, as with their own constituent granules, they may cluster into contiguous groups sharing flattened or interlocking boundaries. This pattern of recurrent aggregation is illustrated in figure 5.

(ii) *Distribution of organic components*

The pervasion and durability of the organic constituents of the *Discina* shell, which account for 25% of the exoskeletal dry weight of the related genus *Discinisca* (Jope 1965, p. H158), can be shown by comparing the microtextures of sections of dried valves. Backscattered electron scans may show an overwhelming dominance of calcium phosphate within untreated successions. Yet membranous laminae occur throughout the shell and organic tissue can so shroud other laminae as to obscure the spherular texture of their biomineral components. This fine texture can usually be seen on untreated fracture surfaces and on internal surfaces stripped of epithelium (figure 10), but not in untreated polished sections where resin has impregnated the organic constituents of the shell.

The chemical and enzymic treatment of fracture surfaces and resin-mounted sections has helped to determine the distribution of the principal, extracrystalline, organic components of the *Discina* shell not only in relation to apatitic granules and their aggregates but also throughout laminar successions. It therefore seems appropriate at this juncture to describe the distribution, suggested by the present study, at all structural levels within the shell.

Bleaching a surface or section with sodium hypochlorite degraded most of its organic constituents irrespective of their composition and revealed that they coated granules and spherules and formed a pervasive matrix in all apatitic laminae. Even so, layers of spherules as thin as 400 nm, frequently retained some flexibility after treatment, indicating the persistence of some organic residue (figures 11 and 12).

In contrast, enzymes differentially digested the various organic components although with varying efficacy. The proteinases, papain, trypsin and subtilisin, removed some of the coating of spherules which were consequently more clearly seen under the SEM than were those in untreated or buffered specimens; while even the most specific of the enzymes used, trypsin, degraded granular coats. However, proteolysis of the organic framework of the shell was differential. Judging from the textures of exposed interfaces

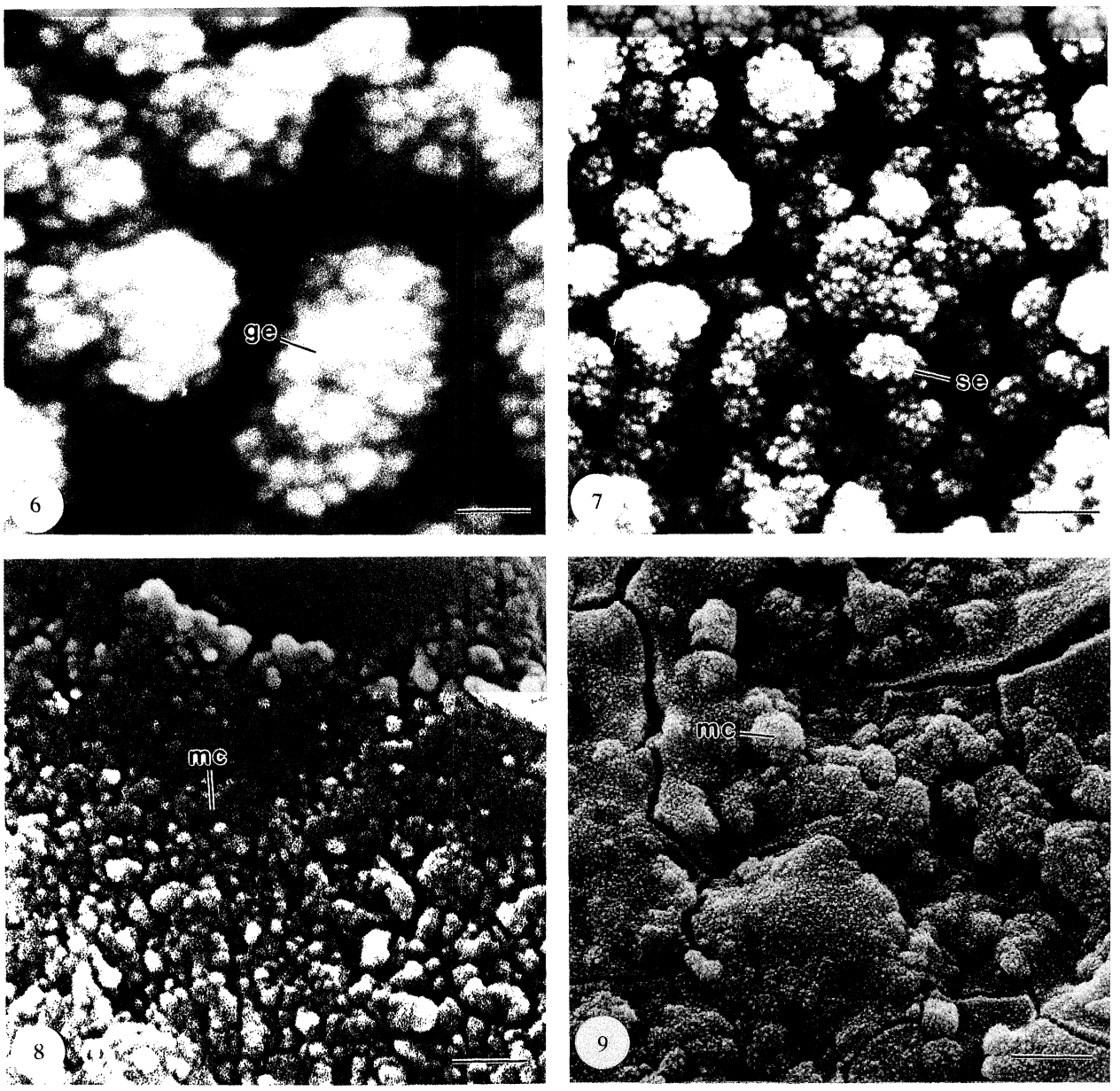

Figure 6–9. Scanning electron micrographs of dried dorsal valves of *Discina striata*.

Figure 6. Vertical fracture surface digested in chitinase (2 mM in phosphate buffer) and coated with gold–palladium to show the granular nature (ge) of apatitic spherules. Scale bar = 15 nm.

Figure 7. Vertical fracture surface digested in trypsin (1 mM in phosphate buffer) and coated with gold-palladium to show the aggregation of spherules (se) into mosaics. Scale bar = 40 mm.

Figure 8. Bleached, internal surface coated with carbon then gold to show the flattened aspect of apatitic mosaics (mc). Scale bar = 500 nm.

Figure 9. Bleached, internal surface coated with carbon then gold to show the spheroidal aspect of aggregations of apatitic mosaics (mc). Scale bar = 4 μm.

within shell successions, organic laminae tended to survive papain cleavage but were removed by trypsin and especially subtilisin, as were most interstratal membranes in both rubbly and stratified laminae. The organic content of the baculate laminae proved to be even more complex (figures 13 and 14). When treated with papain and lower (200 μM) concentrations of trypsin, the apatitic rods remained shrouded and separated from one another by membranous drapes as was also so in bleached sections (figure 13), although depressions, up to 4 μm across, developed during digestion by trypsin. Digestion by subtilisin, however, clearly exposed all baculae at the surface of a section and further degraded the proteinaceous matrix (figure 14).

Papain, trypsin and subtilisin (figures 36 and 37) removed the contents of canals and, in one fracture section, papain additionally degraded membranes forming outer coats to canal walls of spherular apatite between 150 and 200 nm thick (figure 39). Subtilisin and collagenase stripped the vertical canal system and anastomosing tunnels within the shell of their membranous linings (figure 36). Collagenase was used in an attempt to trace the distribution of the amino acid,

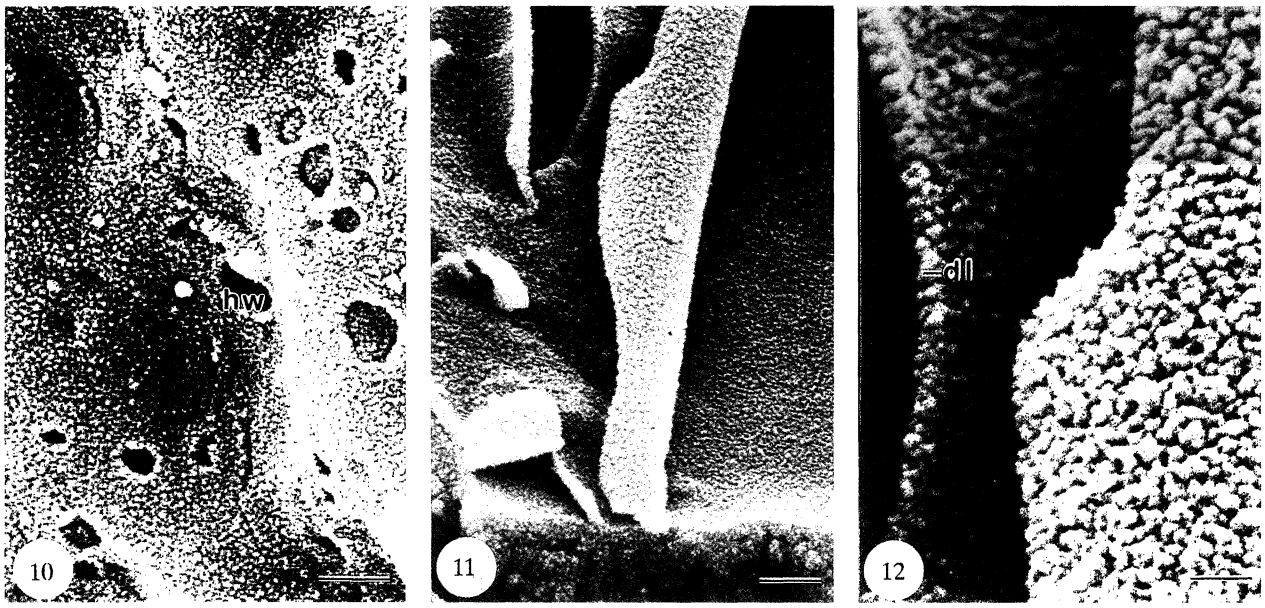

Figures 10–12. Scanning electron micrographs of dried dorsal valves of *Discina striata*.

Figure 10. Untreated, internal surface coated with carbon then gold to show the differential aggregation of spherules in the most recently secreted member of a stratified lamina; the subcircular hollows (hw) are assumed to represent the sites of flattened exocytosed vesicles. Scale bar = 2.5 μm.

Figure 11. Bleached, internal surface coated with carbon then gold to show the flexible nature of the most recent member of a stratified lamina. Scale bar = 2 μm.

Figure 12. Detail of the superficial coat featured in figure 11 to show that the biomineral components of the coat are apatitic spherules usually arranged in a double layer (dl). Scale bar = 500 nm.

hydroxyproline, within the shell as hydroxyproline and hydroxylysine are present in very few proteins other than the fibrous protein, collagen. Collagenase digestion of canal linings contrasts with its ineffectual degradation of other structures although it did accentuate the laminar succession of the shell.

Chitinase digestion, at both 1 and 2 nM concentrations, had a different effect on shell fabric. After

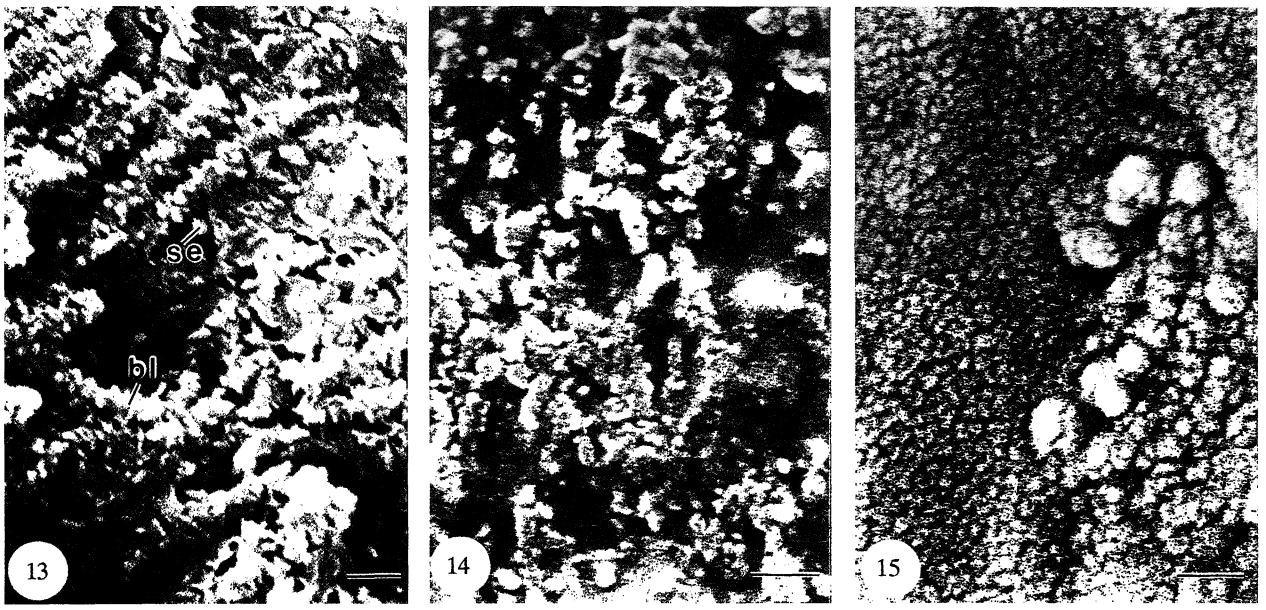

Figures 13–15. Scanning electron micrographs of dried dorsal valves of *Discina striata*.

Figure 13. Bleached, vertical fracture surface coated with gold to reveal rods or baculae (bl) of spherular apatite aligned within an organic matrix which also contains scattered aggregates of spherules (se). Scale bar = 500 nm.

Figure 14. Resin-mounted section digested by subtilisin (2 mM) and chitinase (0.2 mM) in phosphate buffer and coated with carbon then gold to reveal the disposition of rods (baculae) and isolated spherules of apatite relative to the plane of the section. Scale bar = 500 nm.

Figure 15. Vertical fracture surface digested by chitinase (1 mM in phosphate buffer) and coated with carbon then gold to reveal the reticulate network of grooves outlining spherules of apatite. Scale bar = 200 nm.

treatment, all apatitic laminae were veined with a fine network of grooves which occasionally ran in continuous curves for over 1 μm but usually formed a close, angular mesh with numerous triple junctions, discontinuities and discrete perforations all on a nanometric scale (figure 15). This reticulate pattern was etched with equal clarity on all biomineral surfaces and delineated their spherular constituents. Indeed, chitinase also degraded granular coats (figure 6) and was as effective as subtilisin in exposing baculae and even more so in removing some interstratal membranes (figure 20). However, there was no evidence of it having digested canal linings.

In summary, it appears that the organic coats and matrix of the apatitic constituents of the *Discina* shell are chitino-proteinaceous. The chitin and protein of these coats may occur as ordered sheets. Chitin and protein can also occur separately as interstratal membranes but chitin does not contribute to the linings of canals which may contain collagen.

(*b*) *Lamination of the Discina shell*

In the context of this paper, membranous laminae need no more than a passing reference although, in the secretion of the *Discina* shell, they play a key role as substrates for succeeding apatitic laminae (see figure 17). They are seldom more than a micron thick and are normally featureless except for canals and sporadically occurring patches of shallow depressions arranged like negative bubble rafts, which may be casts of exocytosed vesicles. The other kinds of laminae are variably phosphatic, although they are readily distinguishable from one another especially in strip sections orthogonal to the shell exterior. When traced laterally, phosphatic laminae almost invariably lose their distinctiveness by grading into one another or are frequently overstepped by succeeding laminae (figures 1, 2 and 4).

(i) *Compact laminae*

Under the SEM, compact laminae are the most distinctive feature of the *Discina* shell for their seeming homogeneity makes them easy marker horizons to follow within laminar successions (figure 16). Individual laminae are typically between 6–7 μm thick but can thin out laterally within 200 μm or become part of a continuous compact succession up to 100 μm thick.

The general absence of such widespread microstructural features as vertical jointing seems to be linked to the compaction of apatite, the dominant constituent. In polished sections of an adult dorsal valve, digested by both chitinase and subtilisin at optimal concentrations, apatite occupied 88%, 38% and 35% of 4 μm^2 of surface areas of compact, stratified and baculate laminae respectively. The effects of compaction is best seen on smoother patches of fracture (figure 17) and natural surfaces where aggregations of spherules tend to be closely packed into three dimensional jigsaws with pieces, between 100 and 200 nm across, varying in shape from spheroids and polygons to twisted cylindroids, all delineated in bleached and digested surfaces by grooves up to 25 nm wide. More usually, however, the spherules themselves aggregate into mosaics, especially sporadically distributed spheroids, which can be found in various stages of development up to 3 μm in size on internal surfaces (compare figure 9).

Spherules forming the walls of canals are not differentiated except in being so arranged as to form

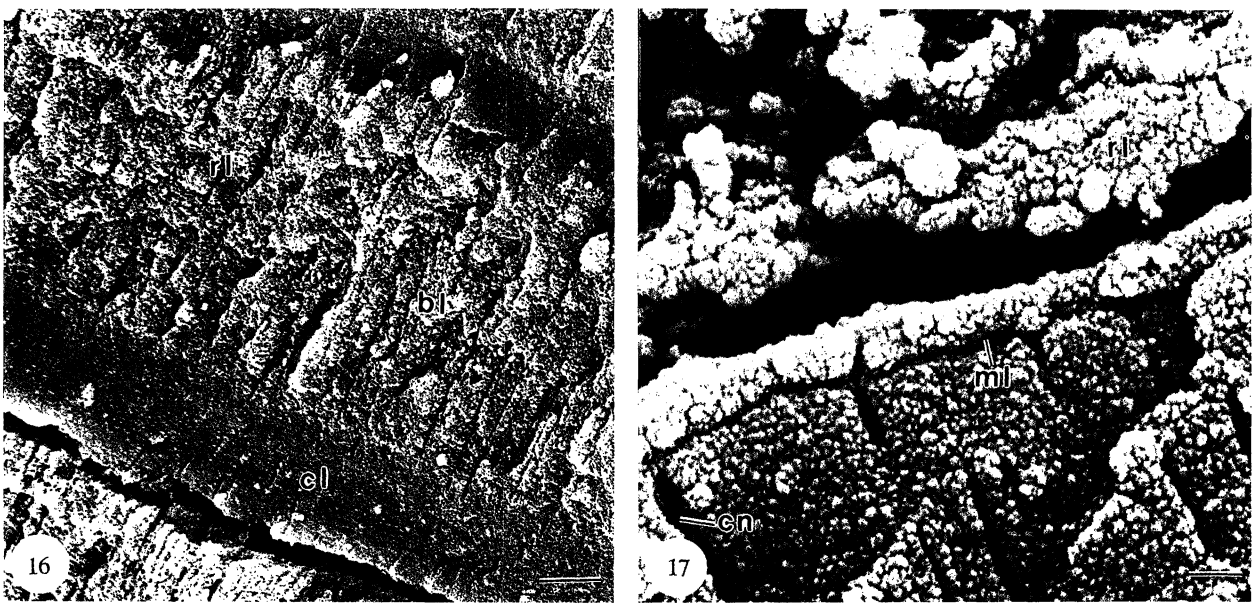

Figure 16–17. Scanning electron micrographs of a dried dorsal valve of *Discina striata*.

Figure 16. Bleached, vertical fracture surface coated with carbon then gold to reveal compact laminae (cl) separated by rubbly (rl) and baculate successions (bl). Scale bar = 5 μm.

Figure 17. Untreated, vertical fracture surface coated with carbon then gold to reveal the junction (presumably the former site of a membrane (ml)) between a graded compact lamina with canals (cn) and a rubbly lamina (rl) with conspicuous spheroidal aggregates of spherular mosaics. Scale bar = 1 μm.

smooth interfaces with the organic linings of the canals. Spherules at the boundaries of compact laminae are similarly undifferentiated although their distribution is affected by the amount of organic material present. Thus, the outer laminar boundary is sharp when shared with a membrane which contains no apatite; while the inner interface is marked only by a more gradual increase in organic content, representing the onset of the succeeding rubbly, stratified or baculate lamina (figure 17).

(ii) *Rubbly laminae*

Rubbly horizons of apatite usually mark a transition between other phosphatic laminae especially the compact and baculate types (figures 16 and 18). As such, this kind of lamination, which is jointed and

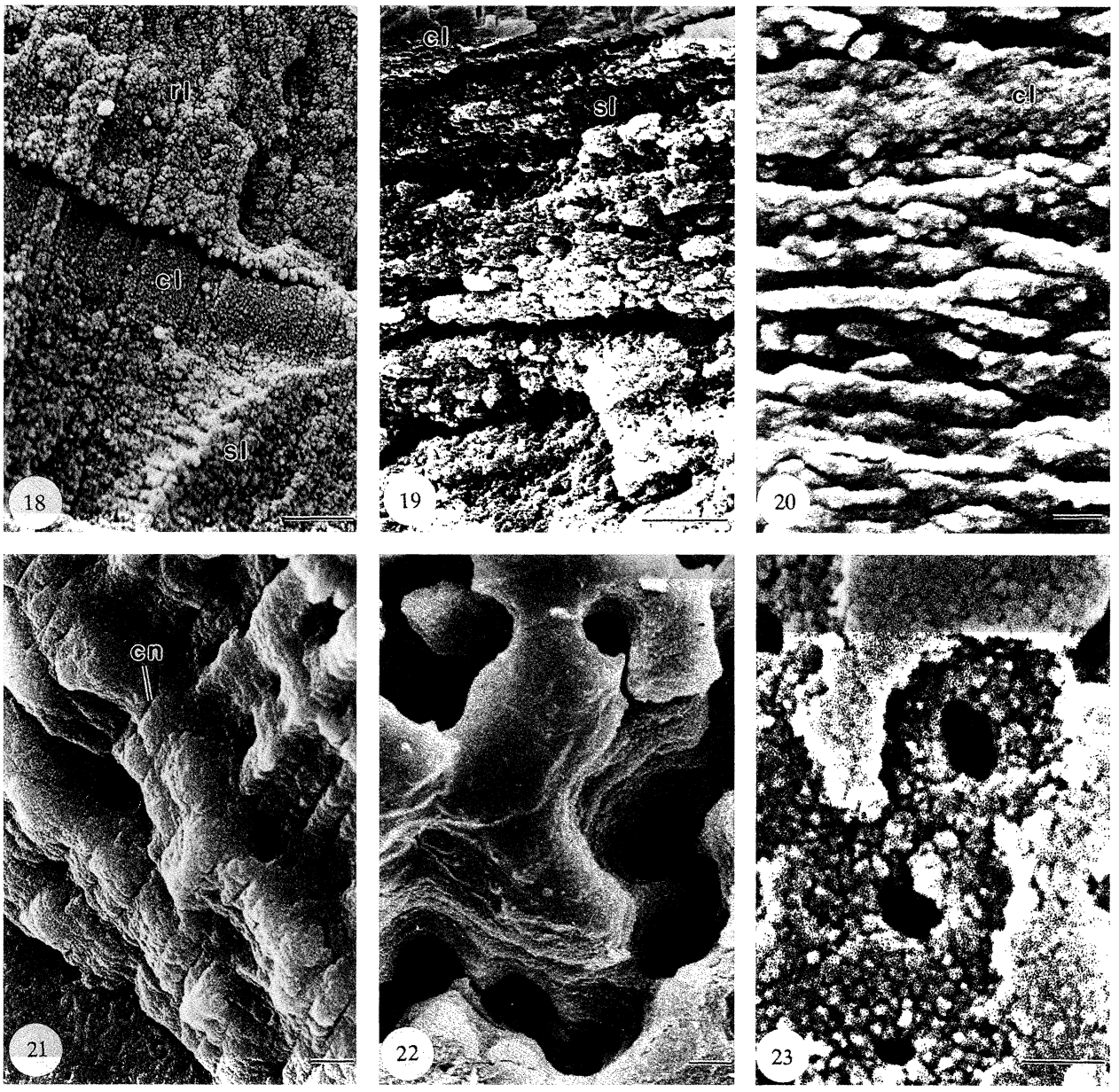

Figures 18–23. Scanning electron micrographs of dried dorsal valves of *Discina striata*.

Figure 18. Bleached, vertical fracture surface coated with carbon then gold to reveal rubbly (rl) and stratified (sl) and rubbly laminae separated by a compact lamina (cl). Scale bar = 5 μm.

Figure 19. Vertical fracture surface digested by trypsin (0.2 mM in phosphate buffer) and coated with carbon then gold to reveal a stratified lamina (sl) underlying a compact one (cl). Scale bar = 5 μm.

Figure 20. Vertical fracture surface digested by chitinase (0.2 mM in MES buffer) and coated with carbon then gold to reveal stratified laminae with an intercalated compact lamina (cl). Scale bar = 500 nm.

Figure 21. Oblique internal view of the margin of a bleached valve coated with carbon then gold to show the disposition of finely stratified laminae pervaded by fine canals (cn). Scale bar = 2 μm.

Figure 22. Internal view of the labyrinthine canal system pervading stratified laminae at the margin of a bleached valve, coated with carbon then gold. Scale bar = 2 μm.

Figure 23. Internal surface of a stratified lamina at the margin of a bleached valve coated with carbon then gold to show the flattened sub-ovoid mosaics making up individual strata. Scale bar = 500 nm.

seamed with canals, is intermediate in apatitic content (46% of a bleached fracture surface, 5.7 μm^2 in area) and can vary greatly in thickness, exceptionally forming multiple laminar lenses up to 50 μm thick.

Rubbly laminae are essentially poorly bedded successions of apatitic nodules and lenses, up to 1 μm thick but more commonly ranging between 200 and 500 nm and spreading laterally for about 2–3 μm. The nodules and lenses are horizontal rafts of spherules between membranes but interconnected with one another by shafts of spherular apatite piercing the organic envelopes (figures 36–38).

(iii) *Stratified laminae*

These laminae, stratified into fine, platy alternations of organic- and apatitic-rich compounds, immediately succeed the primary layer of the *Discina* shell (figures 21 and 22). Indeed, the appearance of these laminae in radial sections of mature valves, as *en echelon* successions of marginal wedges, confirms that they are secreted as an advancing circumferential belt immediately behind the expanding margin of primary shell. The wedges thin out medially into compact lamination, extensions of which periodically reach the shell margin and thereby break the stratified belts into discrete laminae. Stratified laminae of this kind are normally gently flexured inwardly or outwardly in phase with the disposition of the external, concentric growth lamellae of the valve and are succeeded unconformably by other kinds of laminae forming the inner, mature shell (figure 2).

A rougher stratification is also found in the more mature parts of the shell succession and commonly marks the transition between rubbly and compact laminae (figures 19 and 20).

The apatitic strata of marginal laminae are composed of spherules, about 60 nm in size, which normally cluster into flattened sub-ovoid mosaics about 900 nm in maximum diameter (figure 23). These successions are permeated by canals with walls which tend to be conspicuous on fracture surfaces as hollow columns extending through 20 or more consecutive strata (figure 21). Towards the edge of a valve, the inner part of a marginal stratified lamina is pierced by closely distributed holes and consequently has a labyrinthine topography (figure 22). Some of these holes, with diameters 200 and 300 nm, are identical with canals pervading the entire *Discina* secondary shell. There are, however, significantly larger ones with diameters up to 2.7 μm. Some of these are formed by the convergence of canals; others penetrate to the primary layer and may contain a rod(s) of stratified apatite.

(iv) *Baculate laminae*

Baculate lamination has been so named (Holmer 1989, p. 31) for successions within organo-phosphatic shells, which consist of apatitic rods crossing one another at angles of about 60° to the vertical axis. The term can be used in describing similar structures in the *Discina* although their configuration is more complex and more variable than is presently conceded.

Baculate laminae are restricted to the more mature part of the shell and are usually asymmetrically lenticular in shape (figure 2) with maximum thicknesses of 100 μm or more in areas undergoing accelerations in shell deposition as in the development of a median septum or an elevated muscle scar. They are instantly recognizable under the SEM for, in addition to being canalicular and jointed (figure 25), fracture surfaces are indented by subcircular to polygonal depressions, up to 7 μm wide, the lineaments of which are determined by jointing and widely spaced irregular bedding, typically less than 1 μm thick. In BSE scans, the apatitic components of baculate laminae look like scaffolding with vertical or criss-cross struts at several levels between horizontal platform-like beds (figure 24).

All biomineral components are composed of subrounded granules of apatite, within the 4–8 nm range, aggregated into blades, platelets and spherules (figures 29). The rods, averaging 200–300 nmin diameter, are usually made up of blades studded with spherules (figure 29) but they may also be composed of strings of spherules and platelets with no apparent core (figures 27 and 28). Isolated, needle-like crystallites, about 300 × 100 nm in size, may also sporadically occur in the organic matrix but they are actually linear sets of three or four spherules (figure 13).

The disposition of the rods, as seen in sections freed of organic matrix, may be complicated by the collapse of some rods with the removal of membranous support (figure 27). Backscattered electron micrographs, however, reveal undisturbed patterns. Arrays of vertical rods, occasionally gently flexured by stress couples during growth, are common. The criss-cross arrangements of rods are also common; but these are frequently surface views of a three-dimensional hexagonal network of struts composed of spherules and up to 350 nm wide (figure 26). This network is rarely preserved *in situ* in sections which have undergone bleaching or enzymic digestion. However, their presence within the organic matrix of baculate laminae is frequently signalled by the occurrence of regularly arranged depressions up to 600 nm across, which correspond to the openings within hexagonal networks (compare figures 24 and 25).

(*c*) *Vesicular inclusions within the Discina shell*

Two of the many polished sections of *Discina* valves, which had been differentially etched, contained subspherical bodies with characteristics of exocytosed vesicles. One section was bleached (for 24 h in sodium hypochlorite at 10% by volume); the other proteolysed in subtilisin (300 μM in phosphate buffer). The fact that such unambiguous traces of inclusions have not been found in other, similarly treated sections suggests that their incorporation into cell successions was an abnormal event although other discrete bodies, which could have developed in much the same way, have also been revealed by the removal of the organic components of the shell.

In the bleached section of an adult dorsal valve, inclusions were readily found throughout the shell, except for the primary layer and the underlying

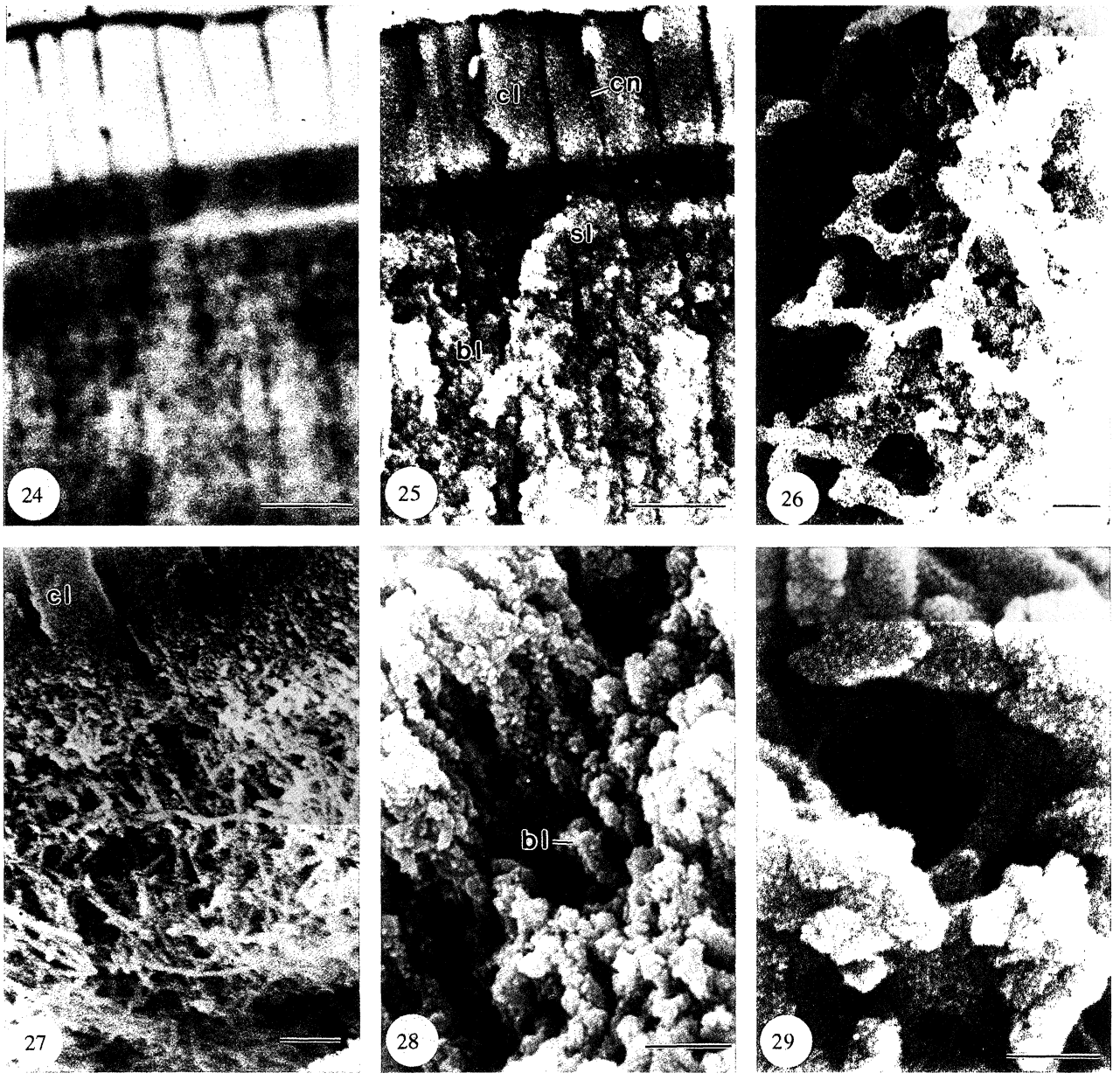

Figures 24–29. Electron micrographs of dried dorsal valves of *Discina striata*.

Figure 24 and 25. Backscattered and scanning electron micrographs of the same part of an untreated, vertical fracture surface coated with carbon and showing the predominant distributions of apatitic and organic components (white and darker shades respectively in figure 24) within baculate (bl), stratified (sl) and compact laminae (cl) pervaded by canals (cn) as identified in figure 25. Scale bar = 5 μm.

Figure 26. Bleached, resin-mounted section coated with carbon then gold to show the hexagonally arranged spherular struts within a tension crack at the interface of a baculate lamina. Scale bar = 500 nm.

Figure 27. Bleached transverse fracture surface of a dorsal septum coated with gold to show the disposition of baculae relative to a compact lamina (cl). Scale bar = 1 μm.

Figure 28. Oblique fracture surface of a dorsal valve digested by trypsin (0.8 mM in phosphate buffer and coated with gold-palladium to show the disposition of an array of baculae (bl) composed of apatitic spherules. Scale bar = 1 μm.

Figure 29. Oblique fracture surface digested by trypsin (0.8 mM in phosphate buffer) and coated with gold-palladium to show the granular structure of spherules and blades forming the baculae around a subcylindrical depression. Scale bar = 100 nm.

succession of stratified laminae, although they were most densely distributed in the rubbly zones (figure 30) between compact or baculate laminae. At low magnifications, their presence is signalled by the finely speckled appearance of those parts of the laminae containing them. This is caused by variably distributed electron-light particles which are typically between 200 and 500 nm in size (figures 31 and 32). At first sight the particles appear to be islands of high relief within an electron-dense labyrinth of deep grooves; but, in fact, they are connected by isthmuses to a lower-lying, medium electron-dense matrix which

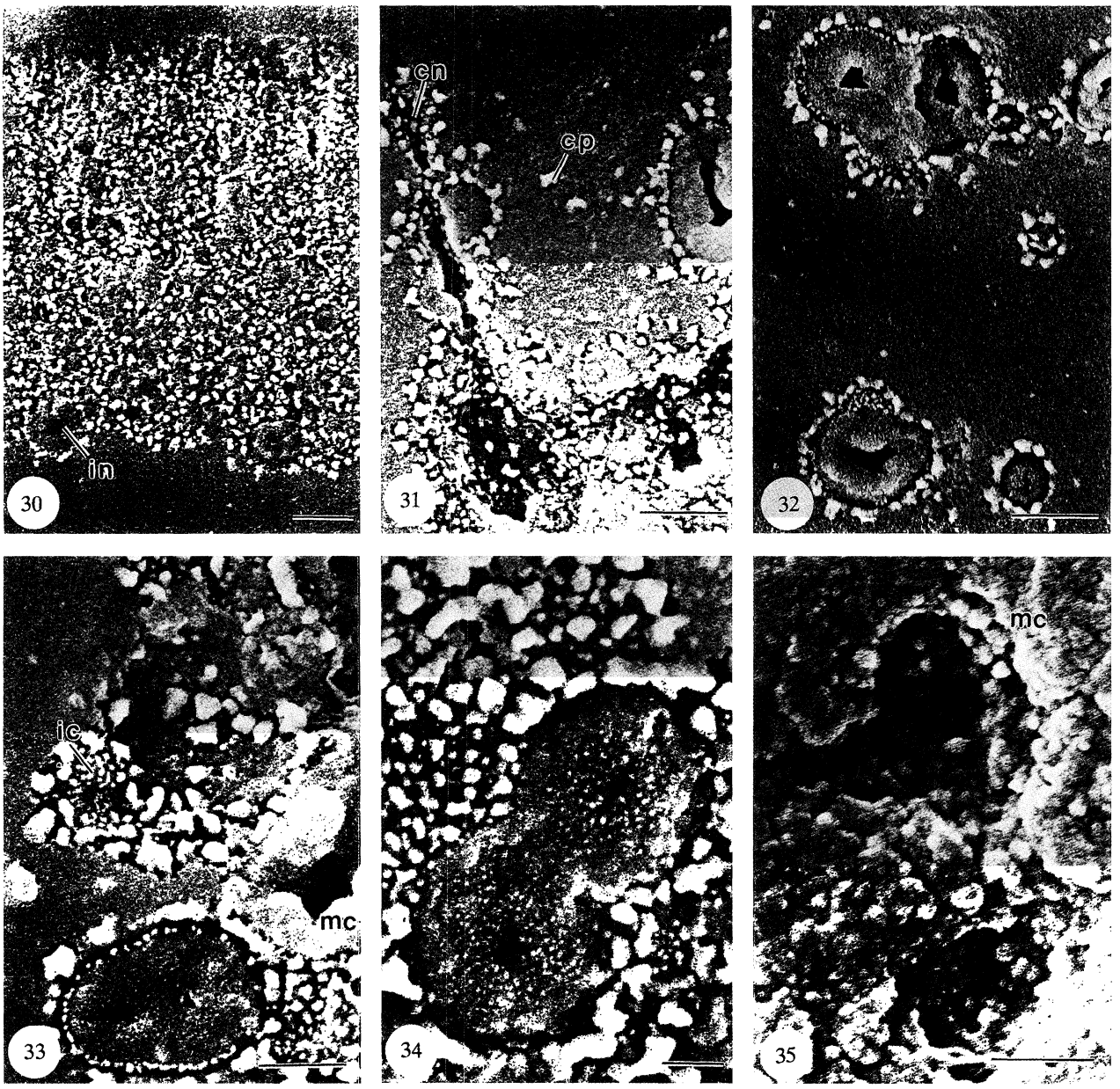

Figures 30–35. Scanning electron micrographs of resin-mounted sections of a dried dorsal valve of *Discina striata* coated with carbon then gold.

Figure 30. Bleached section showing the dense distribution of inclusions (in) and electron-light particles in a rubbly lamina bounded by two compact ones. Scale bar = 2 μm.

Figure 31. Bleached section showing the distribution of inclusions and electron-light particles (cp) in an incipient rubbly lamina and along a canal (cn) traversing a compact lamina. Scale bar = 2 μm.

Figure 32. Bleached section showing the sporadic occurrence of inclusions and associated electron-light particles in a compact lamina. Scale bar = 2 μm.

Figure 33. Bleached section showing an inclusion in the equatorial plane (below), a botryoidal group of spheroidal mosaics (mc) of a larger inclusion (right) and the hollow remaining after the removal of an inclusion with a lining of electron-light particles and part of the inner coat (ic) of electron-light spherules (above). Scale bar = 1 μm.

Figure 34. Bleached section showing the details of two conjoined inclusions, more or less in the equatorial plane. Scale bar = 250 nm.

Figure 35. Complementary section of the same dorsal valve as in figures 30–34 digested in subtilisin (2 mM in phosphate buffer) to reveal hollows lined with particles of spherular mosaics (mc) and assumed to have contained inclusions in the same way as the hollow shown in figure 33. Scale bar = 1 μm.

ramifies in patches throughout the speckled zones (figures 33 and 34). The entire fabric is so unusual as to suggest that it is an artefact of section preparation. However, high resolution examination and EDX analysis of the matrix and particles confirm that both are composed of spherules of apatite, between 30 and 50 nm in size, and that their structural relationships have not been significantly affected by a pervading film of resin no more than 10 nm thick. The electron-light particles vary greatly in shape from reticulate to labyrinthine structures up to 1.5 μm long. In general, however, they tend to be subrounded to subangular in

shape especially those coating inclusions and canals; 30 such particles, at the interfaces with a canal and an inclusion, average 306 nm in maximum width (range 148–593 nm).

The simplest kind of inclusion is a spheroid with an average diameter of 1.05 μm (range 0.65–1.8 μm in 15 measurements), excluding the circumferential coat of particles just described (figure 32). They can be relatively densely distributed with 31, for example, occurring in 100 μm^2 of a compact lamina. The boundaries of such patches are so sharply defined, that horizontally aligned spheroids, with their coats of electron-light particles, may intrude into the finely textured matrix of the succeeding lamina (figure 30). Variations in the shape of the inclusions, which are seldom deformed along axes of compression, appear to be related to the host lamina. Those occurring in compact laminae are typically spheroidal, but two or three may amalgamate into dumbbell-shaped (figures 32 and 34) or trilobed bodies. In rubbly and baculate laminae, on the other hand, clusters of spheroidal inclusions may aggregate into botryoidal structures (figure 33) with long axes parallel with the laminar boundaries and subsidiary outgrowths developing around canals (figure 31). Indeed, spheroids, flattened at the surfaces of attachment or even reduced to dome-like structures, can be found draped along the sides of canals, which also directly supported adherent electron-light apatitic particles.

Irrespective of shape, radial successions to the centres of inclusions are almost invariably the same. The outermost coat of electron-light particles is more or less separated from the contents of the inclusion by a deep groove up to 150 nm wide. The inner boundary of that groove is marked by regularly arranged, electron-light spherules about 50–100 nm in diameter (figure 33). These form the outer coat to a medium electron-dense mass, speckled with electron-light spherules, up to 70 nm across, with a central cavity varying from a curved slit (figure 31) to a hole (figure 32), no more than 250 nm across, constricted by curved sides. This mass is further seen to consist of merged spheroidal mosaics, the inner curved surfaces of which define the central cavity (figure 33), whether it be a slit or a hole.

This succession determines the appearance of tangential sections of the spheroidal inclusions. Thus, some small, circular, convex, medium electron-dense patches are ornamented by well-ordered, electron-light spherules and are sections revealing the inner biomineral coat of deeply embedded inclusions. Shallow, concave depressions, similarly ornamented, represent the same coat of inclusions which were removed when the section was cut or later bleached. Such patches are usually surrounded by a broad, circular zone of the coarser outer apatitic coat and, more rarely, the latter alone survives in the plane of the section as the final trace of an inclusion that has all but been removed (figure 33).

The inclusions, found in the section of an immature ventral valve digested by subtilisin, occur as moulds which have been stripped of organic contents as, indeed, have their host laminae as a whole. They were developed throughout the secondary shell but are especially prevalent in rubbly and stratified laminae. In such laminae, the apatitic spherules are arranged more or less linearly in a series of string-like, interconnected arcs and loops to form a three-dimensional mesh. Within this biomineral framework, the most conspicuous set of ramifying spaces consist of regular tunnels (figures 36 and 37) with an average diameter of 420 nm (range 290–590 nm for 20 measurements). They occur as holes or, superficially, as elliptical furrows or strips with rounded ends, up to 3 μm long (figure 36) which appear to be disposed mainly subparallel with, or oblique to, the plane of lamination. They are evidently transverse, oblique or sagittal sections of membrane-lined canals or cylindroid strands of tissue, which were strongly curved and occasionally branched.

The moulds of the inclusions are variably distributed (figure 36) but can occur in swarms (178 were counted in a surface area of 2500 μm^2) and tend to be concentrated in bands up to 50 μm thick more or less parallel with laminar boundaries. They are also variable in size, ranging in diameter from 450 nm to 8.5 μm in the case of a few exceptionally large bodies which may be amalgamations of smaller ones. The average diameter of 20 inclusions featured in one micrograph was 1.1 μm. The moulds vary from hemispherical bowls to flat-bottomed subcircular depressions (figures 37 and 38). Their sloping sides have the same smooth-surface mesh found in the moulds of the interconnected canals but the bottoms of the depressions may be more spherular than reticulate in appearance.

The inclusions revealed by papain digestion (40 μM with mercaptoethanol (50 μM)) of a fracture surface of a mature dorsal valve, are actually thickly coated segments of vertical canals. They are best developed in compact laminae although traces of them persist within rubbly horizons of the succession. In naturally occurring transverse sections on the exposed interfaces between successive laminae, the inclusions are seen as thick rings of spherular apatite bulging inwardly and separated from the laminar matrix of the same composition by moat-like grooves (figure 39). The average external and internal diameters of 20 rings were 775 and 260 nm respectively. The rings themselves are uniformly thick at about 250 nm although localized swellings, incorporating additional spherular mosaics, do occur and, exceptionally, can restrict the canal to less than 100 nm in diameter.

The rings are densely distributed with a count of 65 within an area of 100 μm^2. They normally occur singly in linear arrays although a pair may be so close together as to share an outer groove and may even join into a figure of eight (figure 39). Their complete structures, however, are shown, in oblique and vertical sections of the host laminae, to be hollow cylinders of apatite up to 1 μm in length. Indeed, a group of protruding rings along the boundary of one lamina could be matched with a set of vertical channels of the same outer diameters extending for 5 μm throughout the succeeding lamina.

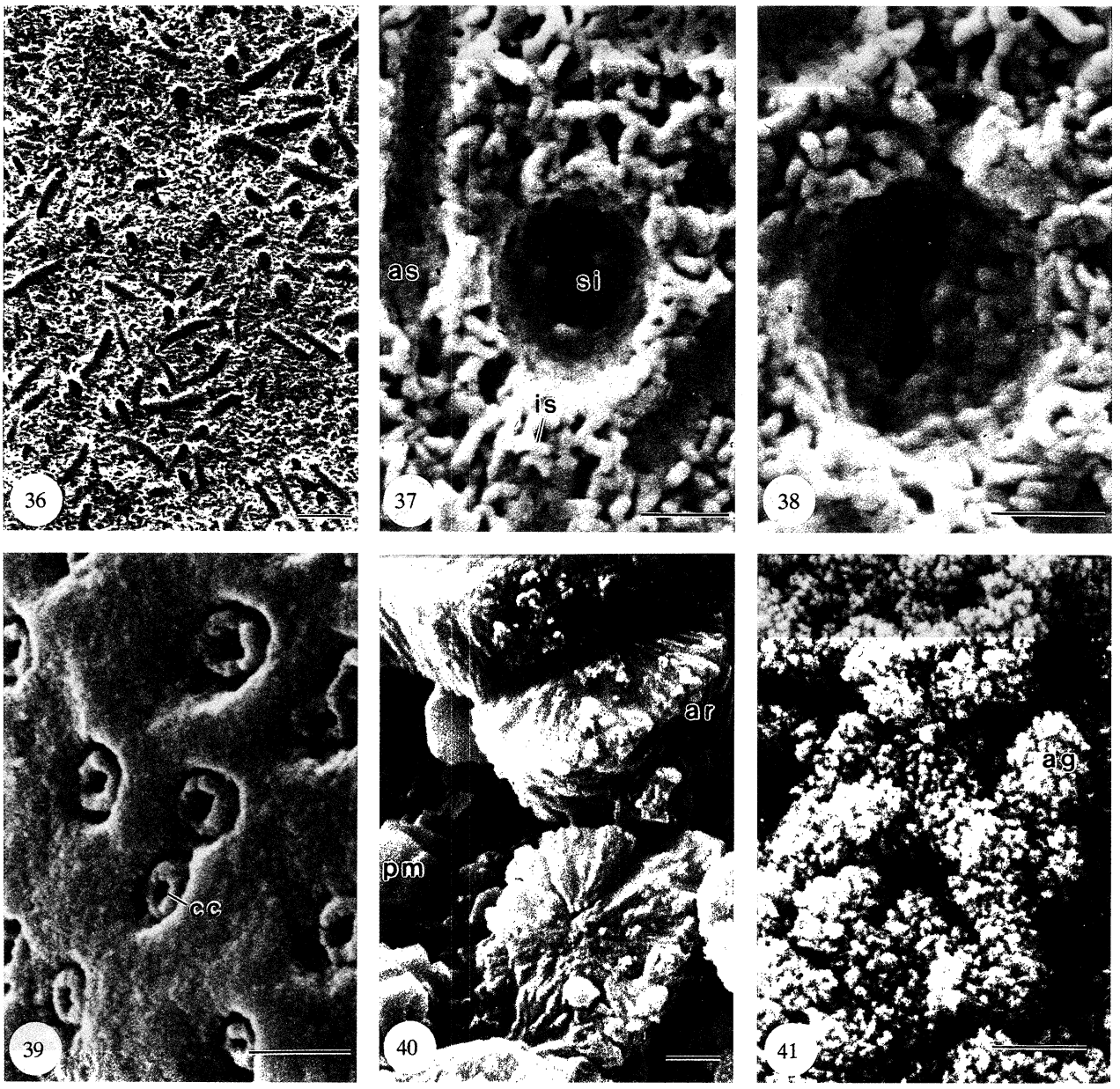

Figures 36–38. Scanning electron micrographs of a resin-mounted section of a ventral valve of *Discina striata* digested in subtilisin (2 mM in phosphate buffer) and coated in carbon then gold.

Figure 36. General view showing the distribution of hemispherical and hemicylindroid hollows in rubbly laminae. Scale bar = 2 μm.

Figure 37 and 38. Details of section showing the nature of the apatitic mesh of interconnected spherules (is) and the way it lines the hollows assumed to have accommodated anastomosing strands (as) and spheroidal inclusions (si) mainly of organic tissue. Scale bars = 500 nm.

Figures 39–41. Scanning electron micrographs of various organo-phosphatic brachiopods.

Figure 39. A vertical fracture surface of a dorsal valve of *Discina striata* digested by papain (40 μM with mercaptoethanol at 50 μM in phosphate buffer) and coated in carbon then gold to show the development of discrete coats (cc) of spherular apatite around canals on the inner surface of a compact lamina. Scale bar = 1 μm.

Figure 40. Acicular spherulites (ar) and prisms (pm) of apatite between the lamellae bounding a columnar lamina in an untreated fracture surface of *Apsotreta expansa* Palmer, Upper Cambrian Wilberns Formation, Threadgill Creek, Texas. Scale bar = 1 μm.

Figure 41. Aggregates (ag) of spheroidal apatite in an untreated, vertical fracture surface of *Dictyonina* cf. *ornatella* (Linn.), Middle Cambrian Sosiuk Formation, Turkey. Scale bar = 1 μm.

(*d*) *Outer epithelium and associated shell*

The outer epithelium (figure 42) consists of low cells standing about 4.5 μm above the basal lamina to which they are usually steeply inclined posteromedianly. The lateral cell membranes are highly interdigitated and frequently distended to delineate electron-lucent areas. The cell membranes, apical of the tight junctions, are prolonged as a series of prostrate, secretory tubes, 150 nm or so in diameter (figures 42

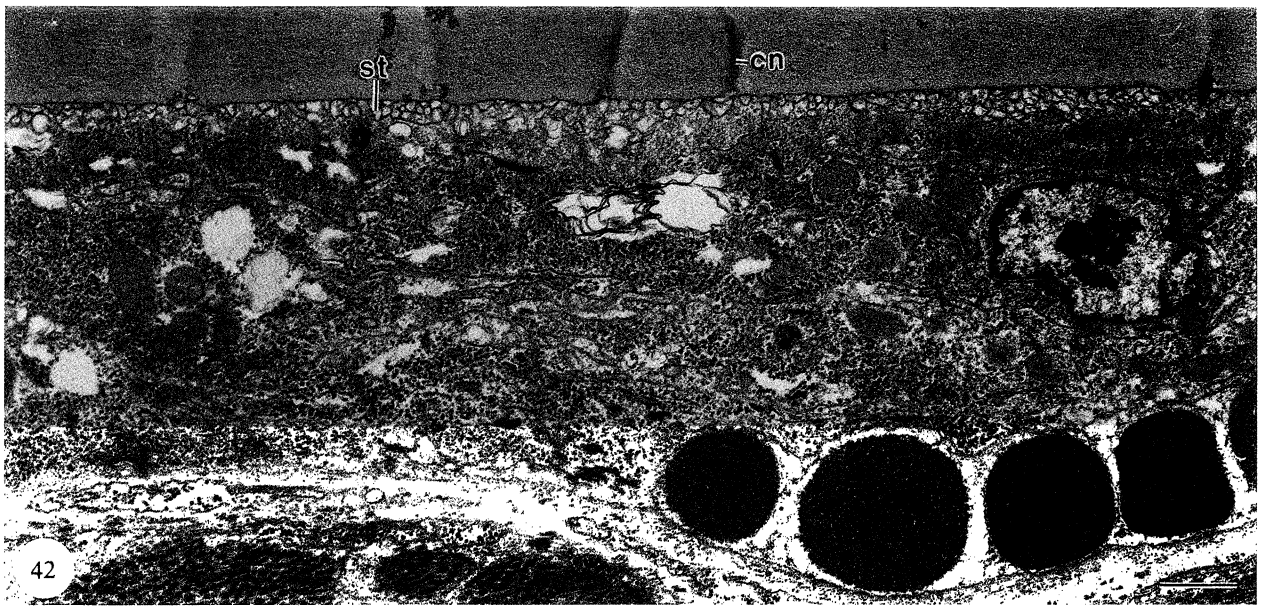

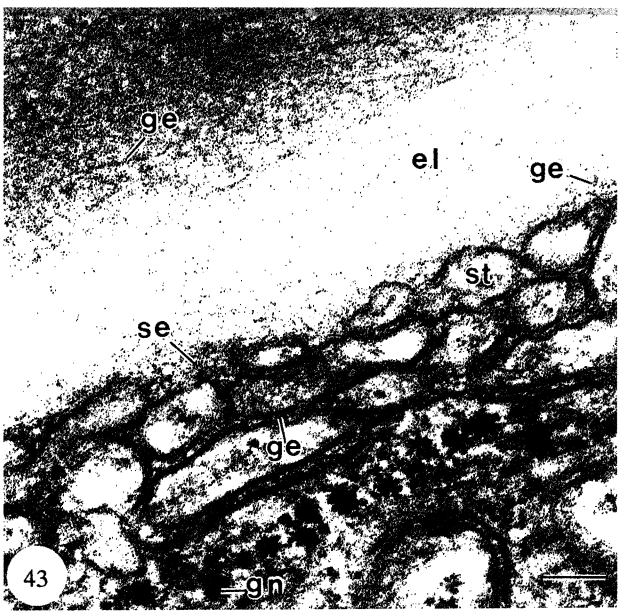

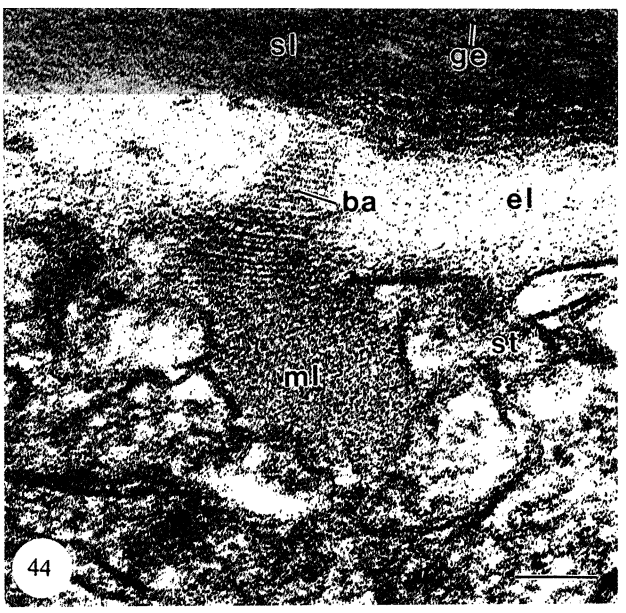

Figures 42–44. Transmission electron micrographs of decalcified sections of dorsal valves of *Discina striata*.

Figure 42. General view of outer epithelium underlying stratified laminae, showing the disposition of interdigitating secretory tubes (st) along the interface with the shell which is pierced by canals (cn). Scale bar = 1 μm.

Figure 43. Outer epithelial secretory tubes (st) underlying a compact lamina, from which they are separated by an electron-lucent zone (el) containing (along with the shell and the tubes) coats of apatitic granules (ge), some in spherular aggregates (se); glyogen (gn) is abundant in the apical part of the cell. Scale bar = 100 nm.

Figure 44. The organic contents and lining of a canal originating within the zone of interdigitating secretory tubes (st) and penetrating an electron-lucent band (el) and a stratified lamina (sl) with aligned granular coats (ge); the basal close-packed assemblage of electron-lucent and medium electron-dense particles (ml) grades apically into banded arrays (ba). Scale bar = 100 nm.

and 43). The secretory tubes of adjacent cells interdigitate with one another to form a layer up to three or four deep and up to 750 nm thick, from which are exuded most of the constituents of the overlying shell. The nucleus, about 2 μm in diameter, is basally situated; the Golgi apparatus is more apical and has dilated cisternae. Mitochondria, which are comparatively rare, are rounded and have a dense matrix and tubular cristae. Rough endoplasmic reticulum is a dominant feature of the cytosol although smooth endoplasmic reticulum has rarely been seen. Lysosomes are rare but membrane-bound vesicles, about 300 nm in diameter, are common, more so than membrane-free, electron-lucent areas of the same size. Glycogen is densely distributed especially in the basal part of the cell; membrane-coated lipids and medium electron-dense proteinaceous complexes occur sporadically usually in clusters.

The distribution of the main biomineral components in the shell and associated outer epithelium has been determined in both decalcified and untreated sections prepared for the TEM. In untreated succes-

sions, the spherical basic unit, up to 10 nm in size, consists of an apatitic granule with a medium electron-dense coat which is unaffected by decalcification. Variation in the density distribution of these units is a key to the identification of the different types of laminae in TEM sections. Electron-dense bands are correlatives of compact laminae as seen under the SEM with the matrix, which is indistinguishable from the organic coats of hexagonally close-packed apatitic granules, tending to mask the biomineral components.

In untreated (or decalcified) sections of other laminae, with a higher organic content, the basic units are dispersed as discrete clumps, rods or linear trails in an electron-lucent matrix with a very faint but close network of strands and particles, especially between adjacent clusters of coated granules. This arrangement is well seen in sections showing the first stages in the secretion of a baculate lamina (figure 45). Electron-dense baculae, composed of coated granules, are either continuous between the outer epithelium and the terminating surface of the overlying compact lamina (with which they subtended angles of 45–60°) or contiguous with only the interdigitating tubes of the outer epithelium. Between the compact lamina and outer epithelium, baculae are suspended in a fine network of electron-lucent strands and particles streaming from the plasma membranes of the interdigitating tubes (figures 45 and 46). Sporadically distributed granules also occur but are densely distributed in the intertubular spaces (figure 43) and are also common in the apical region of the cells including some of the vesicles. An electron-lucent band, up to 300 nm thick, may intervene between the shell and outer epithelium but its fine structure is variable (figures 43–45). In sections showing outer epithelium underlying stratified and compact laminae, the bands contain electron-lucent versions of the organic coats around trails and arrays of granules characterizing the overlying lamina. We have assumed that such networks are an integral part of the overlying lamina, which have not been completely polymerized.

The organic constituents of the vertical canal system are assembled independently of those incorporated into the shell (figure 44). They are exocytosed deep within the interdigitating tubes as a bulbous assemblage of medium and lucent electron-dense particles. As these particles emerge from the apical surfaces of the secretory tubes, they polymerize into horizontally disposed, alternating bands of electron-lucent and darker beaded lineations with a combined periodicity of 15 nm. The beading may represent sets of horizontally aligned granules. The occurrence of this banded constituent as elliptical patches within the plane of the section suggests that it is the lining of the canals.

5. CONCLUSIONS

(*a*) *Inferred secretion of Discina shell*

The secretion of the *Discina* shell can be inferred by determining the distribution of the biomineral and organic components throughout the shell itself and its associated outer epithelium. These components, however, could not always be unambiguously identified so that precise comparisons of relevant shell sections were attended by uncertainties at two levels in the processing of data. First, the components exposed on natural and fracture surfaces could not always be matched in detail with those on polished sections because of the

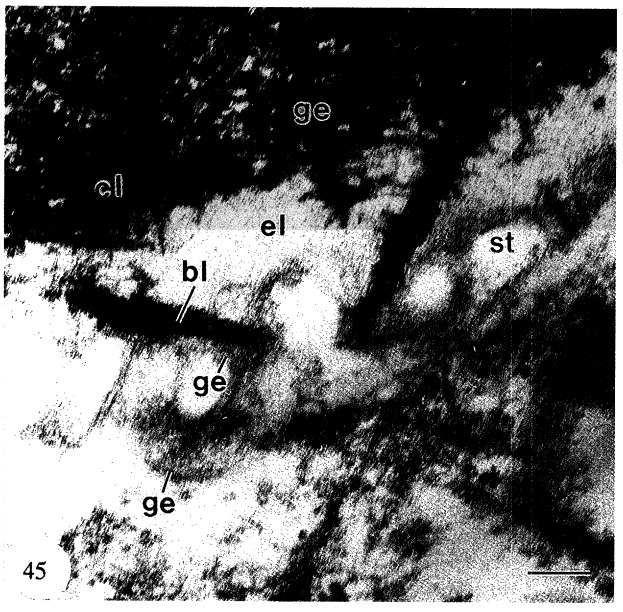

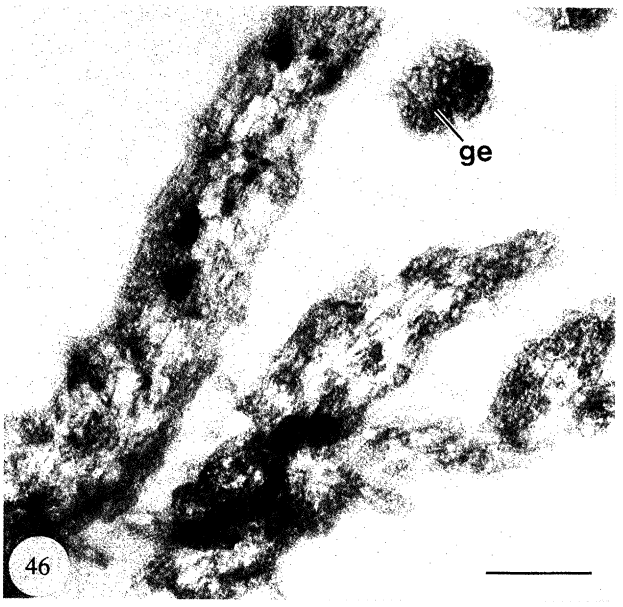

Figures 45–46. Transmission electron micrographs of shell and associated outer epithelium of a dorsal valve of *Discina striata*.

Figure 45. The secretory tubes (st) of outer epithelium in relation to baculae (bl) within or spanning an electron-lucent zone (el) underlying a compact lamina (cl); coated apatitic granules (ge) occur throughout. Scale bar = 100 nm.

Figure 46. Details of a baculate lamina within the shell succession showing the distribution of aggregates of coated apatitic granules (ge). Scale bar = 100 nm.

differential penetration of such surfaces by the various reagents used in this study. Where possible, therefore, ambiguities in interpretation were reduced by preparing successive polished surfaces of the same resin-mounted specimens for sequences of enzymic digestion and bleaching. The second difficulty arose, not so much in correlating untreated sections of shell and epithelium with those of decalcified specimens as in comparing both kinds with sections of dried shells as seen under the SEM. There were, however, some reliable markers for intersectional comparisons. In particular, the basic granule and compact and baculate laminae could be readily identified in all sections irrespective of the nature of their preparation and have played a key role in formulating the conclusions outlined below.

The basic biomineral unit of *Discina*, the coated, subrounded granule of apatite, is readily identified in both the dried shell and the fixed shell with epithelium. In sections of the latter, granules occur in varying concentrations in the apical parts of the outer epithelium, especially within and between the interdigiting secretory tubes at the interface of mantle and shell (figures 43 and 45). The granules are well defined by fibrillar, organic coats of varying electron density in untreated and decalcified sections of outer epithelium (and associated shell). They are also equally well delineated in sections of dried shell digested by chitinase and subtilisin. We have, therefore, concluded that the granular coat is chitinoproteinaceous. This is consistent with the findings in *Lingula* that the chitin: protein ratio is higher in biomineral laminae than in organic ones (Iijima *et al.* 1991, p. 381).

The aggregation of coated granules into spherules can take place in intra-cellular vesicles and in intercellular spaces between the interdigitating tubes of outer epithelium and presumably involves the enmeshment of contiguous fibrillar coats. Further aggregation is completed extracellularly but all biomineral features from baculae to finely stratified laminae are initiated and progressively assembled within, or at the surfaces of, the more distal interdigitating tubes. Accordingly, the main components of every type of lamination occur in what appears to be their final crystalline or polymerized states at the interface between the shell and outer epithelium. This kind of secretion precludes the existence of a film of 'extrapallial' fluid between newly formed shell and mantle, like that found in molluscs (Simkiss & Wilbur 1989, p. 235) and allegedly in lingulid brachiopods (Iijima *et al.* 1991, p. 382; Pan & Watabe 1988, p. 47).

This second order aggregation of spherules, like the first order spherular clustering of granules into spherules, is promoted by organic substrates. In untreated sections, its products – spherular mosaics, baculae, platy strata and so on – are obscured by membranes which are scarcely or only selectively digested by collagenase and chitinase respectively. However, bleaching and proteolysis by trypsin, subtilisin and, to a lesser extent, papain, expose all biomineral structures in sharp relief, which suggests that the organic matrix is mainly protein. At this scale of shell architecture, the distribution of chitin, as indicated by chitinase digestion, appears to be concentrated in the coating of granules and spherular mosaics and, more sporadically, in sheets, associated with stratified and baculate lamination. Even these occurrences, however, are mostly in the presence of protein.

The secondary laminae of *Discina* are arranged in a variety of sequences, most of which conform to a discernible pattern of rhythmic sedimentation. In a mature valve, a typical secretory cycle begins with an organic sheet or a lamina with a high organic content, which grades internally into a predominantly apatitic lamina. Thus, a commonly occurring rhythmic unit consists of rubbly or baculate laminae (usually succeeding an organic sheet) grading inwardly into a compact lamina which terminates at a sharply defined interface with the succeeding unit (figures 16–18). Rhythmic units characterize the shells of other organo-phosphatic brachiopods (Iwata 1981, p. 41; Watabe & Pan 1984, p. 979) but the relationships between consecutive laminae have not been precisely described. In any event, laminae grade laterally into one another so that all kinds are usually being simultaneously secreted on some part or other of the valve floor. Consequently, a succession along a vertical traverse of a valve may be structurally (but not rhythmically) unique.

Laminar periodicity reflects environmental rhythms as well as recurrent physiological changes in the outer epithelium, not least those arising from the maturation and, possibly, the differentiation of the mantle. Such relationships are complex and their effect on the *Discina* shell have still to be analysed. It is, however, important to our conclusions to establish whether the mantle of *Discina* undergoes the differentiation reported by Watabe & Pan (1984, p. 982) for the lingulid *Glottidia*. According to them, the anterior part of the squamous (i.e. outer) epithelium secretes 'mineralized' layers and has smooth plasma membranes whereas the more posterior cells secrete 'chitin' layers (with biomineral components) and are microvillous. We found no such differentiation in any of our sections of shell and epithelium. In fact, a comparison of sections, showing outer epithelium contiguous with each of the five types of laminae described herein, did not reveal significant structural differences among the secreting cells all of which were prolonged distally into prostrate, interdigitating tubes (compare figures 42, 43 and 45). This is consistent with the anchoring of the epithelium to the valve floor by the canals pervading the *Discina* shell. The canal linings, which are proteinaceous (with hydroxyproline), are assembled well within the interdigitating tubes of outer epithelium and can usually be traced through several consecutive laminae. Each such lamina must, therefore, have been secreted in turn by the same assemblage of cells so that the compositional differences of laminae arise through periodic physiochemical, rather than structural, changes in the secreting cells.

(*b*) *Inferred origin of inclusions*

Two inferences, so far made, have played a key role

in our interpretion of inclusions in the *Discina* shell. The first is that the shell is more or less in the final stages of crystallization and polymerization of its components as it is being secreted by outer epithelium. Secondly, the structural and compositional differences, characterizing successive laminae, are related to changes in the physio-chemical milieu of the same cell(s). During secretion, some *in situ* cell division and replacement takes place, as is indicated by the convergence of canals into branching systems, especially in areas of shell thickening. However, such adjustments in the spread of the secreting plasma membranes would not greatly affect the overall permanency of the mantle relative to the valve floor nor inhibit deviations in the rhythmic secretory cycles of the outer epithelium.

In respect of the inclusions found in abundance in a dorsal valve, five aspects of their occurrence lead to the same conclusion: (i) they are not regular manifestations of the *Discina* secretory regime; (ii) when they occur, they do so in swarms concentrated in zones conformable with lamination; (iii) they occur throughout the secondary shell succession more or less irrespective of the nature of lamination; (iv) they are normally spherical in shape with only occasional evidence of post-formational compaction; and (v) they almost invariably have a central space.

The inclusions have been most completely revealed in a bleached section of a resin-embedded dorsal valve; but subtilisin digestion of the counterpart confirms that the grooves separating the inclusions from the coarse, apatitic particles were the sites of organic coats, certainly proteinaceous (compare figures 34 and 35) but also with some chitin if inclusions are variants of spheroidal mosaics (figure 15). Spherular aggregates, comparable with the coarse particles in size and distribution, also emerge after subtilisin digestion (figure 35). It is, therefore, assumed that the particles are the coarser nodes of an interconnected framework of spherular apatite enveloped in a proteinaceous matrix. The coats of each inclusion, embedded in this framework, would have acted as a substrate not only for the external nodes of apatite but also for an internal layer of smaller, regularly formed apatitic spherules. The latter were the foundation for the accretionary growth of botryoidal mosaics of apatitic spherules. In most inclusions, such aggregates all but filled the spaces enclosed by the coats, leaving small central cavities or slits confined by the curved surfaces of the mosaics. In larger, botryoidal inclusions, however, cavities were relatively extensive and contained perfectly spherical mosaics which must have crystallized freely in a space circumscribed, without much subsequent volumetric change, by the bounding coat when it was first formed (figure 47).

The inclusions, complete with their mainly proteinaceous coats, are interpreted as having been produced by sporadic, abnormal outpourings from the outer epithelium, mainly in one sector of the valve during an otherwise normal secretion of the shell as a whole. These prolifically generated bodies appear not only to have been assembled in vesicles within the cells but, there, also to have undergone sufficient polymerization and crystallization to have acquired rigid apatitic linings to their protein coats before exocytosis took place. This assumption is prompted by the retention of the spheroidal shape of the great majority of inclusions, with comparatively few signs of post-deformational compression, after their incorporation into the shell succession. Moreover, the way inclusions occasionally formed a closely stacked layer, like a cobbled pavement, over which laminar infill with a stratum of coarse particles had been secreted as a mould, confirms that they were exocytosed in their present shape and, thereafter, buried in the organo-phosphatic framework of the shell (figure 30). This seems to have been the sequence of deposition as there are no signs, within the host laminae, of the

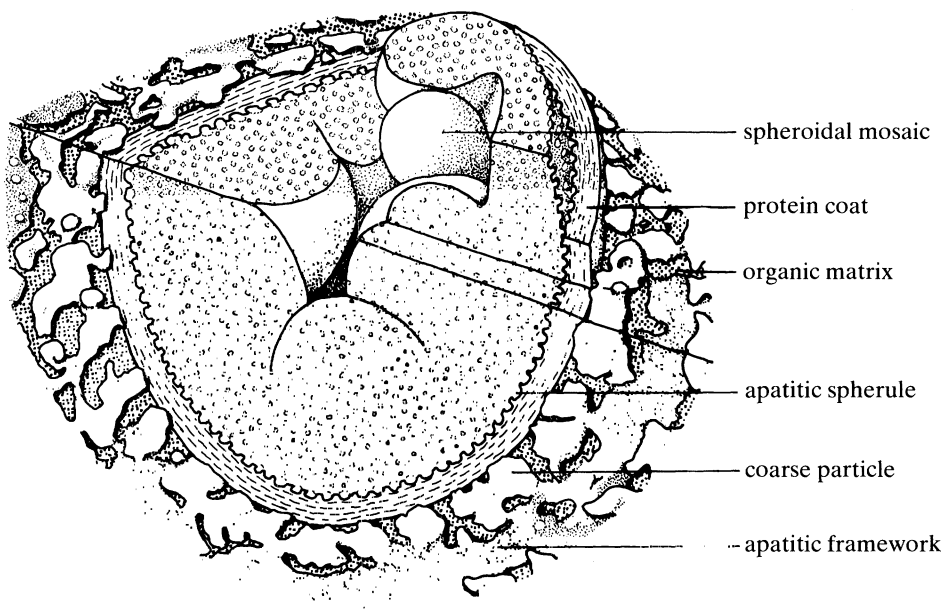

Figure 47. A reconstruction of a botryoidal inclusion of apatitic mosaics and its chitino-proteinaceous coat within the anastomosing strands of the organo-apatitic framework.

kind of deformational strain that is associated with post-depositional concretionary growth within a plastic/brittle medium.

Of course, the final stages in the solidification of the inclusions could have taken place extracellularly during consolidation of the shell itself. Conjoined inclusions, which share a protein coat, could have been exocytosed contemporaneously by vesicles overlapping at the plasma membrane and then merged before the protein coats had polymerized. Indeed, groups of inclusions adhering to canal linings must have been formed in a rapid sequence of vesicular ejections at practically the same loci on plasma membranes (figure 31). Botryoidal masses, however, which can involve a complex of inclusions extending, for up to 7 μm or so, vertically along canals and horizontally parallel with a laminar boundary, could only have been assembled by sustained exocystosis of the amalgamating contents of vesicles from two or more cells (figure 33).

The inferred origin of the coarse particles, which typically constitute spherular nodes within the apatitic framework as well as external coats to inclusions, is also noteworthy. Their size suggests that their aggregation began before they became part of the apatitic framework. This assumption is supported by the sporadic occurrences of single layers or dispersed scatters of discrete particles, each with its protein coat, within compact laminae. It is, therefore, possible that the spherular components of the coarse particles were assembled within the cytosol immediately before their exocytosis as precursors to, or associates of, inclusions (figure 47). In that context, the particles forming the outermost coat of inclusions are an integral part of the zoned succession of those bodies even though they are connected with the matrix of the host lamina. This would account for a solitary inclusion, isolated from an antecedent swarm by 2 μm of spherular apatite, having a well-developed external coat of coarse particles (compare figure 32).

Traces of inclusions found in digested sections of a ventral valve are almost exclusively empty moulds of spheroidal or discoidal bodies within an apatitic framework permeated by anastomosing tunnels as well as the ubiquitous vertical canal system. The digestion of counterpart sections by subtilisin and chitinase confirmed that the coats of these bodies and the tunnels and the infill around the biomineral frame were mainly protein, with little chitin except in some membranous interleaves in stratified laminae. The contents of the spheroidal moulds (and tunnels) could have been exclusively organic. Yet the absence of any morphological evidence of such a component from sections treated with chitinase and the mass removal by subtilisin of the coats and the biomineralized contents of inclusions already described, suggest that the empty moulds in life probably contained loosely adherent spherular mosaics.

The apatitic cylindroid bodies, revealed in a dorsal valve by papain digestion, are not inclusions but walls of spherular mosaics enclosing vertical canals. Their protrusion above the general level of a laminar surface suggests that they were secreted as spherular mosaics around the cylindroid proteinaceous linings of the vertical canals and assembled deep among the interdigitating tubes of outer epithelium. In turn, the external surfaces of these intrusive stacks were substrates for more or less continuous coats of protein.

(*c*) *Phylogenetic significance of the Discina shell structure*

The granular spherules, the principal structural components of the *Discina* shell, are phylogenetically significant in two respects. First, they are crystallographically different from the spherulites of acicular crystallites which characterize the lingulid *Glottidia* (Pan & Watabe 1988, p. 45). Secondly, both kinds of aggregates appear to be sufficiently stable, at least in their overall shape, to survive in a recognizable form almost indefinitely under propitious conditions of fossilization. There can be little doubt, for example, that the spheroidal fabric of the Middle Cambrian organo-phosphatic paterinide *Dictyonina* cf. *ornatella* (Linn.) (figure 41) is original even on a nanometric scale. These spheroidal mosaics are more likely to be relicts of the standard fabric of the paterinide shell than the polygonal arrays of coarse crystallites, discovered by Popov & Ushatinskaya (1987, p. 1228) in the Lower Cambrian *Cryptotreta*. Such arrays may represent recrystallized casts of secreting cuboidal epithelium, like those found in linguloid skeletal successions (Curry & Williams 1983). This interpretation does not presume that the *Dictyonina* shell was free of recrystallization. It has yet to be determined whether the *Dictyonina* spheroids were secreted as aggregates of granules or of acicular crystallites. Indeed, it may not presently be possible to draw such a fine crystallographic distinction. Spherulites of radiating acicular crystallites (figure 40) can be found in the skeletal successions of Lower Palaeozoic acrotretoids (Williams & Holmer 1992). The general shape of these common constituents of the acrotretoid shell is too much like those of living organo-phosphatic skeletons to be anything but original. Yet the acicular texture is lingulid rather than discinoid; and, although it may have resulted from post-mortem recrystallization, further study may show it to be original. In any event, the effects of fossilization on organo-phosphatic shells are in urgent need of review following the pioneering but controversial researches of Popov & Ushatinskaya (1986).

There is also abundant evidence of spheroidal or discoidal inclusions within the original integument of many extinct organo-phosphatic brachiopods. Pits, normally not more than 1 μm in size, indent the surfaces of all acrotretoid larval shells and the exteriors of an adult linguloid (*Rowellella*) and some discinoids (*Schizotreta* and *Orbiculoidea*). They have been interpreted as the casts of vesicular periostraca impressed on a very fine organo-apatitic paste which quickly set on secretion to form the primary layer (Biernat & Williams 1970). This interpretation gained credence from the inclusion within the periostracum of living terebratuloids of abundant, thick-walled vesicles of comparable dimensions (Williams & Mackay 1978). However, these periostracal vesicles are not

impressed on the surface of the underlying carbonate layer of the terebratuloid primary shell, a phenomenon which has hitherto been attributed to the blanketing effects of a thickly developed basal layer which can exceed 350 nm in *Macandrevia* (Williams & Mackay 1978, p. 201). An alternative explanation can now be offered in that the periostracal vesicles of extinct organo-phosphatic brachiopods could have been filled with spherular apatite comparable not only with the *Discina* inclusions but also with those found in the periostracum of the mytiloid bivalve *Lithophaga* (Carter 1990, p. 281).

The tubercules ornamenting the larval shell of paterinides, on the other hand, have cores of apatitic spherules 2 μm or more in diameter. Their regular arrangement beneath a superficial layer of apatite 500 nm thick suggests that a monolayer of vesicular inclusions dominated the larval shell succession of those early Palaeozoic brachiopods.

Finally, the sporadic development of discrete walls of spherular mosaics enclosing vertical canals, as revealed by papain digestion of the *Discina* shell, is a clue to the origin of an extraordinary skeletal fabric of many acrotretoids. In these species, the secondary shell consists of lenticular laminae made up of bounding walls connected by orthogonally disposed hollow columns of apatite (Poulsen 1971). Williams & Holmer (1992) have interpreted the columns (and associated domes) as original structures and have assumed that the intralaminar spaces containing them were filled, in life, with an organo-apatitic mesh which would not normally have survived in the fossil state. The more rubbly laminae of *Discina* approach this condition and constitute a feasible living model for one of the most bizarre skeletal successions within the brachiopod phylum.

The specimens of *Discina* used in this study were collected in The Gambia and we are indebted to Professor Nils Spjeldnaes of Oslo University for having alerted us to their presence in that country; and to the Director and staff of ITC, including our intermediary, Professor Max Murray of Glasgow University, and especially Derek J. Clifford and Ousman Jin Njie for respectively affording A.W. generous facilities in the laboratory and expert technical assistance in the field. The ancillary study of fossil organo-phosphatic brachiopods was greatly helped by the loan of etched paterinide specimens expeditiously arranged by Dr M. G. Bassett of the National Museum of Wales.

Most of the work was carried out in our respective Departments; and we express our gratitude for all the facilities and technical and photographic assistance we have received from these sources. In addition, we have benefited from the expertise of Laurence Tetley of the Electron Microscopy Centre and Douglas Macintyre and David Gourlay of the Department of Electronic and Electrical Engineering. It is a pleasure to record the multi-disciplinary co-operation available in the University of Glasgow.

Finally, our studies have been underwritten by various grants. A.W. and M.C. have enjoyed the support of the Royal Society; A.W. and S.M. the enhancement of electron microscopy facilities by the NERC; and A.W. a generous continuation of funding from the Leverhulme Trust.

REFERENCES

Biernat, G. & Williams, A. 1970 Ultrastructure of the protegulum of some acrotretide brachiopods. *Palaeontology* **13**, 491–502.

Carter, J.G. 1990 Evolutionary significance of shell microstructure in the Palaeotaxodonta, Pteriomorphia and Isofilibranchia (Bivalvia: Mollusca). In *Skeletal biomineralization: patterns, processes and evolutionary trends* (ed. J. G. Carter), pp. 135–296. New York: Van Nostrand Reinhold.

Carter, J.G. *et al.* Glossary of Skeletal Biomineralization. In *Skeletal biomineralization: patterns, processes and evolutionary trends* (ed. J. G. Carter) pp. 609–671. New York: Van Nostrand Reinhold.

Curry, G.B. & Williams, A. 1983 Epithelial moulds on the shells of the early Palaeozoic brachiopod. *Lingulella. Lethaia* **16**, 111–118.

Geiger, R. & Fritz, H. 1983 Trypsin. In *Methods of enzymatic analysis. V. Enzymes 3: Peptidases, proteinases and their inhibitors* (ed. H. U. Bergmeyer), pp. 119–129. Weinheim: Verlag Chemie.

Holmer, L.E. 1989 Middle Ordovician phosphatic inarticulate brachiopods from Västergötland and Dalarna, Sweden. *Fossils Strata* **26**, 1–172.

Iijima, M., Hiroko, T., Yutaka, M. & Yoshinori, K. 1991 Difference of the organic component between the mineralized and the non-mineralized layers of *Lingula* shell. *Comp. Biochem. Physiol.* **98A**, 379–382.

Iwata, K. 1981 Ultrastructure and mineralization of the shell of *Lingula unguis* Linné (inarticulate brachiopod). *J. Faculty Sci. Hokkaido Univ.* **4,20**, 35–65.

Iwata, K. 1982 Ultrastructure and calcification of the shells in inarticulate brachiopods Part 2. Ultrastructure of the shells of *Glottidia* and *Discinisca*. *J. geol. Soc. Japan.* **88**, 957–966.

Jope, H.M. 1965 Composition of brachiopod shell. In *Treatise on invertebrate paleontology. Part H Brachiopoda* (ed. R. C. Moore), pp. H156–H164. Geological Society of America and University of Kansas Press.

Markland, F.S. & Smith, E.G. 1971 Subtilisin: primary structure, chemical and physical properties. In *The enzymes*, vol III. *(Hydrolysis: peptide bonds)*, 3rd edn (ed. P. D. Boyer), pp. 562–606. New York: Academic Press.

Owen, G. & Williams, A. 1969 The caecum of articulate brachiopods. *Proc. R. Soc. Lond.* B **172**, 187–201.

Pan, C.-M. & Watabe, N. 1988 Shell growth of *Glottidia pyramidata* Stimpson (Brachiopoda: Inarticulata). *J. exp. mar. Biol. Ecol.* **119**, 257–268.

Popov, L.E. & Ushatinskaya, G.T. 1986 O vtorichnykh izmeneniyakh mikrostructury fosfatno-kal'tsievykh rakovin bezzamkovykh brakhiopod. [On secondary changes in the microstructure of calcium-phosphatic shells of inarticulate brachiopods.] *Izvestiya Akademii Nauk SSSR, Seriya Geologicheskaya* **10**, 135–137. [In Russian.]

Popov, L.E. & Ushatinskaya, G.T. 1987 Novyye dannyye o mikrostrukture rakoviny bzzamkovykh brakhiopod otryada Paterinida. [New data on the microstructure of the shell in inarticulate brachiopods of the Order Paterinida.] *Doklady AN SSSR* **293**(5), 1128–1231.

Popov, L.E., Zezina, O.N. & Nõlvak, J. 1982 Mikrostruktura apikal'noj chasti rakoviny bezzamkovykh brakhiopod i ee ekologischeskoe znachenie [Microstructure of the apical parts of inarticulates and its ecological importance.] *Byuleten Moskovskogo abschchestva ispytatelej prirody, otdel biologicheskij* **87**, 94–104.

Poulsen, V. 1971 Notes on an Ordovician acrotretacean brachiopod from the Oslo region. *Bull. geol. Soc. Denmark* **20**, 265–278.

Seifter, S. & Harper, E. 1970 Collagenases. In *Methods in enzymology XIX. Proteolytic enzymes* (ed. G. E. Perlman & L. Lorand), pp. 613–635. New York Academic Press.

Simkiss, K. & Wilbur, K.M. 1989 *Biomineralization cell biology and mineral deposition.* (337 pages). San Diego: Academic Press.

Smith, E.L. & Kimmel, J.R. 1960 *The Enzymes*, vol. 4. (Hydrolytic cleavage (Part A)), 2nd ed (ed. P. D. Boyer, H. Lardy & K. Myrback), p. 133. New York: Academic Press.

Watabe, N. & Pan, C.-M. 1984 Phosphatic shell formation in atremate brachiopods. *Am. Zool.* **24**, 977–985.

Watabe, N. 1990 Calcium phosphate structures in invertebrates and protozoans. In *Skeletal biomineralization: patterns, processes and evolutionary trends* (ed. J. G. Carter), pp. 35–44.

Williams A. & Curry, G.B. 1991 The microarchitecture of some acrotretide brachiopods. In *Brachiopods through time* (ed. D. I. MacKinnon, D. E. Lee & J. D. Campbell), pp. 133–140. Rotterdam: A. A. Balkema.

Williams, A. & Holmer, L.E. 1992 Ornamentation and shell structure of acrotretoid brachiopods. *Palaeontology.* (In the press.)

Williams, A. & Mackay, S. 1978 Secretion and ultrastructure of the periostracum of some terebratulide branchiopods. *Proc. R. Soc. Lond.* B **202,** 191–209.

Williams, A. & Mackay S. 1979 Differentiation of the brachiopod periostracum. *Palaeontology* **22**, 721–736.

Williams, R.J.P. 1984 An introduction to biominerals and the role of organic molecules in their formation. *Phil. Trans. R. Soc. Lond.* B **304**, 411–424.

Received 14 February 1992; accepted 13 March 1992

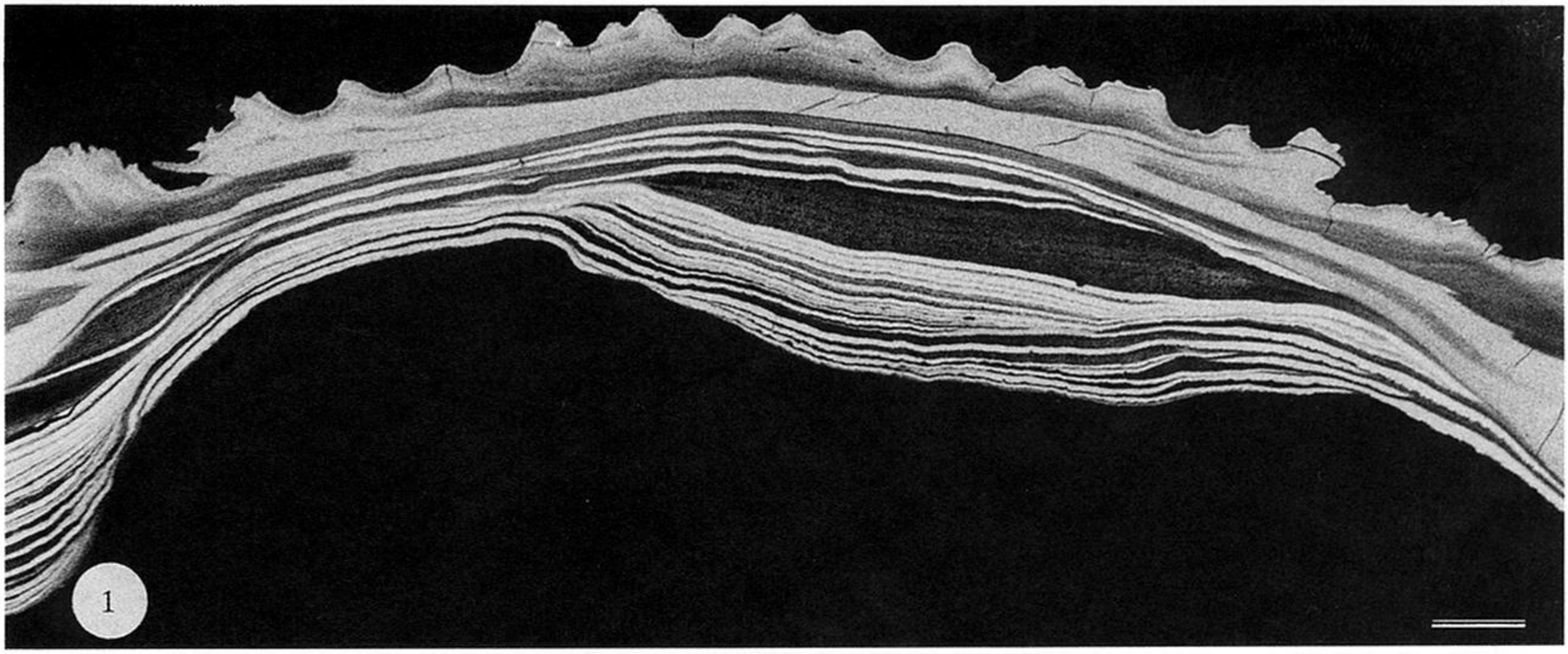

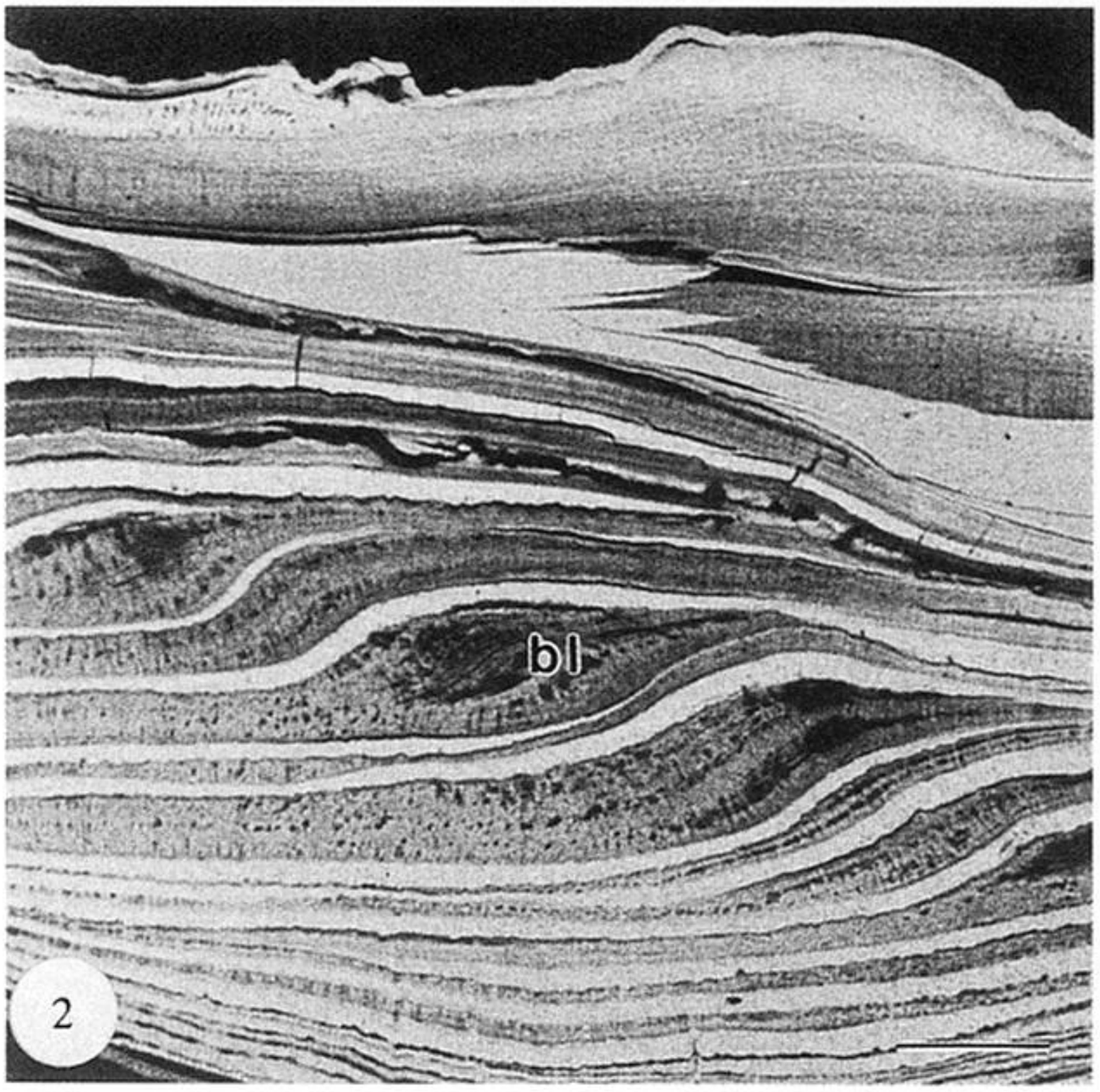

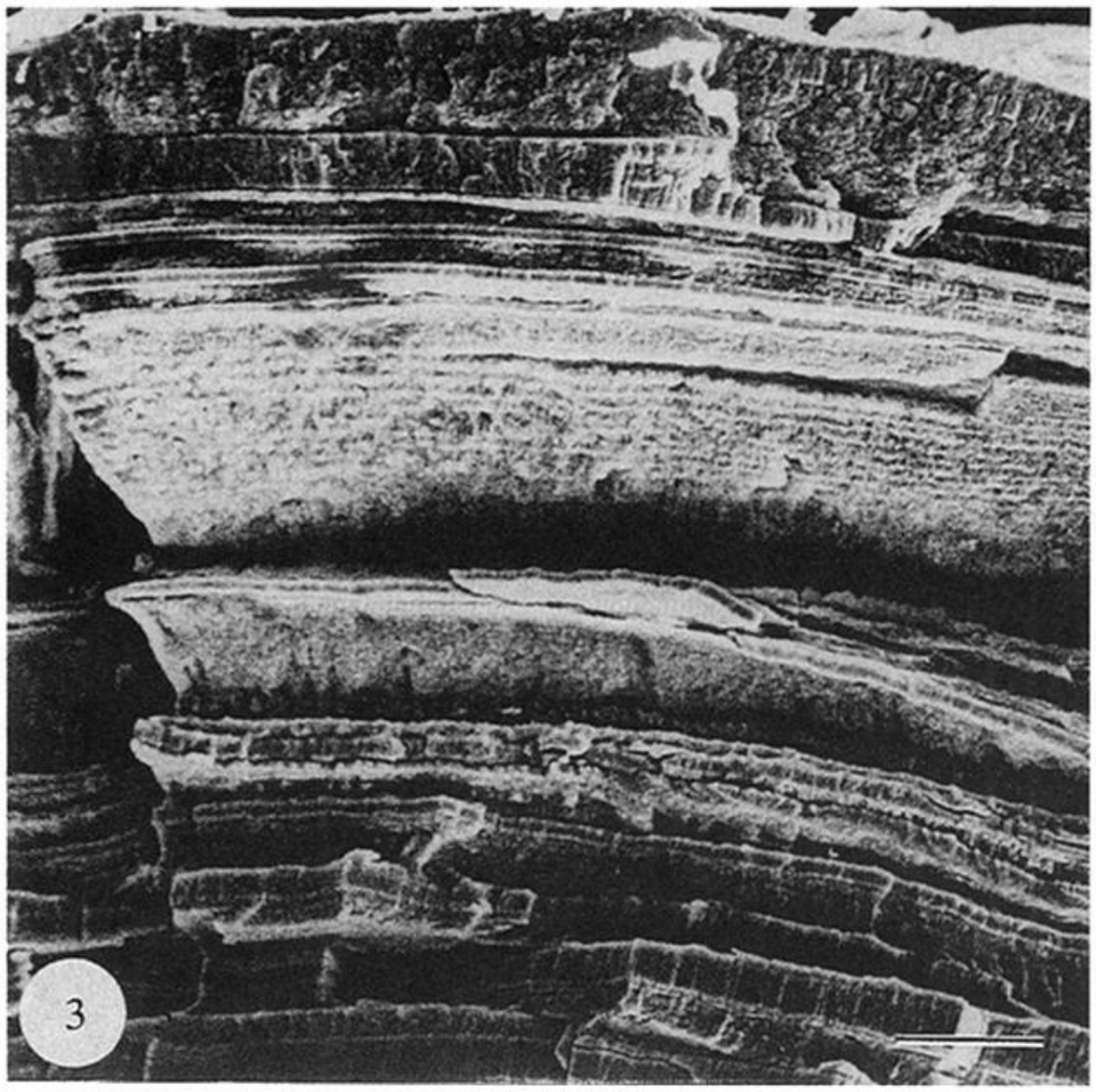

Figures 1–3. Scanning electron micrographs of dried dorsal valves of *Discina striata* with their external surfaces immediately underlain by the primary layer at the top.

Figure 1. Backscattered electron micrograph of a chordal section cut near the umbo and digested in chitinase (0.2 mM in MES buffer) and papain (40 μM in phosphate buffer with mercaptoethanol (50 μM)) and coated with carbon to show the distribution of the apatitic (white) and organic (grey to black) components of the shell succession. Scale bar = 250 μm.

Figure 2. Backscattered electron micrograph of a bleached radial section through the intramarginal zone coated in carbon and showing the distribution of apatitic (white) and organic (grey to black) components of the shell succession with lateral gradations and unconformable oversteps between baculate laminae (bl). Scale bar = 100 μm.

Figure 3. Vertical fracture surface digested in trypsin (1 mM in phosphate buffer) and coated with carbon then gold to show the main types of lamination in a shell succession. Scale bar = 50 μm.

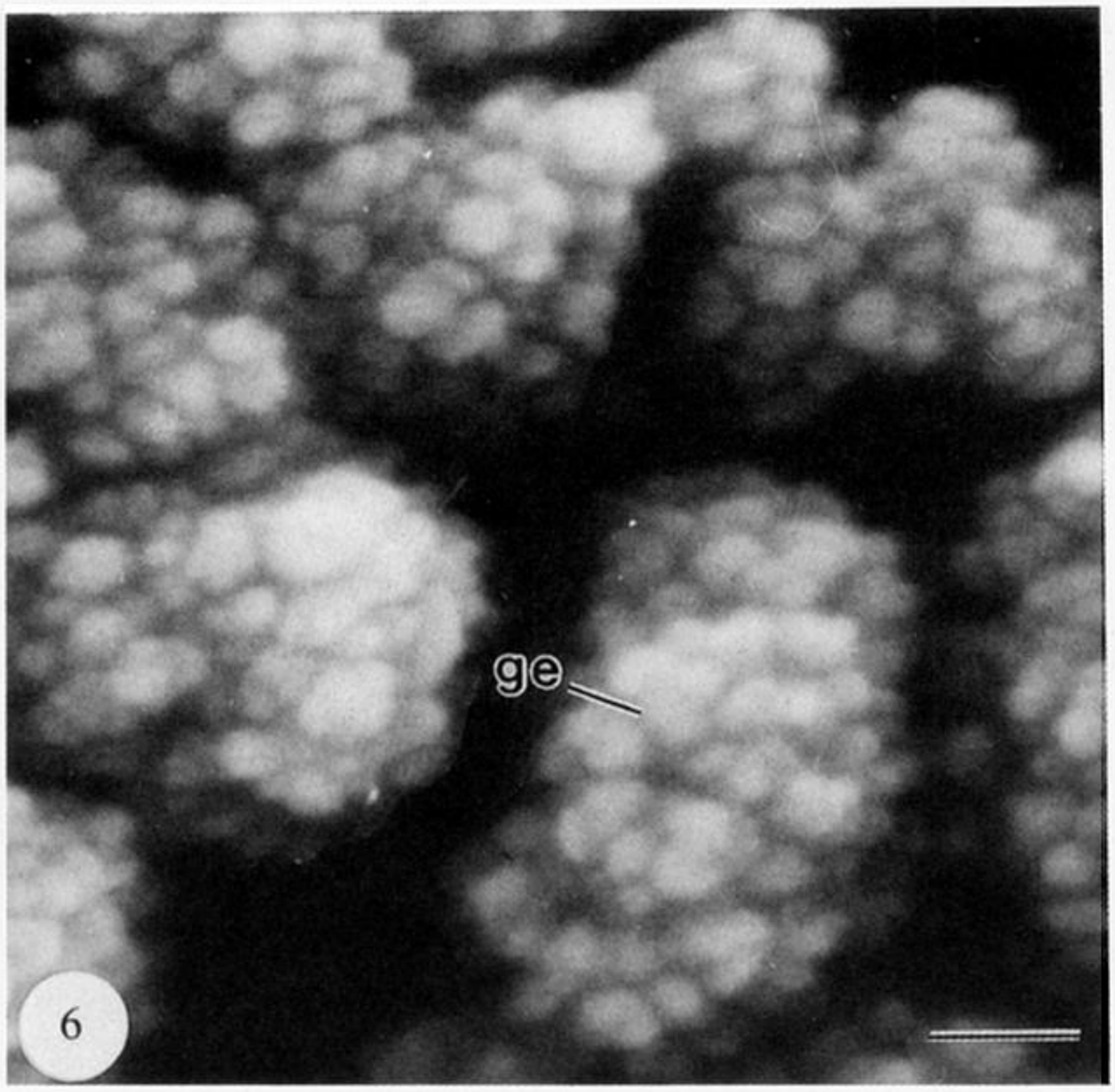

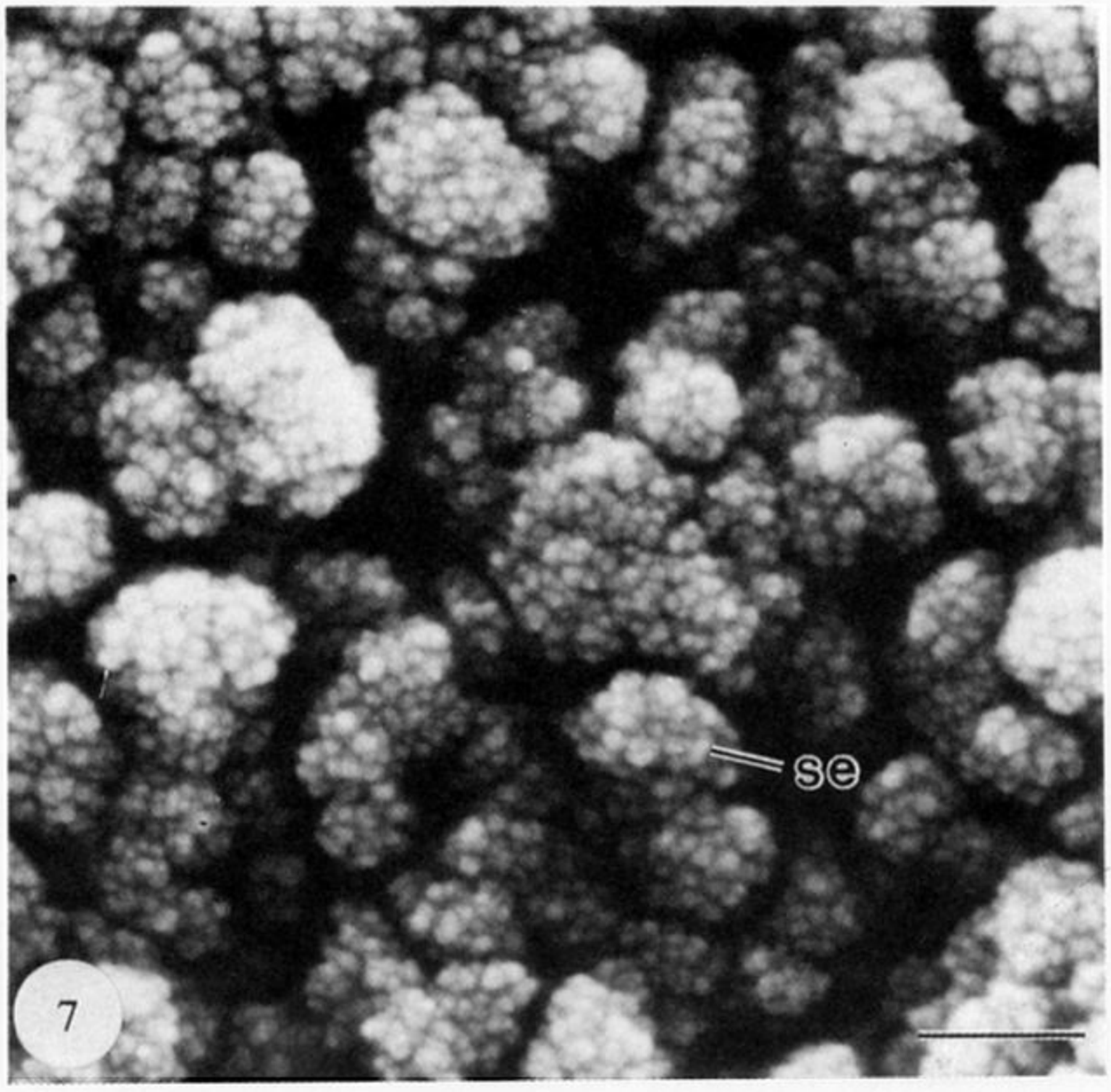

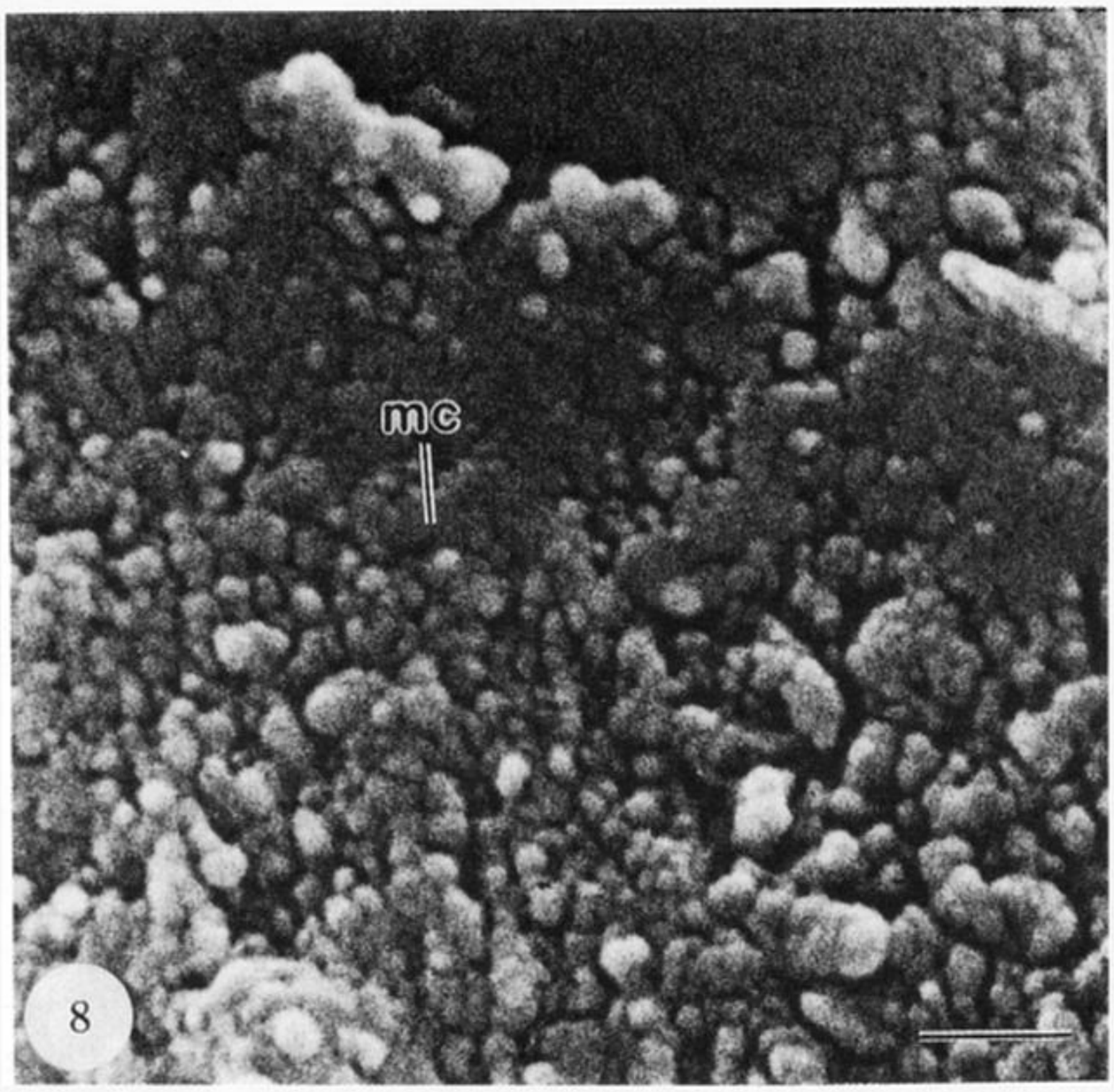

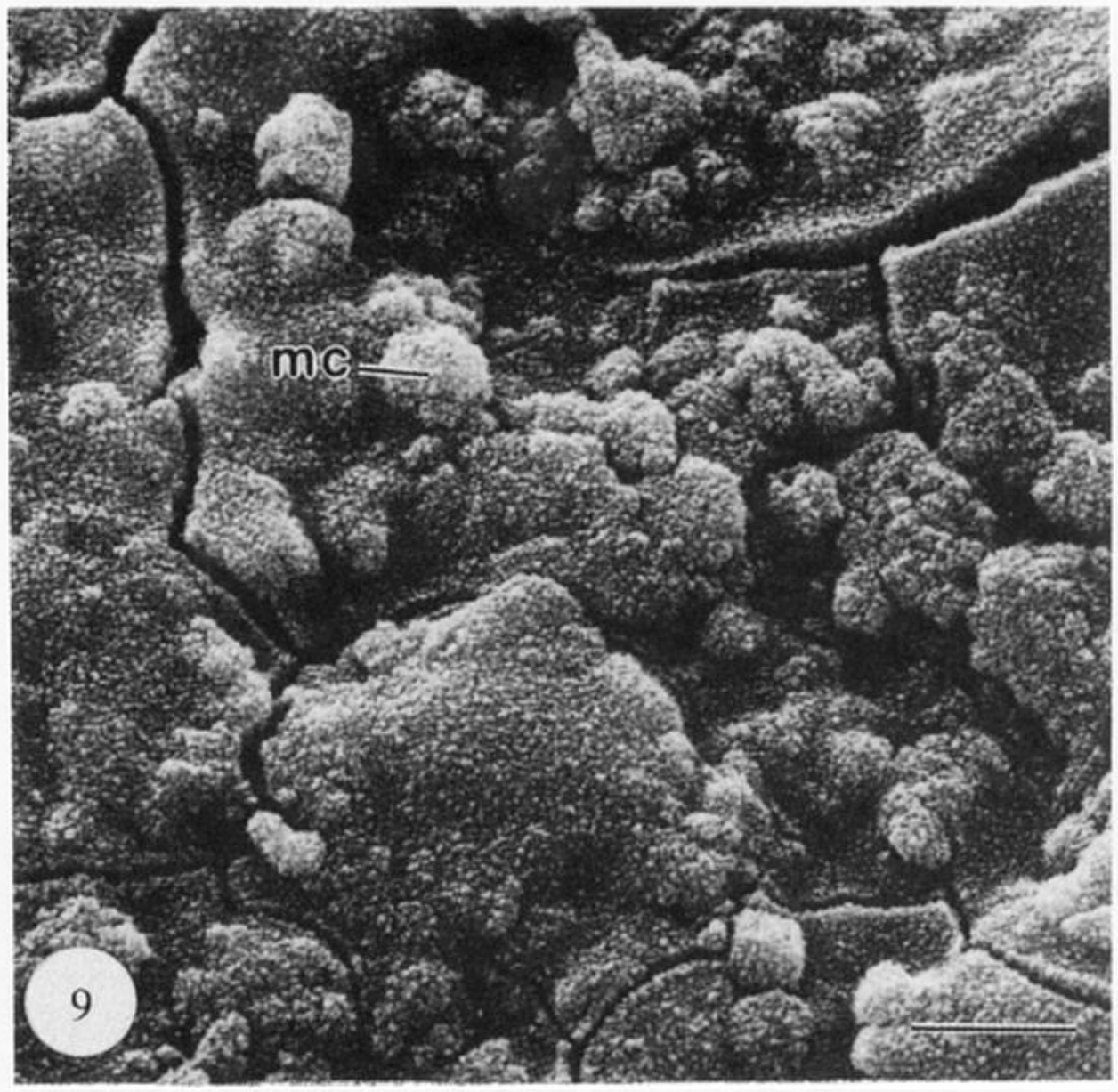

Figure 6–9. Scanning electron micrographs of dried dorsal valves of *Discina striata.*

Figure 6. Vertical fracture surface digested in chitinase (2 mM in phosphate buffer) and coated with gold–palladium to show the granular nature (ge) of apatitic spherules. Scale bar = 15 nm.

Figure 7. Vertical fracture surface digested in trypsin (1 mM in phosphate buffer) and coated with gold-palladium to show the aggregation of spherules (se) into mosaics. Scale bar = 40 mm.

Figure 8. Bleached, internal surface coated with carbon then gold to show the flattened aspect of apatitic mosaics (mc). Scale bar = 500 nm.

Figure 9. Bleached, internal surface coated with carbon then gold to show the spheroidal aspect of aggregations of apatitic mosaics (mc). Scale bar = 4 μm.

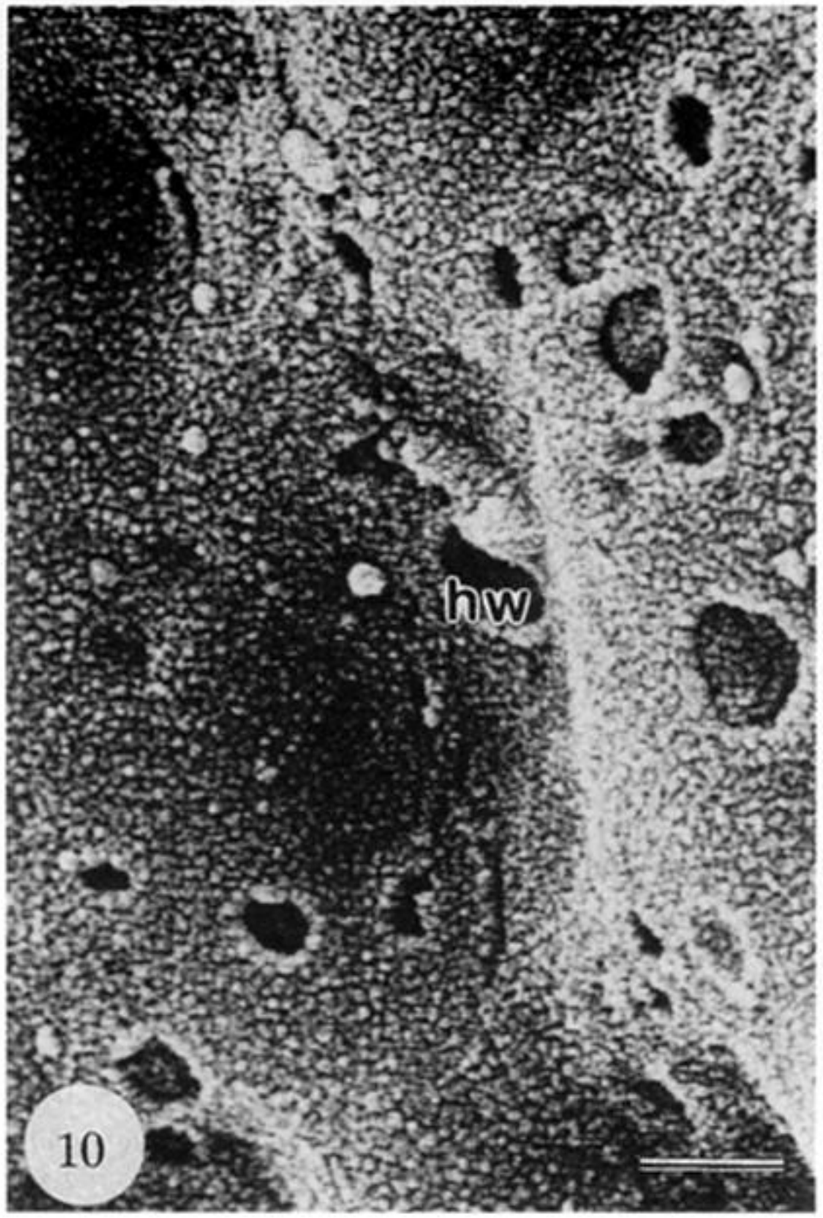

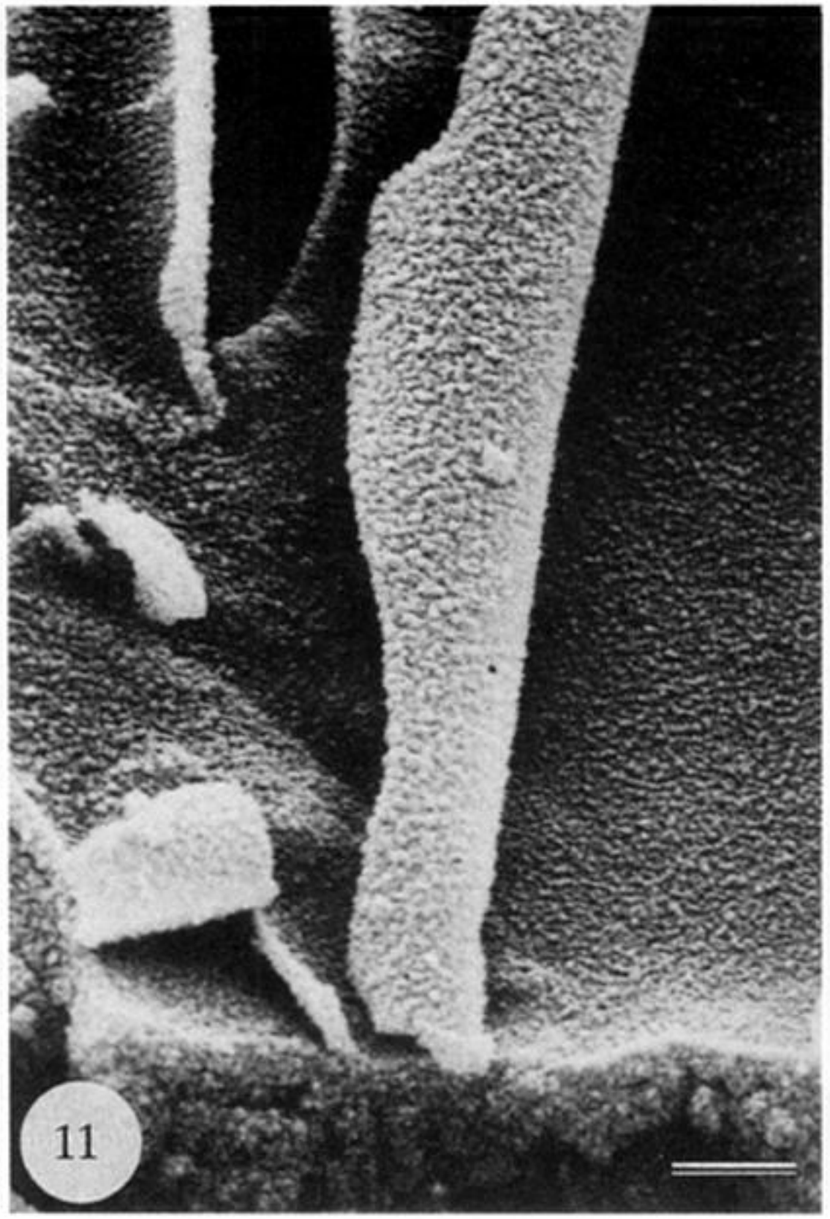

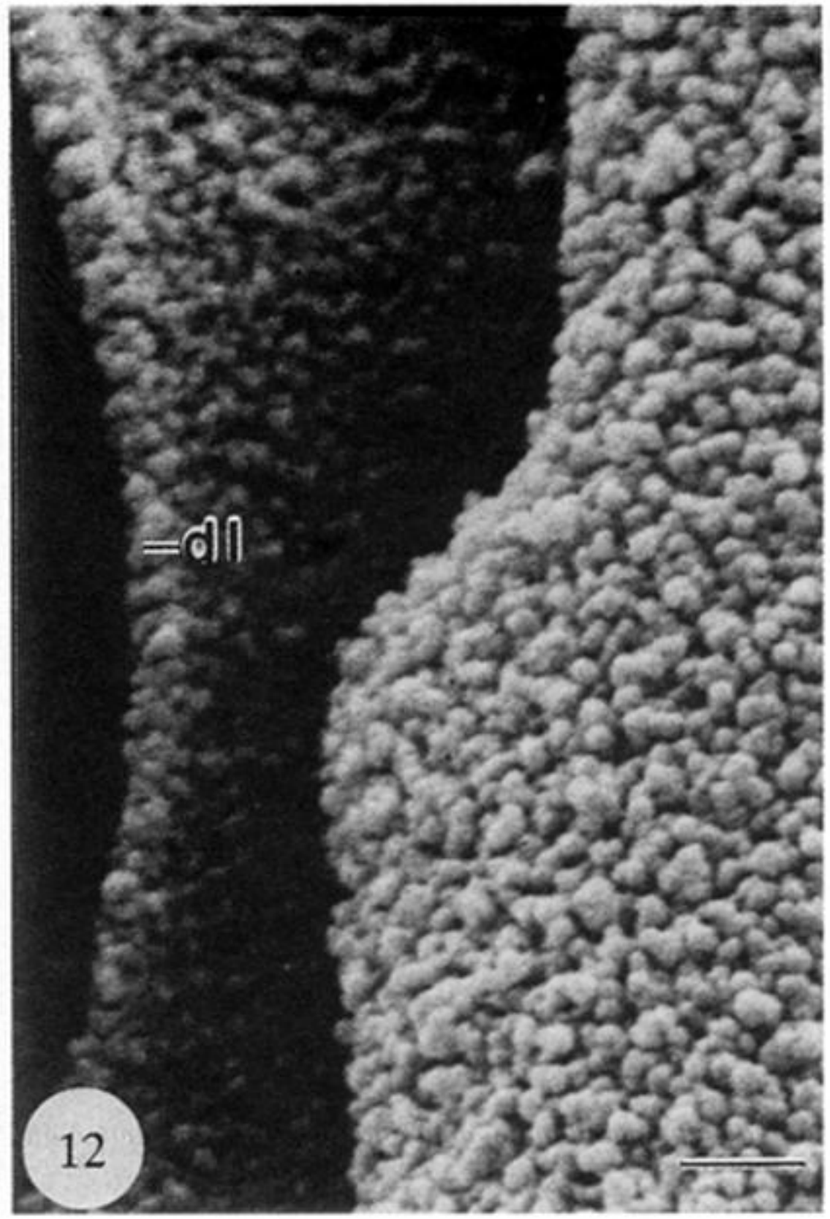

Figures 10–12. Scanning electron micrographs of dried dorsal valves of *Discina striata*.

Figure 10. Untreated, internal surface coated with carbon then gold to show the differential aggregation of spherules in the most recently secreted member of a stratified lamina; the subcircular hollows (hw) are assumed to represent the sites of flattened exocytosed vesicles. Scale bar = 2.5 μm.

Figure 11. Bleached, internal surface coated with carbon then gold to show the flexible nature of the most recent member of a stratified lamina. Scale bar = 2 μm.

Figure 12. Detail of the superficial coat featured in figure 11 to show that the biomineral components of the coat are apatitic spherules usually arranged in a double layer (dl). Scale bar = 500 nm.

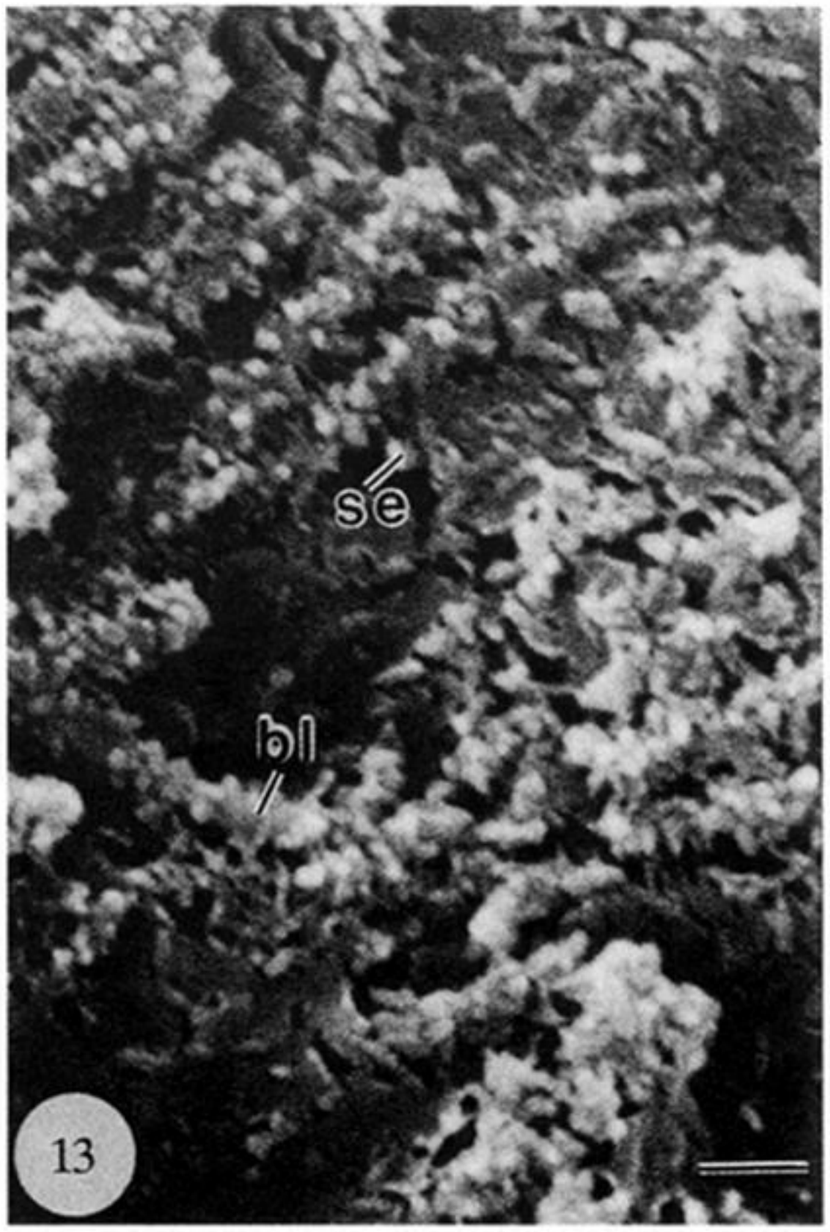

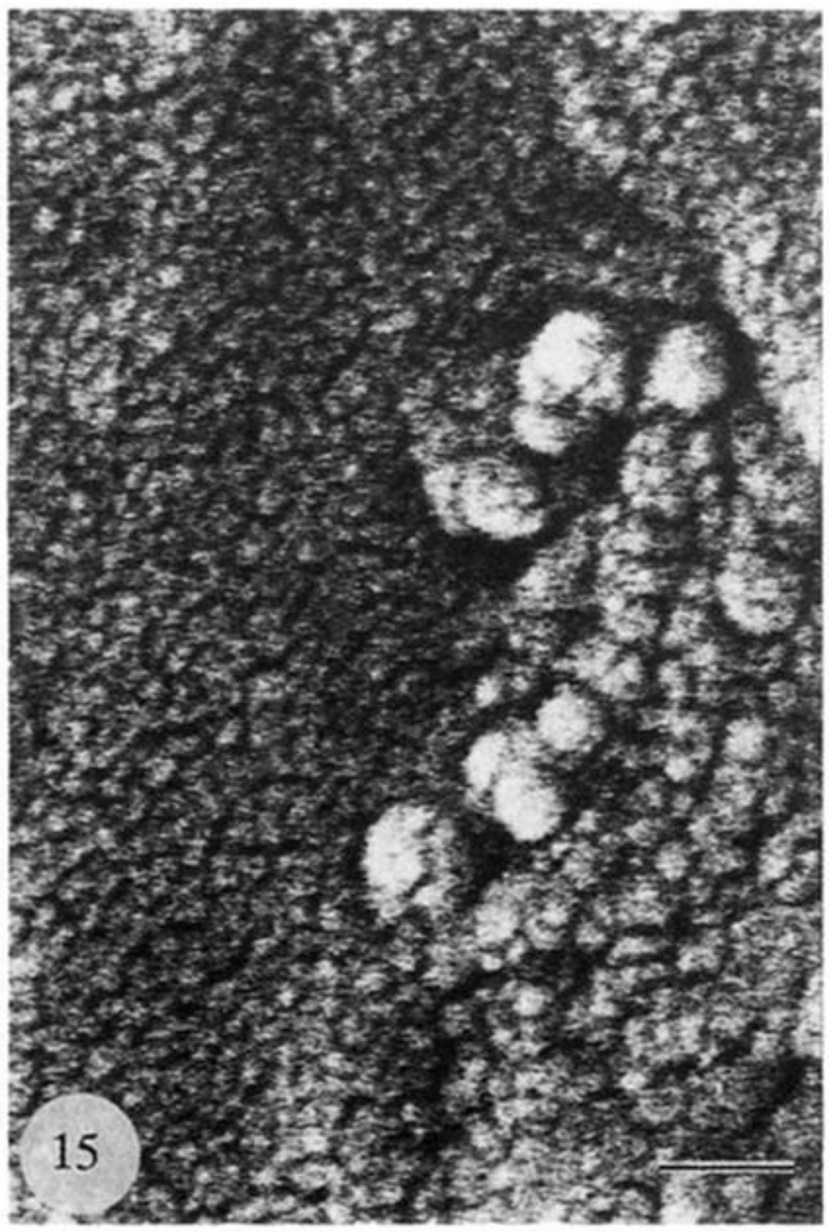

Figures 13–15. Scanning electron micrographs of dried dorsal valves of *Discina striata*.

Figure 13. Bleached, vertical fracture surface coated with gold to reveal rods or baculae (bl) of spherular apatite aligned within an organic matrix which also contains scattered aggregates of spherules (se). Scale bar = 500 nm.

Figure 14. Resin-mounted section digested by subtilisin (2 mM) and chitinase (0.2 mM) in phosphate buffer and coated with carbon then gold to reveal the disposition of rods (baculae) and isolated spherules of apatite relative to the plane of the section. Scale bar = 500 nm.

Figure 15. Vertical fracture surface digested by chitinase (1 mM in phosphate buffer) and coated with carbon then gold to reveal the reticulate network of grooves outlining spherules of apatite. Scale bar = 200 nm.

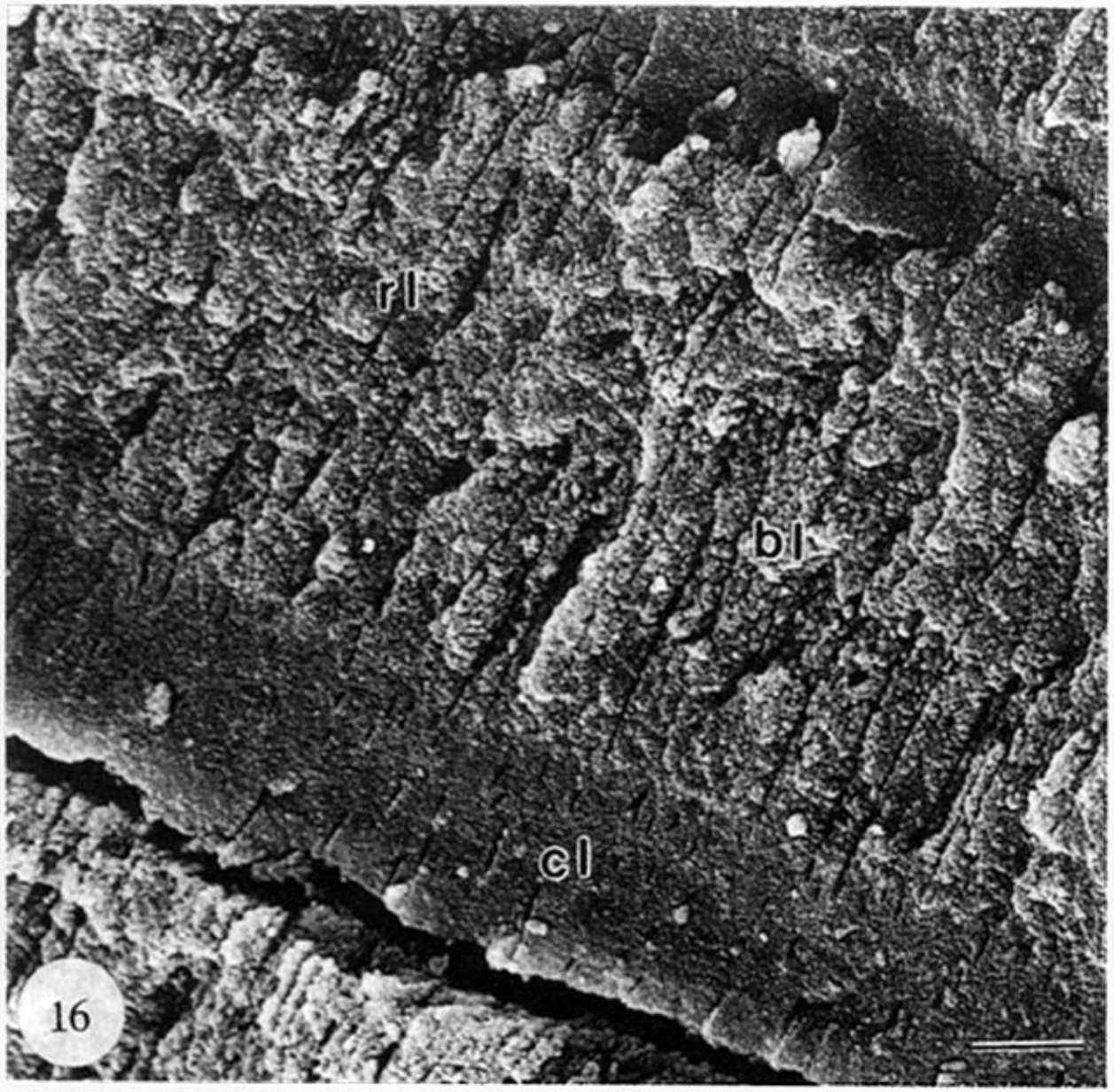

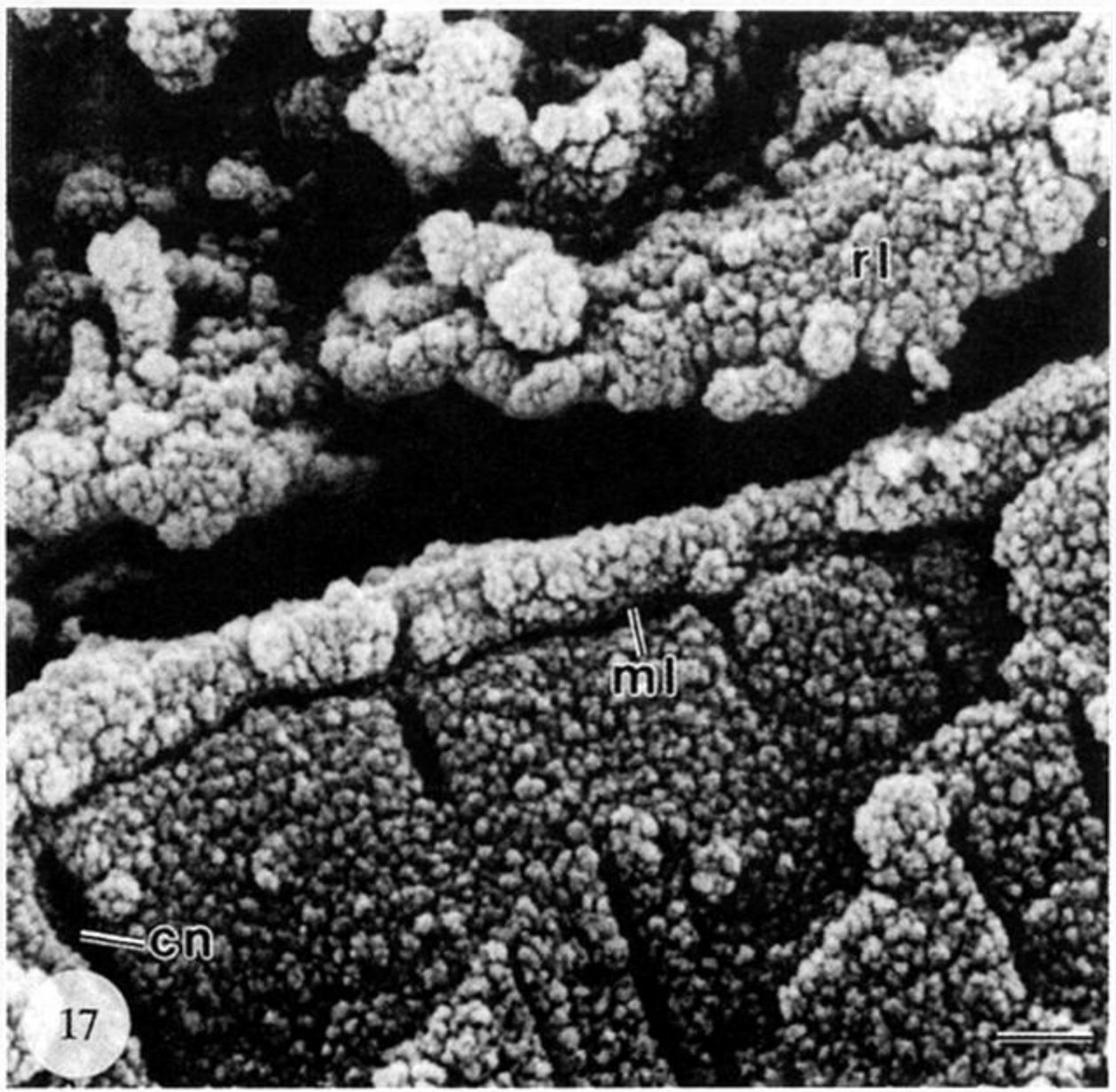

Figure 16–17. Scanning electron micrographs of a dried dorsal valve of *Discina striata*.

Figure 16. Bleached, vertical fracture surface coated with carbon then gold to reveal compact laminae (cl) separated by rubbly (rl) and baculate successions (bl). Scale bar = 5 μm.

Figure 17. Untreated, vertical fracture surface coated with carbon then gold to reveal the junction (presumably the former site of a membrane (ml)) between a graded compact lamina with canals (cn) and a rubbly lamina (rl) with conspicuous spheroidal aggregates of spherular mosaics. Scale bar = 1 μm.

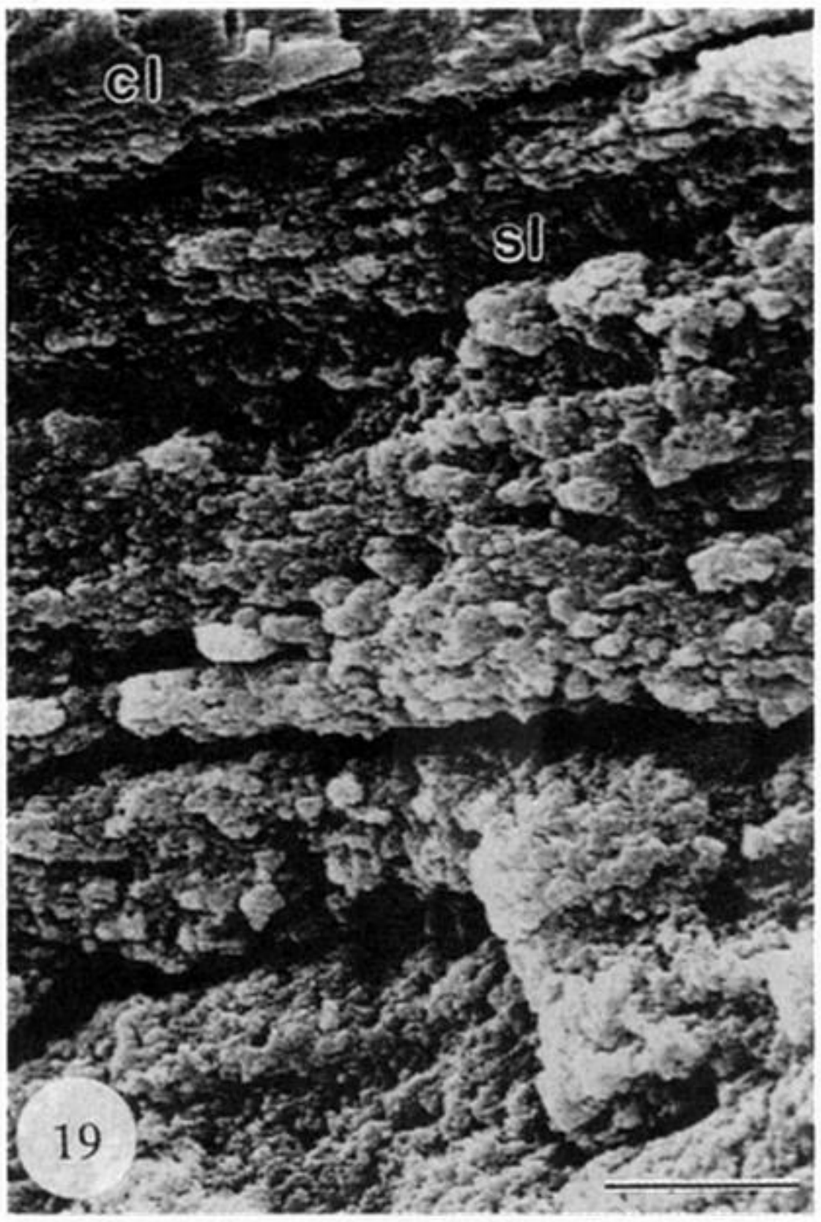

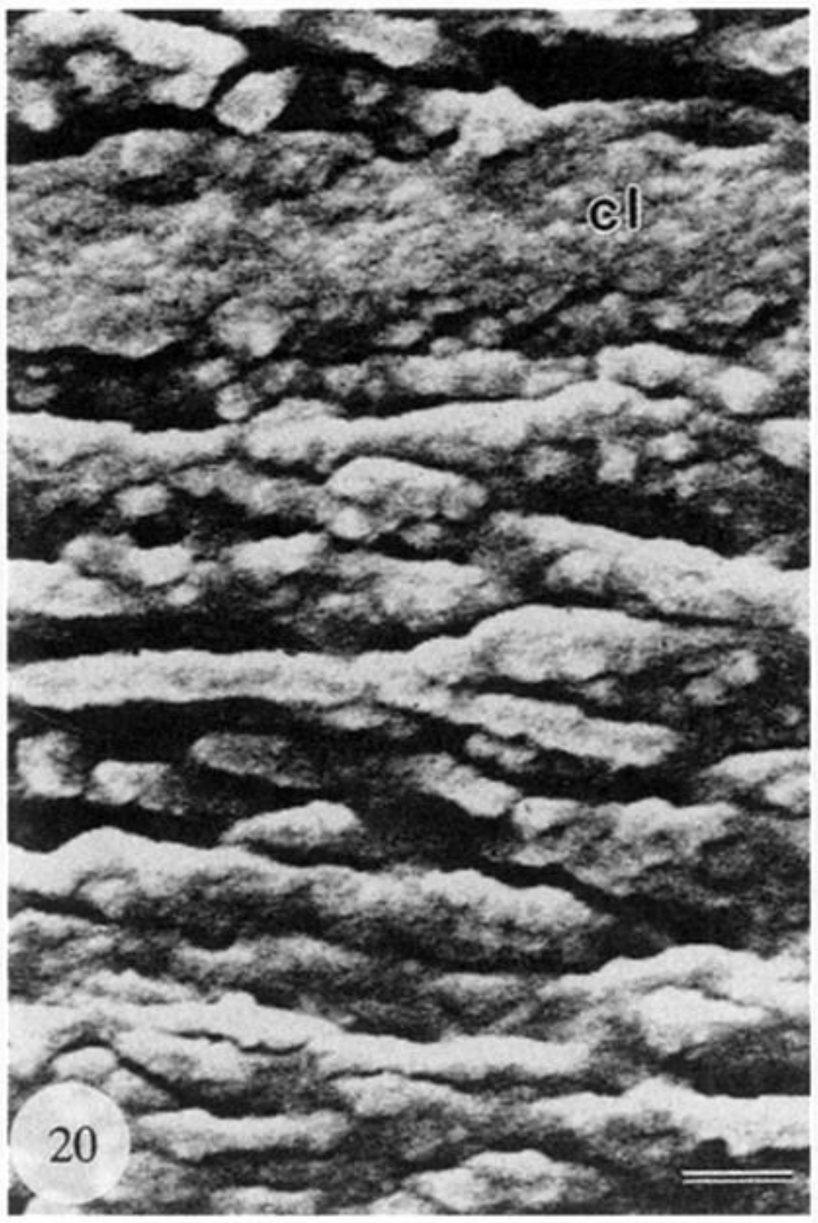

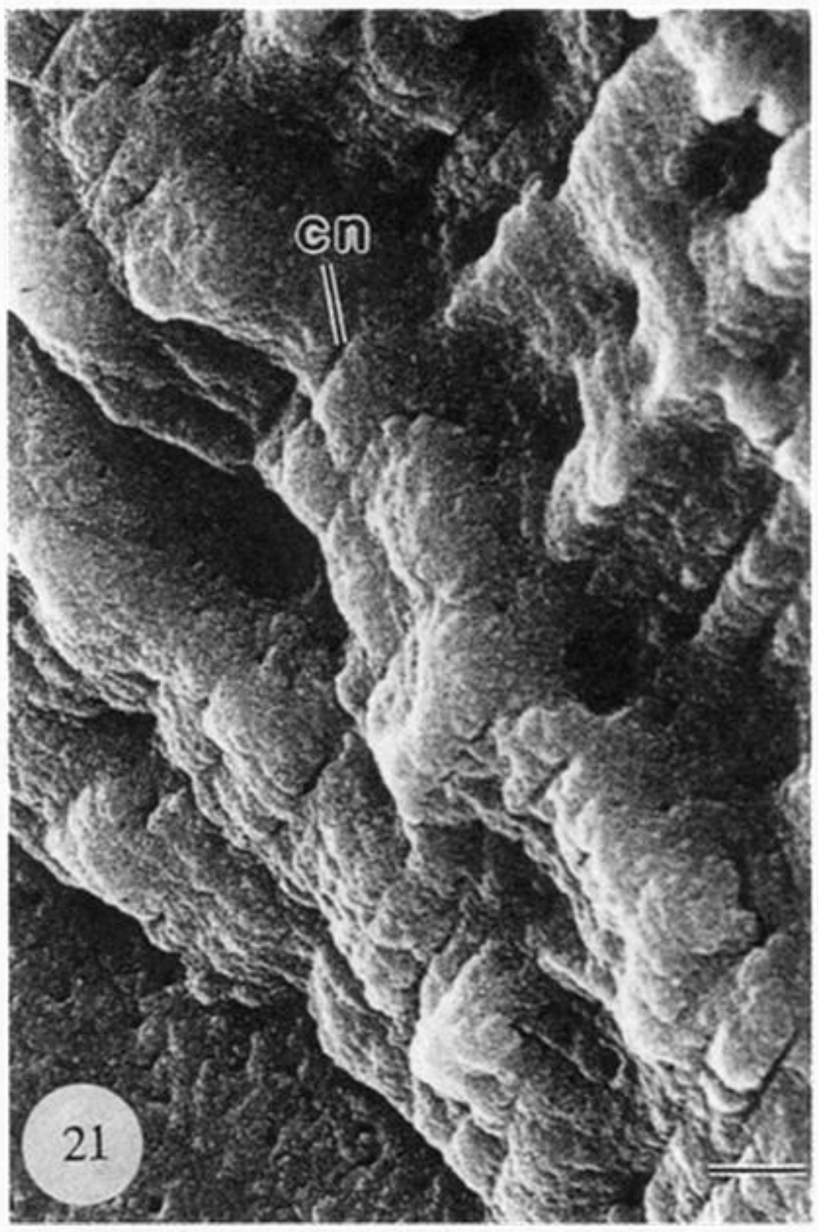

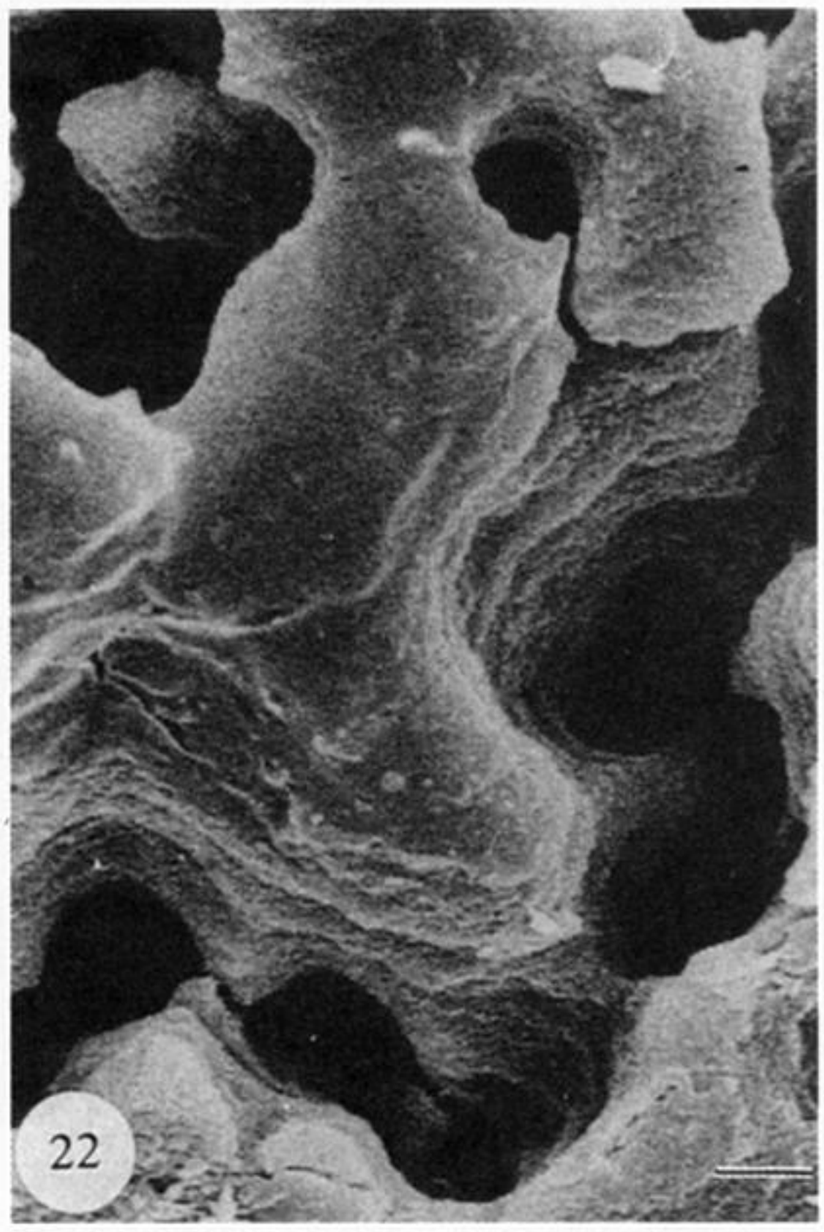

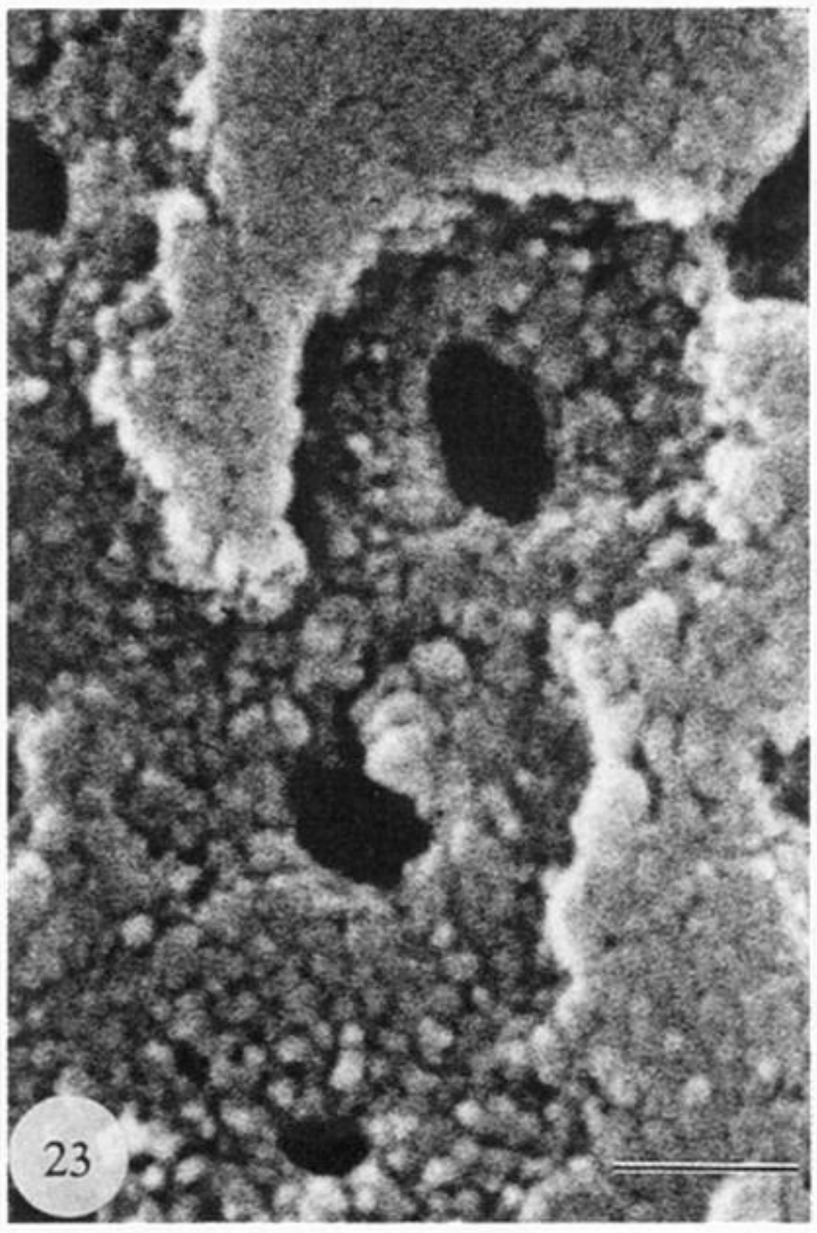

Figures 18–23. Scanning electron micrographs of dried dorsal valves of *Discina striata*.

Figure 18. Bleached, vertical fracture surface coated with carbon then gold to reveal rubbly (rl) and stratified (sl) and rubbly laminae separated by a compact lamina (cl). Scale bar = 5 μm.

Figure 19. Vertical fracture surface digested by trypsin (0.2 mM in phosphate buffer) and coated with carbon then gold to reveal a stratified lamina (sl) underlying a compact one (cl). Scale bar = 5 μm.

Figure 20. Vertical fracture surface digested by chitinase (0.2 mM in MES buffer) and coated with carbon then gold to reveal stratified laminae with an intercalated compact lamina (cl). Scale bar = 500 nm.

Figure 21. Oblique internal view of the margin of a bleached valve coated with carbon then gold to show the disposition of finely stratified laminae pervaded by fine canals (cn). Scale bar = 2 μm.

Figure 22. Internal view of the labyrinthine canal system pervading stratified laminae at the margin of a bleached valve, coated with carbon then gold. Scale bar = 2 μm.

Figure 23. Internal surface of a stratified lamina at the margin of a bleached valve coated with carbon then gold to show the flattened sub-ovoid mosaics making up individual strata. Scale bar = 500 nm.

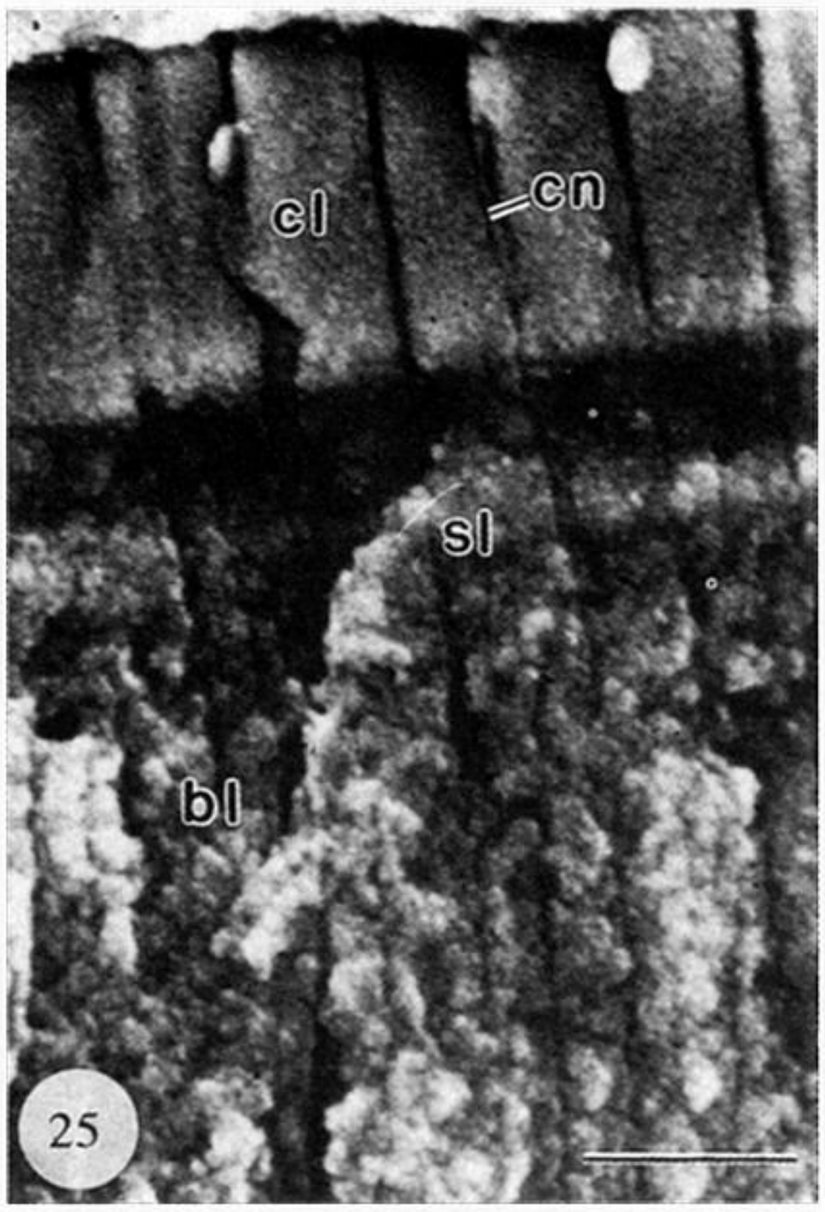

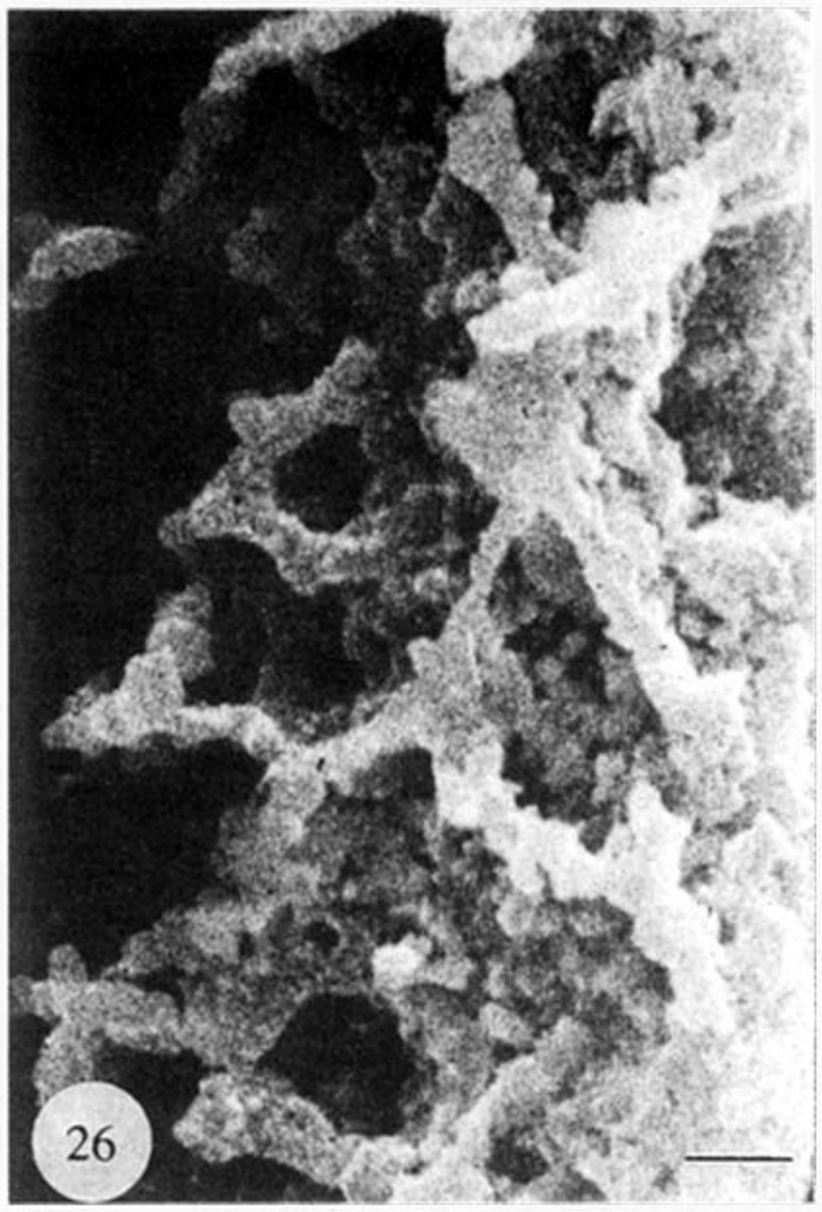

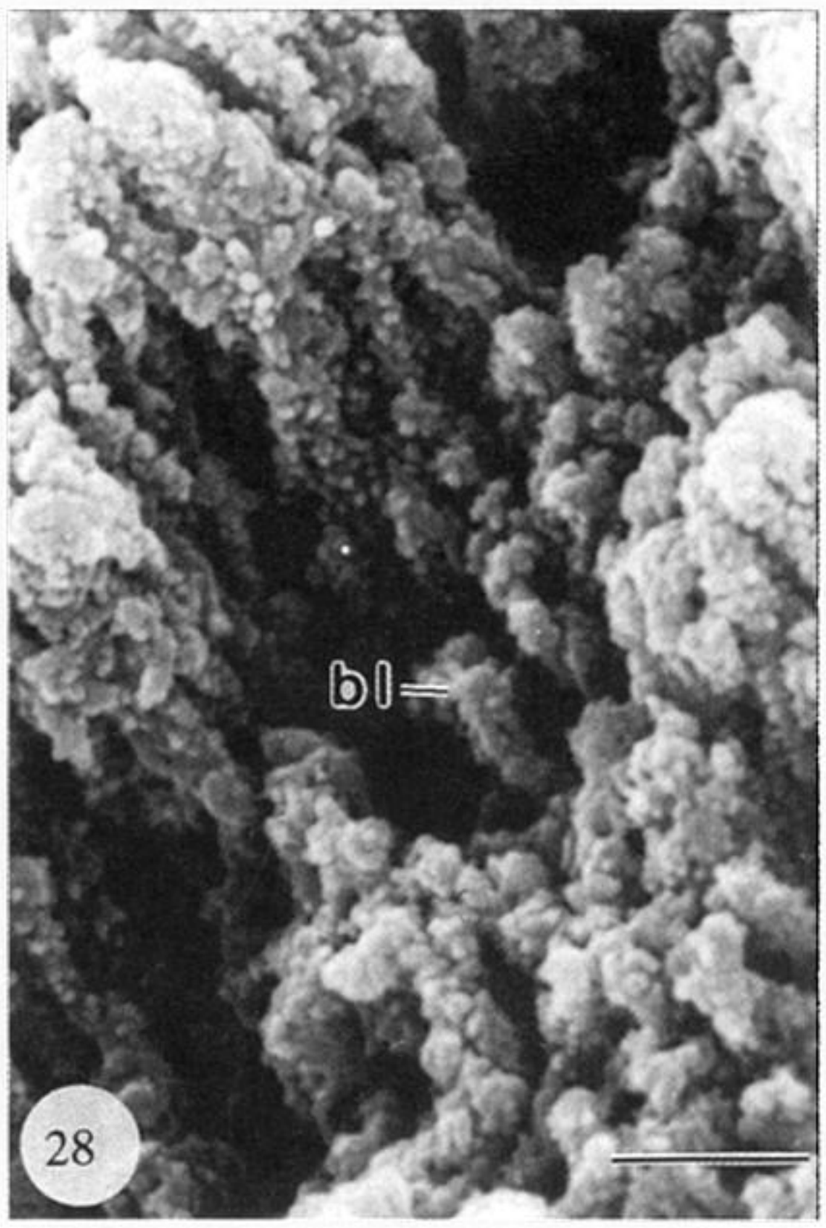

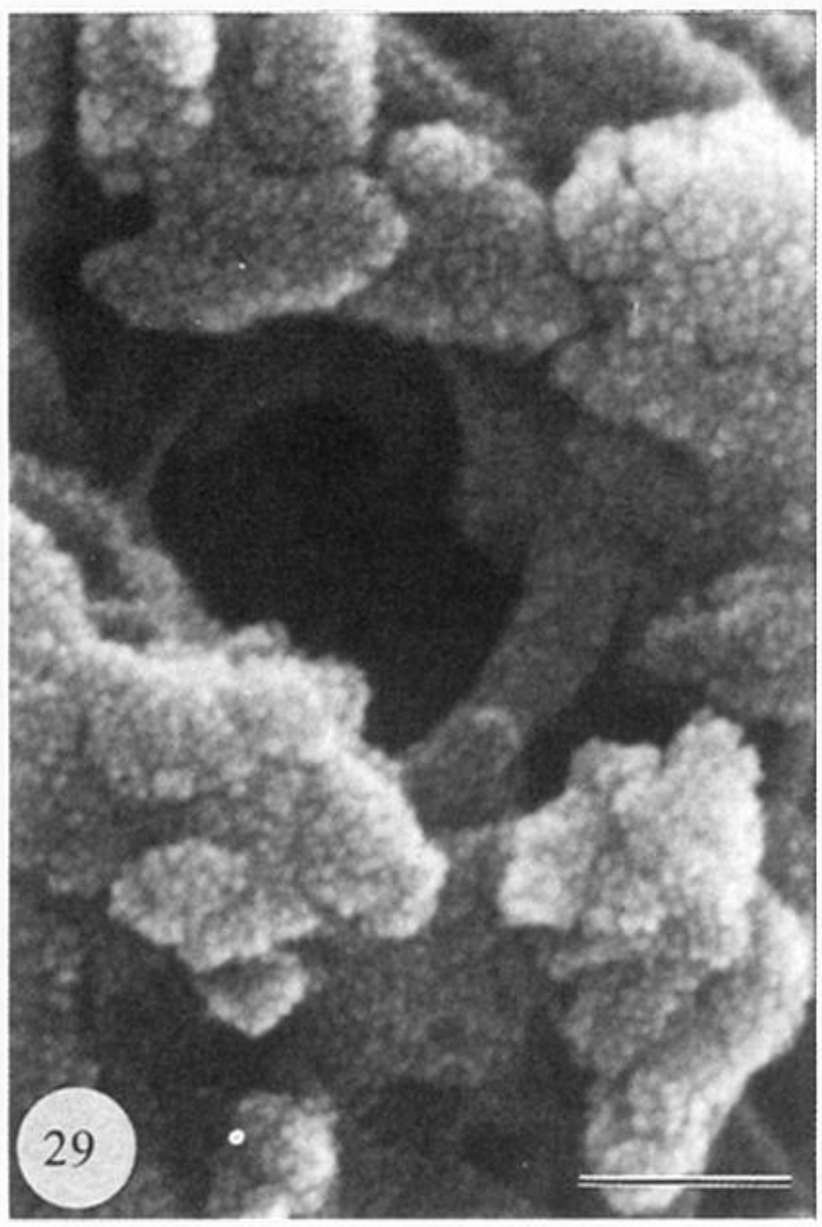

Figures 24–29. Electron micrographs of dried dorsal valves of *Discina striata*.

Figure 24 and 25. Backscattered and scanning electron micrographs of the same part of an untreated, vertical fracture surface coated with carbon and showing the predominant distributions of apatitic and organic components (white and darker shades respectively in figure 24) within baculate (bl), stratified (sl) and compact laminae (cl) pervaded by canals (cn) as identified in figure 25. Scale bar = 5 μm.

Figure 26. Bleached, resin-mounted section coated with carbon then gold to show the hexagonally arranged spherular struts within a tension crack at the interface of a baculate lamina. Scale bar = 500 nm.

Figure 27. Bleached transverse fracture surface of a dorsal septum coated with gold to show the disposition of baculae relative to a compact lamina (cl). Scale bar = 1 μm.

Figure 28. Oblique fracture surface of a dorsal valve digested by trypsin (0.8 mM in phosphate buffer and coated with gold-palladium to show the disposition of an array of baculae (bl) composed of apatitic spherules. Scale bar = 1 μm.

Figure 29. Oblique fracture surface digested by trypsin (0.8 mM in phosphate buffer) and coated with gold-palladium to show the granular structure of spherules and blades forming the baculae around a subcylindrical depression. Scale bar = 100 nm.

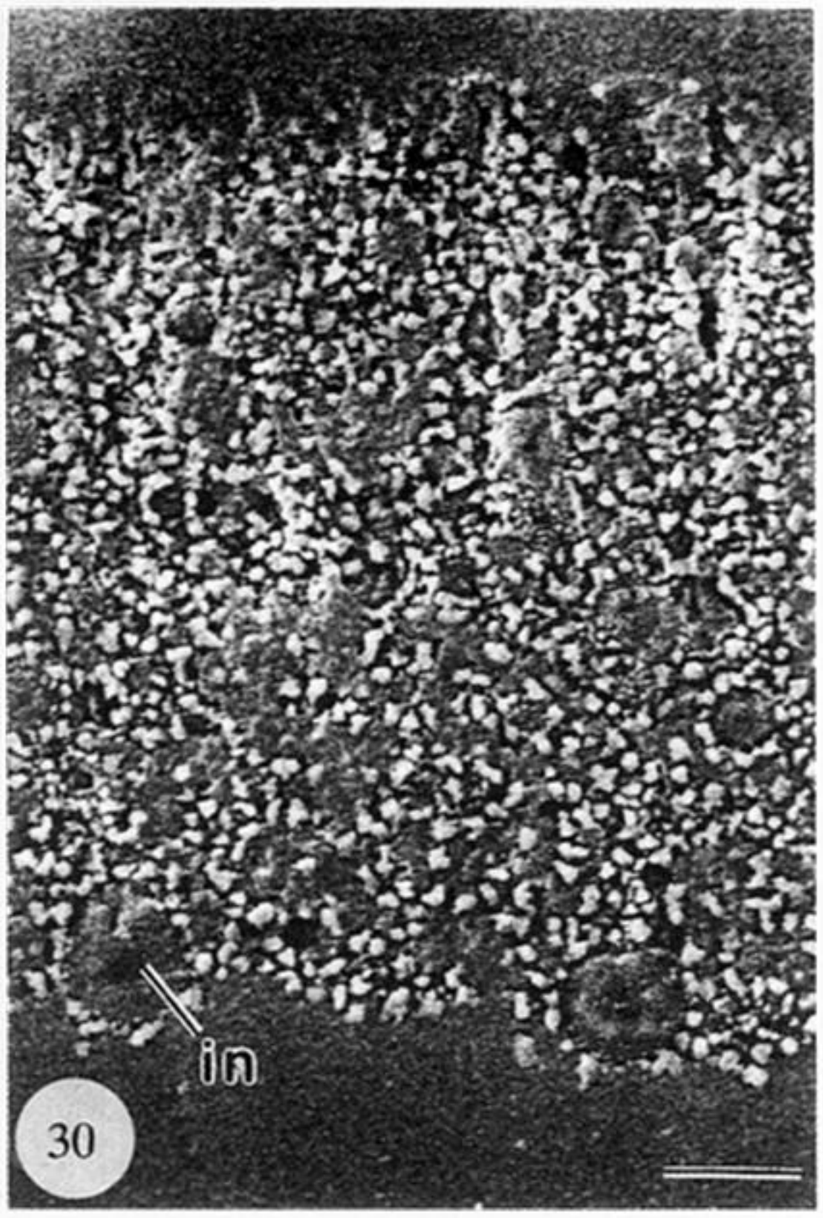

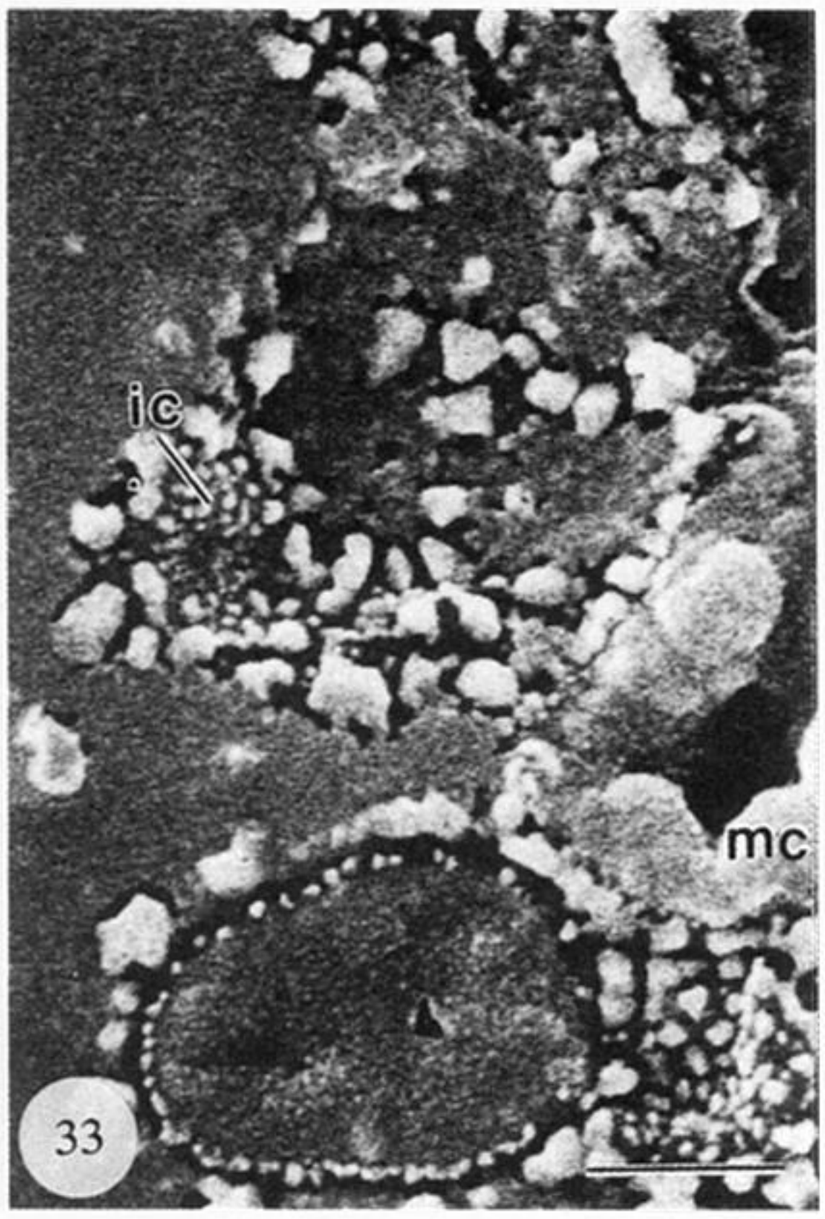

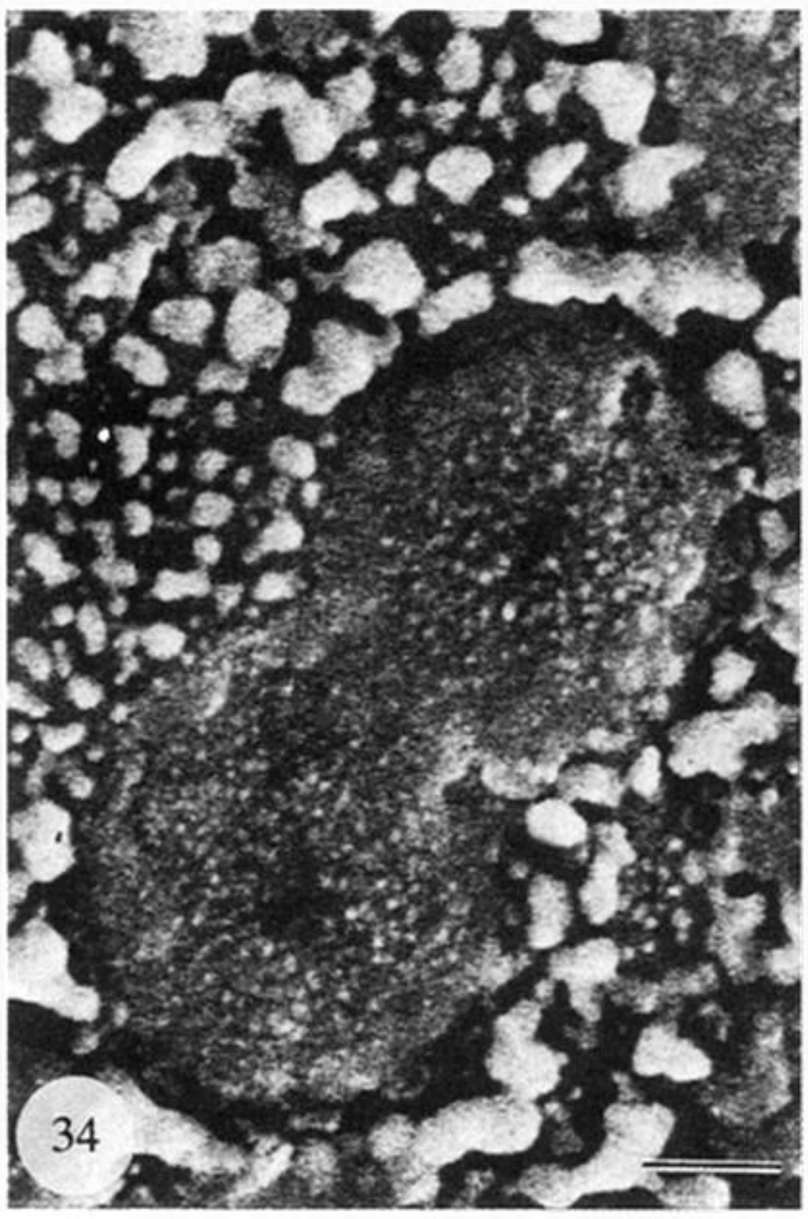

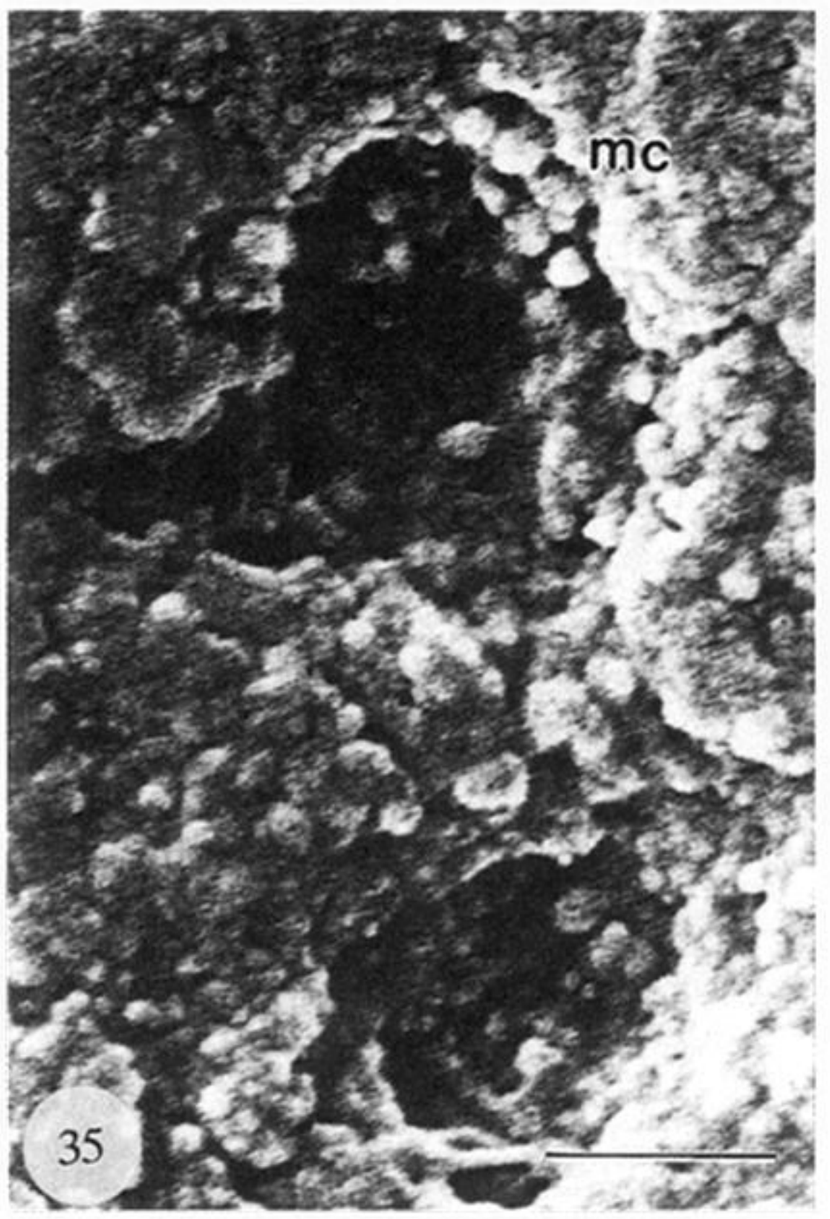

Figures 30–35. Scanning electron micrographs of resin-mounted sections of a dried dorsal valve of *Discina striata* coated with carbon then gold.

Figure 30. Bleached section showing the dense distribution of inclusions (in) and electron-light particles in a rubbly lamina bounded by two compact ones. Scale bar = 2 μm.

Figure 31. Bleached section showing the distribution of inclusions and electron-light particles (cp) in an incipient rubbly lamina and along a canal (cn) traversing a compact lamina. Scale bar = 2 μm.

Figure 32. Bleached section showing the sporadic occurrence of inclusions and associated electron-light particles in a compact lamina. Scale bar = 2 μm.

Figure 33. Bleached section showing an inclusion in the equatorial plane (below), a botryoidal group of spheroidal mosaics (mc) of a larger inclusion (right) and the hollow remaining after the removal of an inclusion with a lining of electron-light particles and part of the inner coat (ic) of electron-light spherules (above). Scale bar = 1 μm.

Figure 34. Bleached section showing the details of two conjoined inclusions, more or less in the equatorial plane. Scale bar = 250 nm.

Figure 35. Complementary section of the same dorsal valve as in figures 30–34 digested in subtilisin (2 mM in phosphate buffer) to reveal hollows lined with particles of spherular mosaics (mc) and assumed to have contained inclusions in the same way as the hollow shown in figure 33. Scale bar = 1 μm.

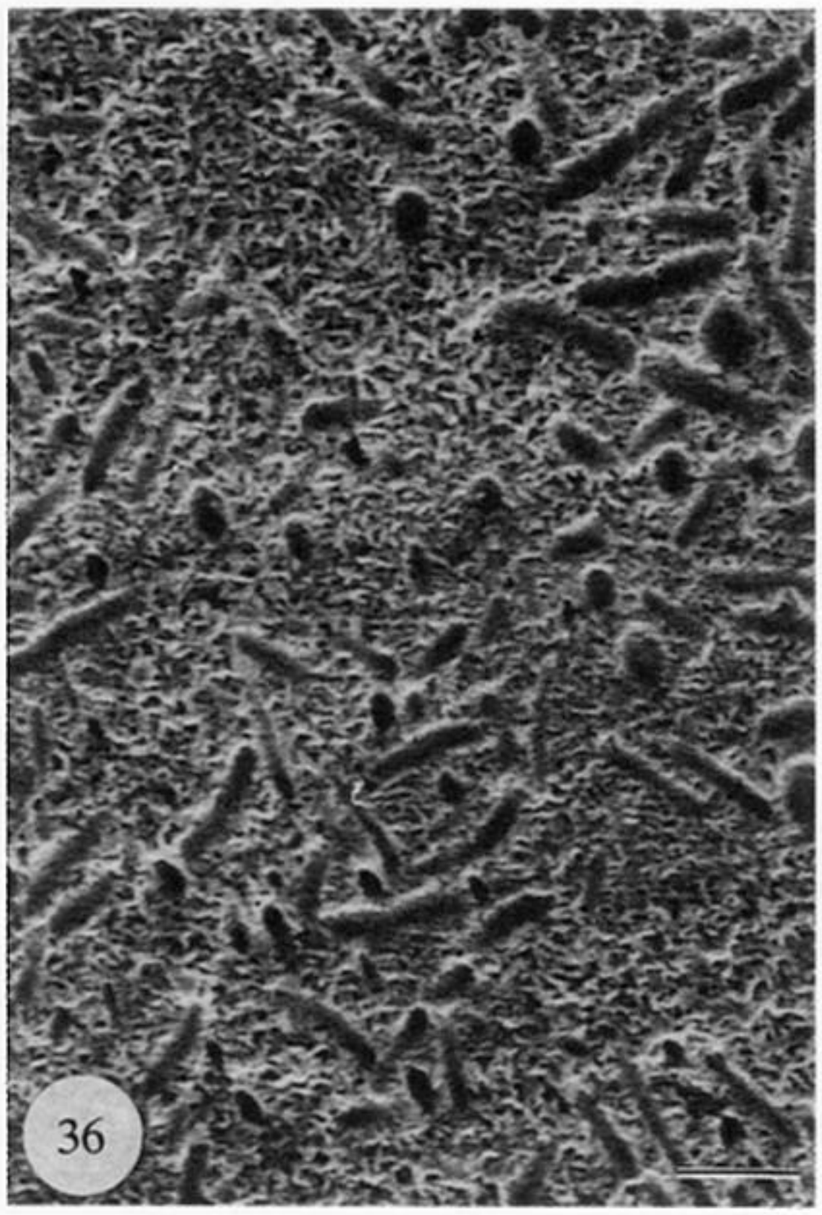

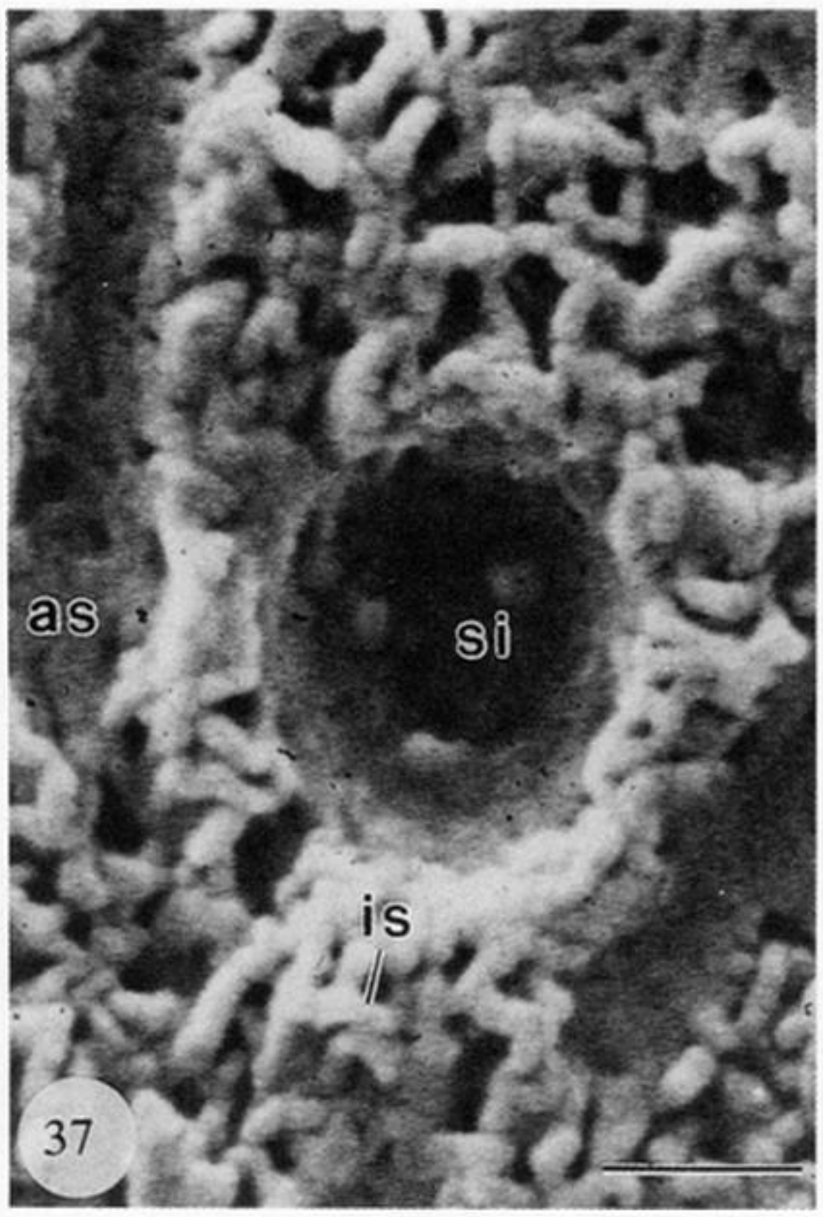

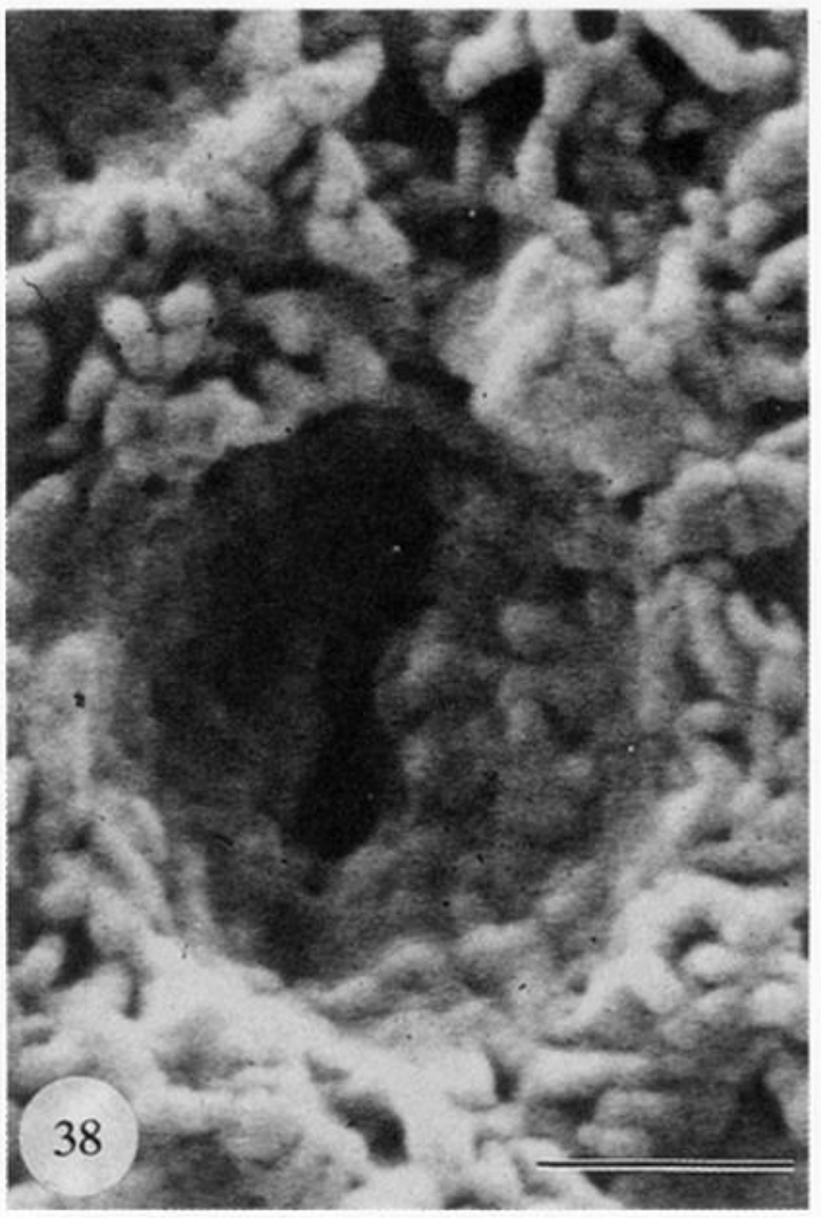

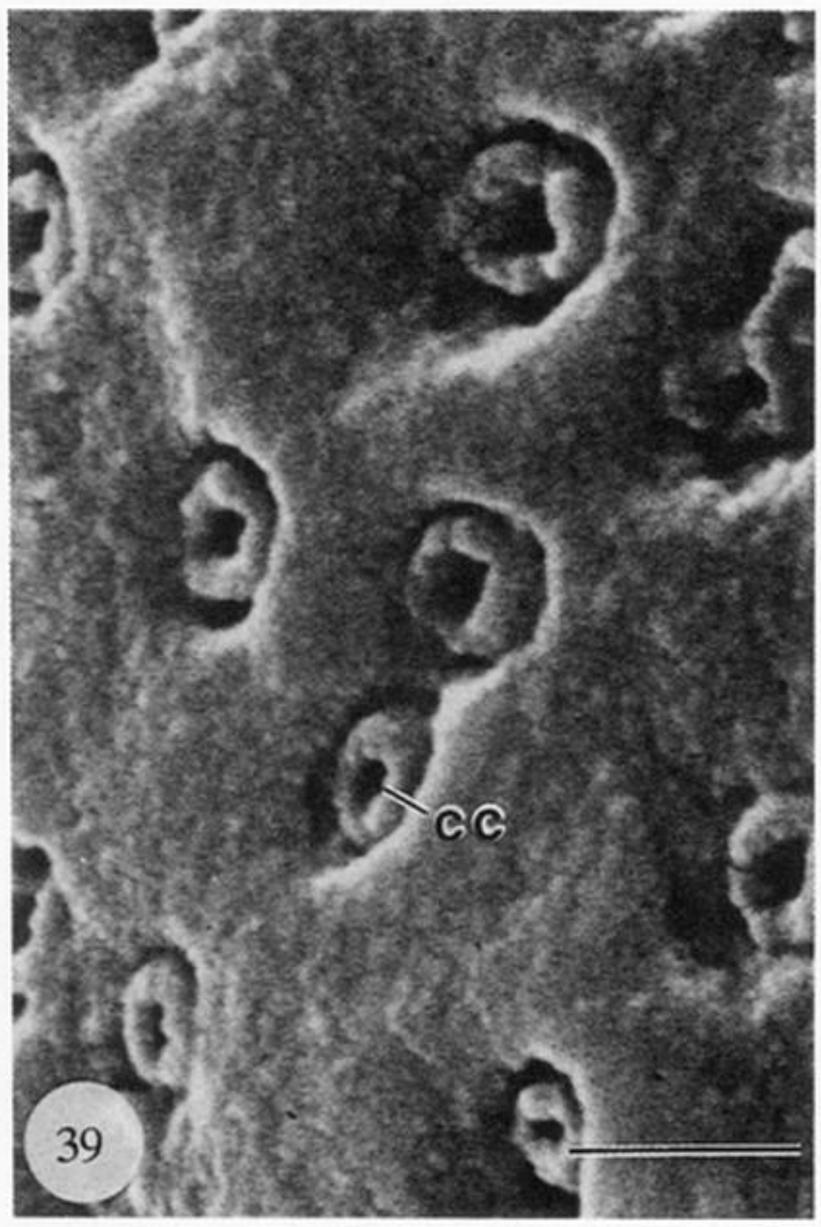

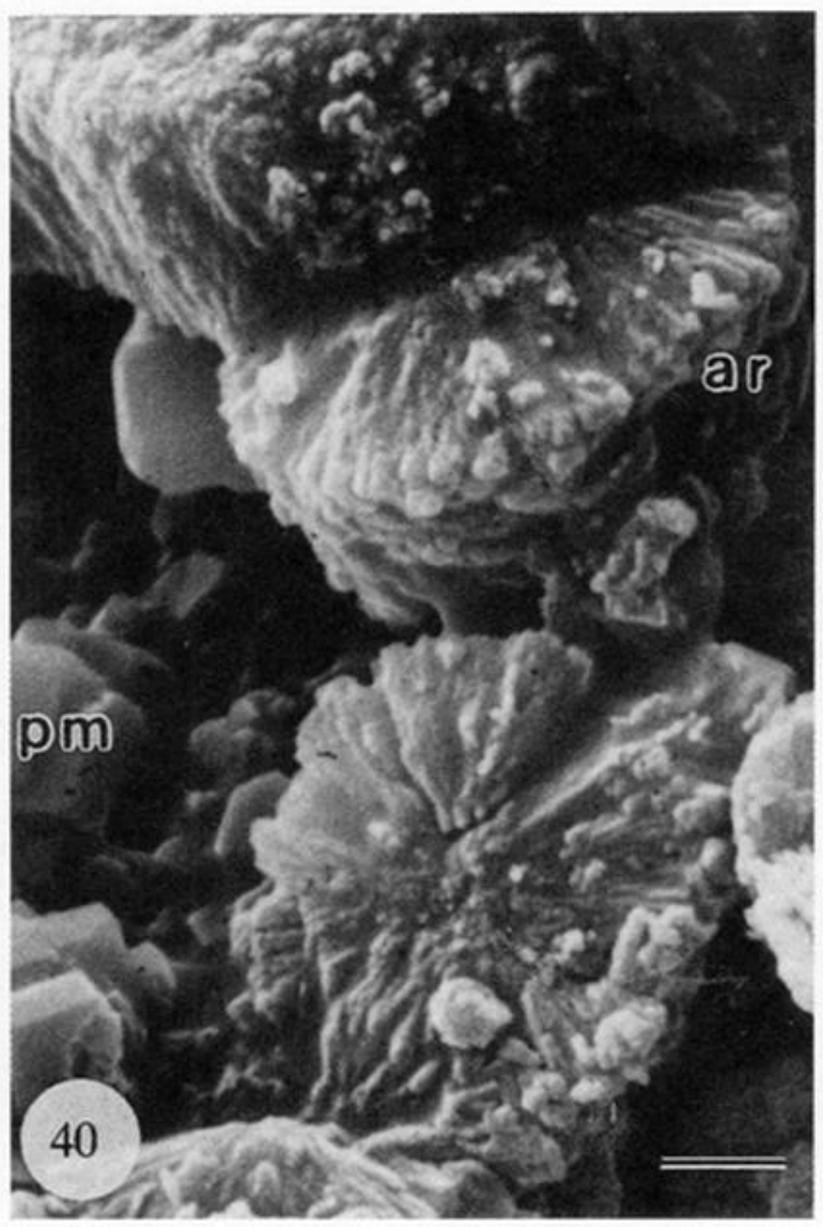

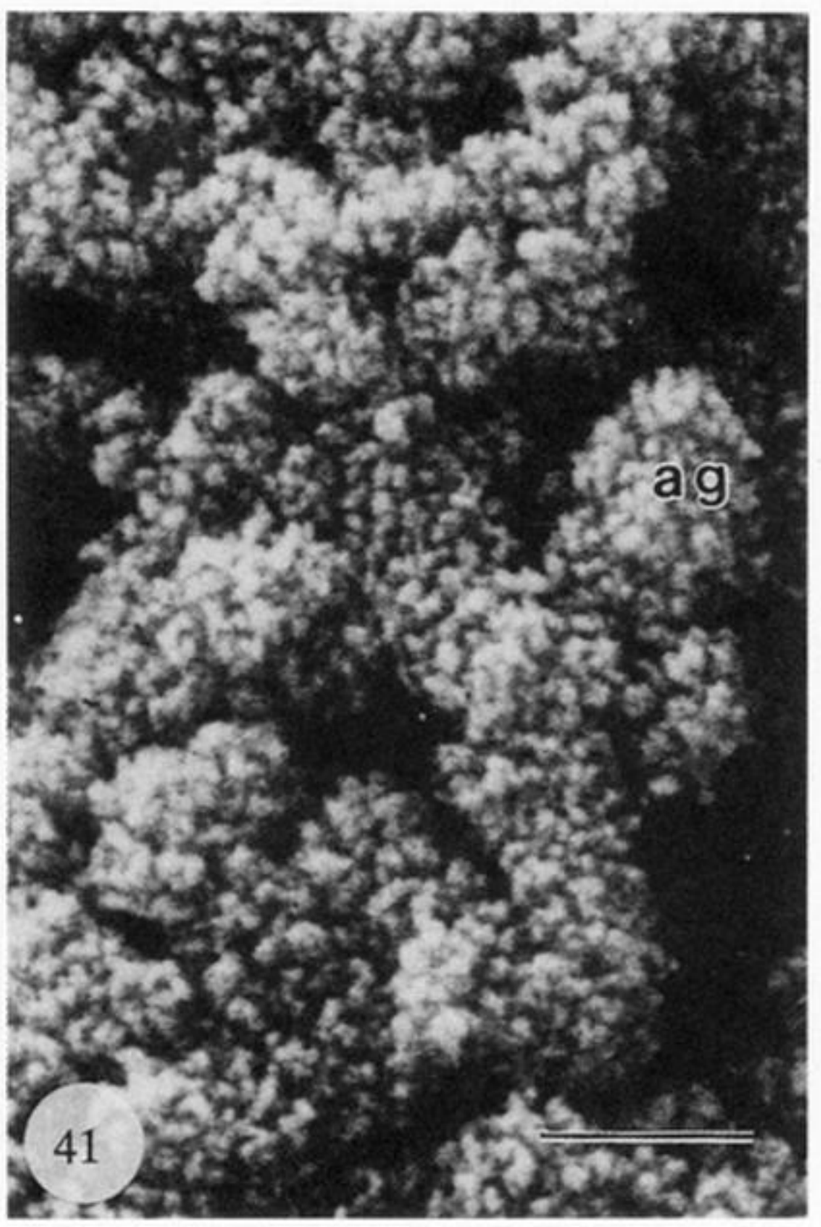

Figures 36–38. Scanning electron micrographs of a resin-mounted section of a ventral valve of *Discina striata* digested in subtilisin (2 mM in phosphate buffer) and coated in carbon then gold.

Figure 36. General view showing the distribution of hemispherical and hemicylindroid hollows in rubbly laminae. Scale bar = 2 μm.

Figure 37 and 38. Details of section showing the nature of the apatitic mesh of interconnected spherules (is) and the way it lines the hollows assumed to have accommodated anastomosing strands (as) and spheroidal inclusions (si) mainly of organic tissue. Scale bars = 500 nm.

Figures 39–41. Scanning electron micrographs of various organo-phosphatic brachiopods.

Figure 39. A vertical fracture surface of a dorsal valve of *Discina striata* digested by papain (40 μM with mercaptoethanol at 50 μM in phosphate buffer) and coated in carbon then gold to show the development of discrete coats (cc) of spherular apatite around canals on the inner surface of a compact lamina. Scale bar = 1 μm.

Figure 40. Acicular spherulites (ar) and prisms (pm) of apatite between the lamellae bounding a columnar lamina in an untreated fracture surface of *Apsotreta expansa* Palmer, Upper Cambrian Wilberns Formation, Threadgill Creek, Texas. Scale bar = 1 μm.

Figure 41. Aggregates (ag) of spheroidal apatite in an untreated, vertical fracture surface of *Dictyonina* cf. *ornatella* (Linn.), Middle Cambrian Sosiuk Formation, Turkey. Scale bar = 1 μm.

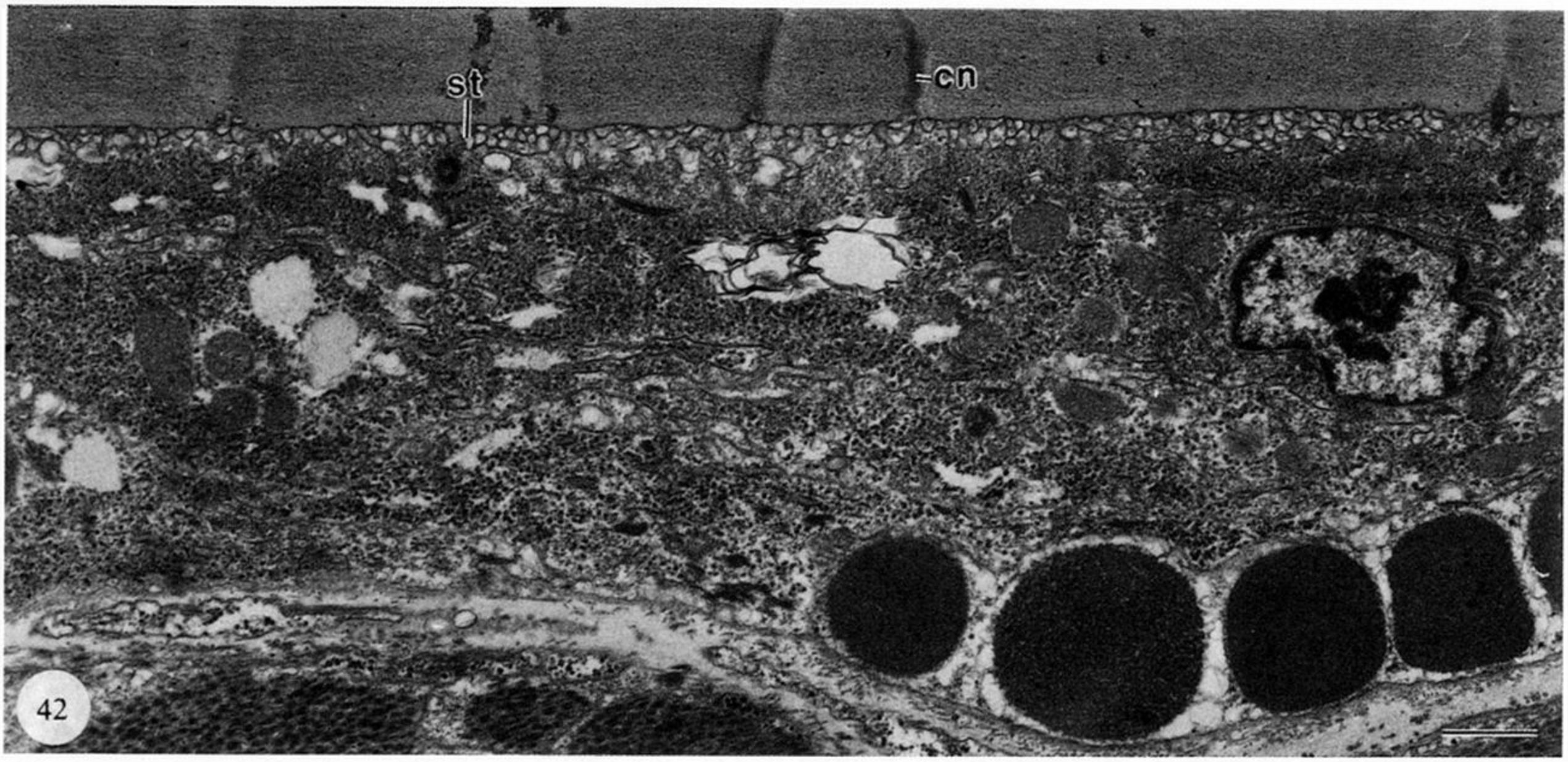

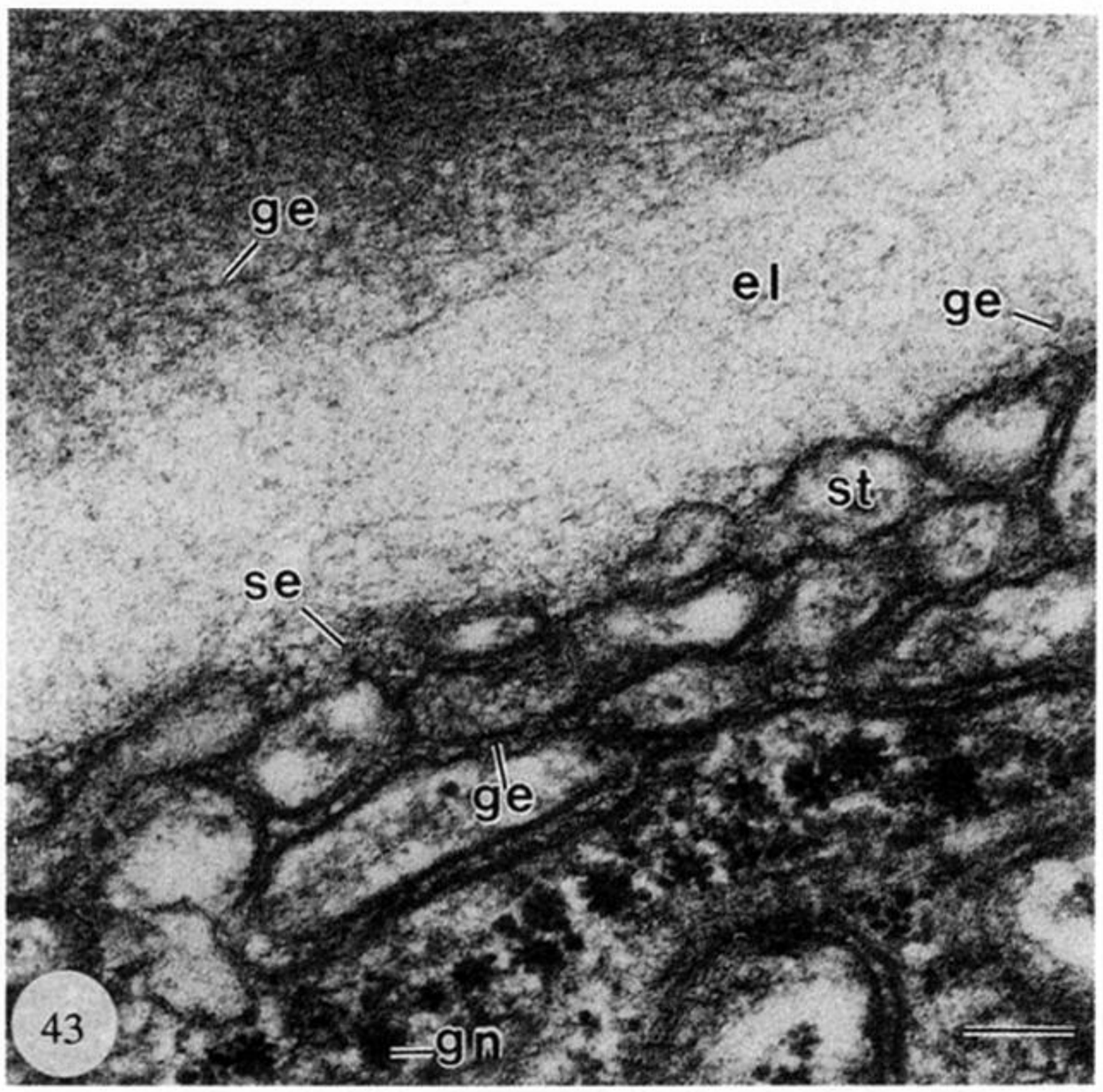

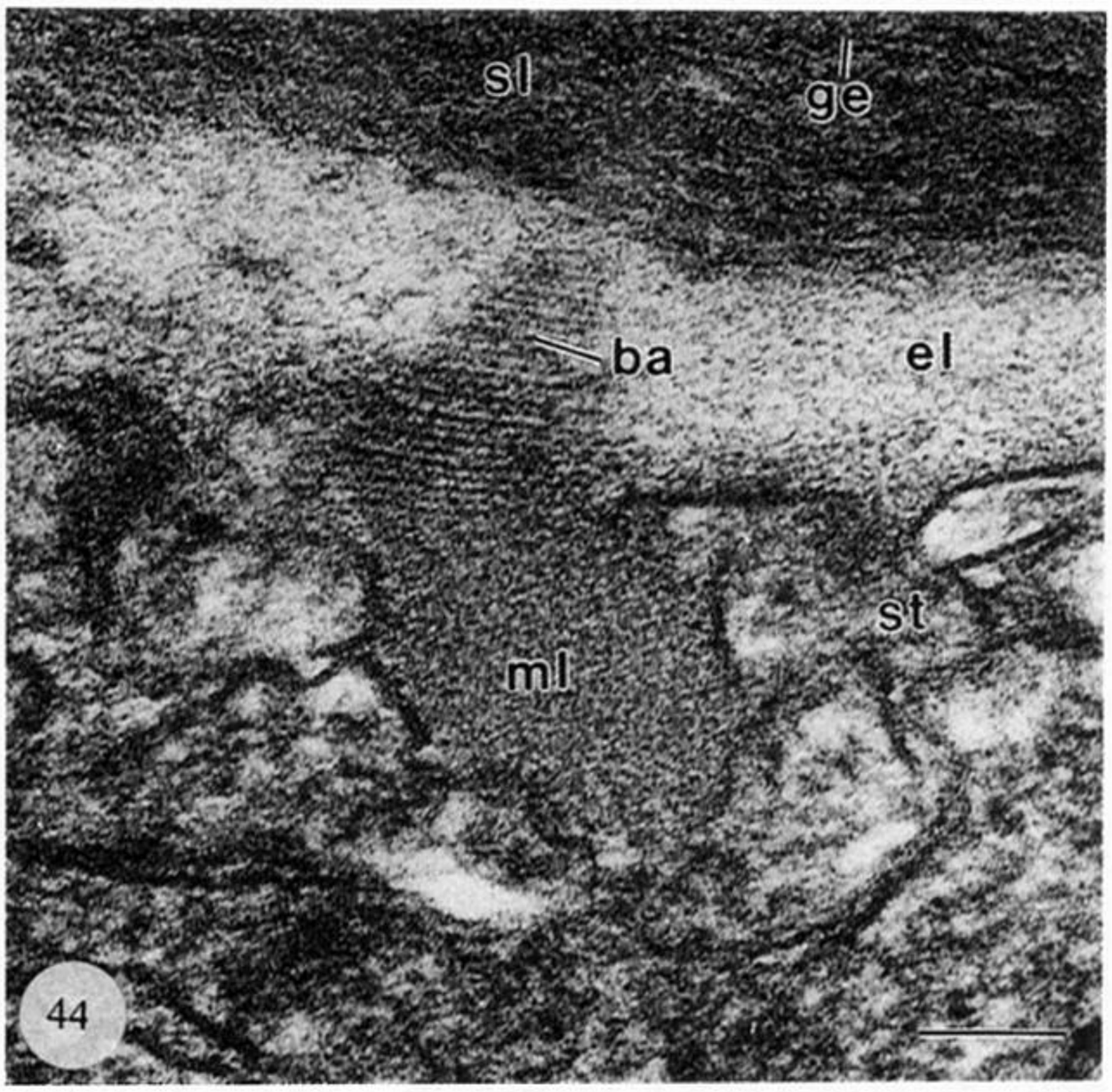

Figures 42–44. Transmission electron micrographs of decalcified sections of dorsal valves of *Discina striata*.

Figure 42. General view of outer epithelium underlying stratified laminae, showing the disposition of interdigitating secretory tubes (st) along the interface with the shell which is pierced by canals (cn). Scale bar = 1 μm.

Figure 43. Outer epithelial secretory tubes (st) underlying a compact lamina, from which they are separated by an electron-lucent zone (el) containing (along with the shell and the tubes) coats of apatitic granules (ge), some in spherular aggregates (se); glyogen (gn) is abundant in the apical part of the cell. Scale bar = 100 nm.

Figure 44. The organic contents and lining of a canal originating within the zone of interdigitating secretory tubes (st) and penetrating an electron-lucent band (el) and a stratified lamina (sl) with aligned granular coats (ge); the basal close-packed assemblage of electron-lucent and medium electron-dense particles (ml) grades apically into banded arrays (ba). Scale bar = 100 nm.

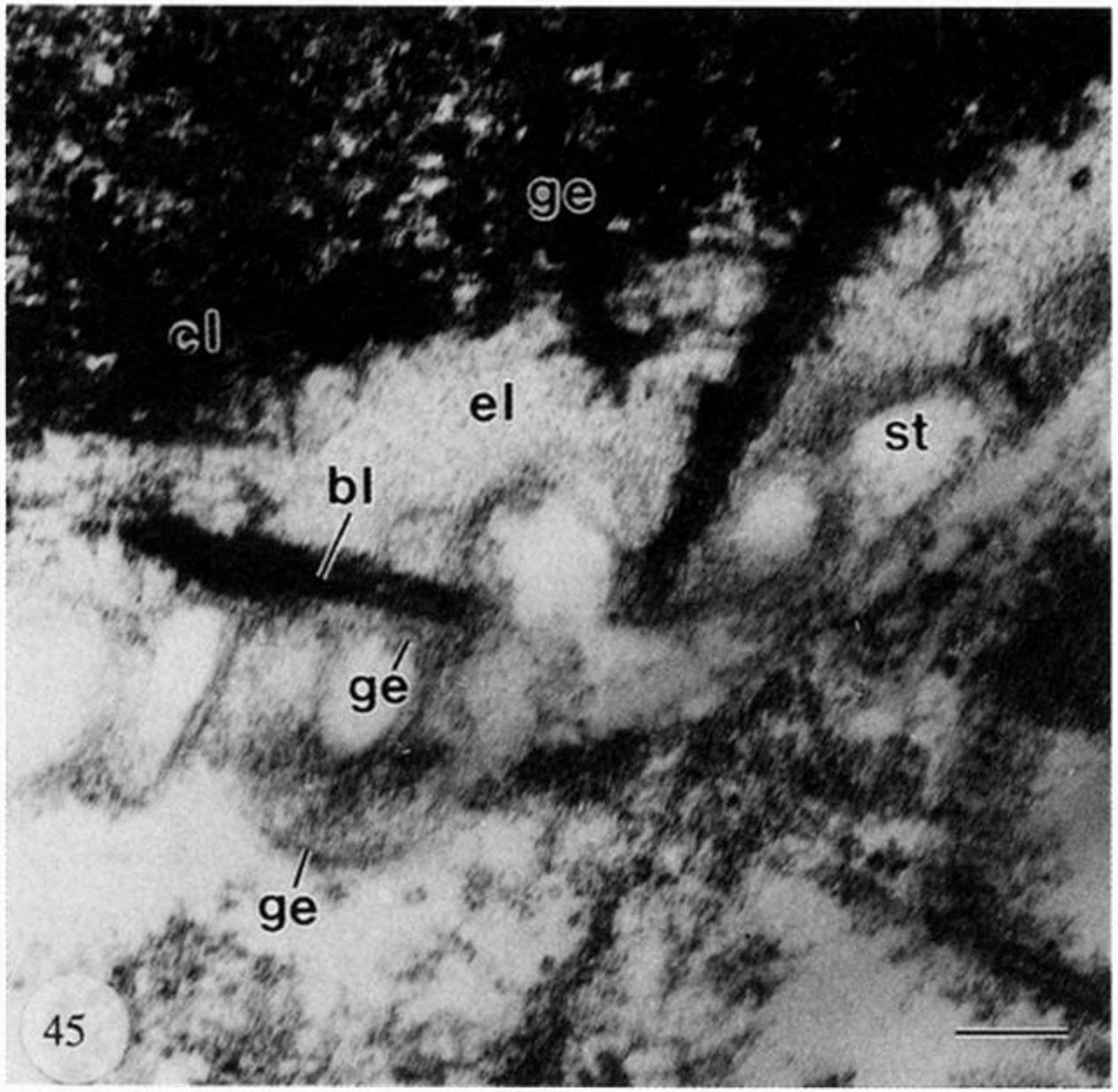

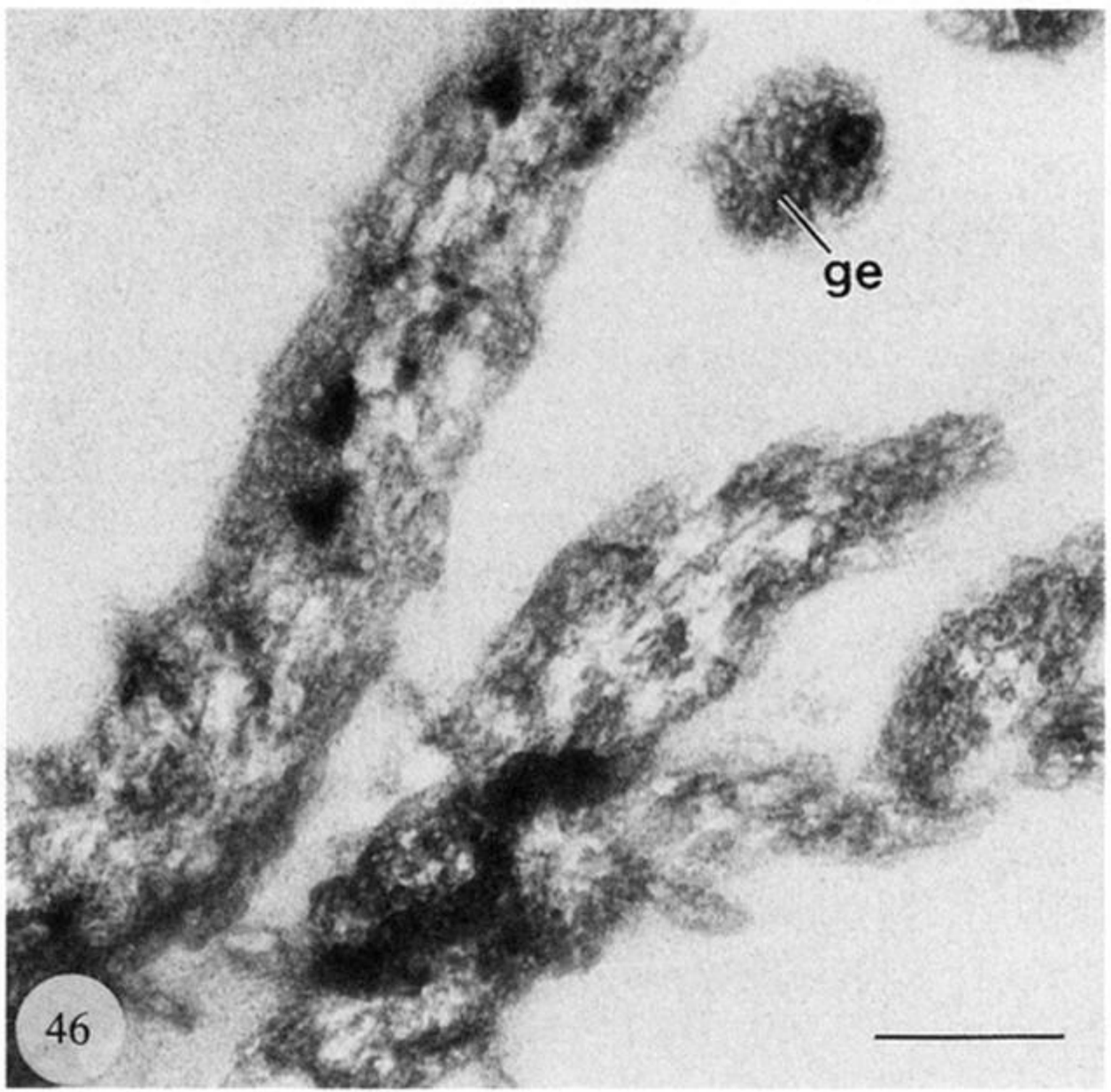

Figures 45–46. Transmission electron micrographs of shell and associated outer epithelium of a dorsal valve of *Discina striata*.

Figure 45. The secretory tubes (st) of outer epithelium in relation to baculae (bl) within or spanning an electron-lucent zone (el) underlying a compact lamina (cl); coated apatitic granules (ge) occur throughout. Scale bar = 100 nm.

Figure 46. Details of a baculate lamina within the shell succession showing the distribution of aggregates of coated apatitic granules (ge). Scale bar = 100 nm.